

W-PM-F1 THEORY FOR THE EQUATION OF STATE OF PHOSPHOLIPID MONOLAYERS

Robert Cantor, Department of Chemistry, Dartmouth College, Hanover, N.H. 03755

We present a semi-empirical statistical mechanical treatment for the interactions among the phospholipids in bilayers and monolayers over a wide range of surface densities, temperatures, and chain lengths. This work draws from three recent efforts: (i) lattice-based interphase theory which explicitly treats the chain conformations in 3-dimensional interfacial phases of short chain molecules, (ii) a recent "equation of state" treatment of van der Waals interactions which predicts volume changes, enthalpies, and temperatures of melting of the "rotator" phases of n-alkanes, and (iii) detailed study of the extensive measurements of Mingins, et al. (*J. Chem. Soc., Farad. Trans. I* (1982) **78**, 323) of pressure-area isotherms of phosphatidylcholines at the heptane/water interface which we have used to assess empirical characteristics of the head group interactions and of the "solid state". This approach rationalizes pressure-area isotherms and phase transitions of monolayers of lecithins of chain lengths from 16 to 22 and predicts temperatures, area, volume changes, and enthalpies of melting of the corresponding bilayers.

W-PM-F2 MEMBRANE HYDRATION AND ITS INFLUENCE ON MEMBRANE PROPERTIES.

A. Sen, S.W. Hui and P.L. Yeagle, Biophysics, Roswell Park Memorial Institute, Buffalo, NY 14263, and Dept. Biochemistry, SUNY/Buffalo School of Medicine, Buffalo, NY 14214.

The water binding capacity of PE, monomethyl PE, dimethyl PE, PC and cholesterol was determined using H labelled water in a two phase partitioning method. PE "bound" 7-9 water molecules, while PC "bound" 45-50 water molecules. The addition of one methyl group to PE did not result in any significant change in the number of water molecules "bound" to the lipid. The addition of the second methyl group increased the number of waters bound to about 20. One molecule of cholesterol bound 2-3 water molecules by the same method. H-2 NMR and O-17 NMR measurements were also used to study the water interacting with PE and PC bilayers. PC showed the appearance of a quadrupole splitting indicative of motionally restricted water in the liquid crystal state, while PE showed little evidence for motionally restricted water. Cholesterol in the bilayer at greater than 25 mole percent increased the motional restriction of the water. Thermodynamic analysis suggested that the surface of PE bilayers was more "hydrophobic" than the surface of PC bilayers. This prediction was supported experimentally by testing the effects of chaotropic agents on the surface properties of PE bilayers. Furthermore, effects of hydration on the lamellar to hexagonal (II) phase transition was examined using P-31 NMR. This phase transition, which is important to membrane stability, and membrane aggregation, which is important to fusion, may be influenced by the hydration of the bilayer surface.

W-PM-F3 THE HYDRATION FORCE AND BILAYER DEFORMATION: A REEVALUATION. T.J. McIntosh and S.A. Simon, Departments of Anatomy and Physiology, Duke University Medical Center, Durham, N.C. 27710.

The main barrier to adhesion of two hydrophilic surfaces in solution is the hydration repulsive force, F_H , which has been determined quantitatively in the pioneering work of Rand, Parsegian, and colleagues (Le Neveu et al., *Biophys. J.* **18**:209-230; Lis et al., *Biophys. J.* **37**:657-666). By use of an elegant "osmotic stress" method, they have found for a variety of lipid bilayer systems that (1) $F_H = F_0 \exp(-d_f/\lambda)$, where d_f is the fluid layer thickness and λ is the decay constant and (2) bilayer thickness, d_b , and area per molecule, A_1 , change significantly as bilayers come together. In these experiments d_f and d_b were set equal to the partial fluid and bilayer thicknesses as determined from the lamellar repeat and gravimetric determination of water content of separate lipid/water mixtures. We have reevaluated these results by using Fourier synthesis methods to determine d_f and d_b for multilayers with applied osmotic pressures of 0 to 38 atm. Our results agree in that we also find that F_H rises exponentially as bilayers move from their equilibrium separation in excess water to within 2 to 4 Å of each other. However, we measure smaller values for λ , 1.3 Å for gel state DPPC and 1.7 Å for liquid-crystalline egg PC. Also, we find that d_b and A_1 remain nearly constant (to within 3%) in this pressure range in agreement with mechanical measurements of bilayer compressibility moduli (Kwok and Evans, *Biophys. J.* **35**:637-652). Conclusions from this Fourier analysis are: (1) λ is not necessarily the size of a water molecule (about 2.8 Å), (2) lipid bilayers are quite incompressible as they are brought together, (3) fully hydrated phosphatidylethanolamine bilayers, both gel and liquid-crystalline, are separated by fluid spaces which could be spanned by only one or two water molecules.

W-PM-F4 MOLECULAR PACKING DIFFERENCES IN LIPOSOMES AND ORIENTED LIPID MULTILAYERS. Stephen H. White, Russell E. Jacobs, and Glen I. King. Department of Physiology and Biophysics, University of California, Irvine, CA 92717

We have measured the partial specific volumes of lipid (\bar{v}_L) and water (\bar{v}_W) in liposomes of egg lecithin at hydrations ranging from 5% to 55% by weight. Ignoring small changes attributable to phase boundaries, \bar{v}_L is 0.983 ± 0.003 cc/g over the entire hydration range. Given the x-ray Bragg spacing (d), one may use the measured value of \bar{v}_L to calculate the area per lipid (A) and the transbilayer phosphate to phosphate spacing (d_{pp}). We have applied this method to the d and d_{pp} data of Torbet and Wilkins (*J. Theor. Biol.* 62:447-458[1976]) for egg lecithin bilayers oriented on glass slides. The calculated values of d and d_{pp} are vastly different at low hydrations. A possible explanation of the result is that the water contents of the oriented and liposomal bilayers are different at a given water activity. We show that this is not the case and conclude that the partial specific volumes of the lipid and water must be quite different in liposomal and oriented bilayers. The difference is attributable to the packing of the head groups. The head groups of egg lecithin in the oriented bilayers appear to occupy a volume of 695 \AA^3 at low hydrations compared to the value of 358 \AA^3 observed in liposomes. (Research supported by the N.S.F.)

W-PM-F5 MOLECULAR MODELING OF THE INTERACTION OF TREHALOSE WITH THE PHOSPHOLIPID BILAYER B. P. Gaber, I. Chandrasekhar and N. Pattiabiraman, Bio/Molecular Engineering Branch, Code 6190, Naval Research Laboratory, Washington, DC 20375-5000 and School of Pharmacy, University of California, San Francisco, CA 94143

Ample evidence now exists that stabilization of organisms against dehydration is, at least in part, a membrane phenomenon. In particular the interaction of the membrane with water and with small molecules, such as the disaccharide trehalose which appears to substitute for water, seems to be critical to our understanding of anhydrobiotic processes at a molecular level. Our approach to studying membrane/water/trehalose interactions uses computer modeling techniques to display accurate graphical representations of phospholipids and the bilayers formed from them. Crystallographic coordinates obtained from the literature have been used to construct a data base from which we have formed computer graphics realizations of the bilayer of dimyristoyl phosphatidylcholine (DMPC). The bilayer models may be displayed either as high-resolution space-filling images, or as skeletal models with van der Waal or solvent-accessible surfaces. The bilayer model includes the waters of crystallization. The location of these tightly bound solvent molecules provides a starting point for modeling a trehalose-bilayer interaction in which the sugar's hydroxyls are assumed to form hydrogen bonds replacing those of the solvent. A model for the trehalose-bilayer complex will be presented in which trehalose forms hydrogen bonds to the unesterified oxygens of the phosphodiester moiety of the type B conformer of DMPC. To accommodate the interaction of trehalose, the bilayer must be expanded slightly, an observation consistent with experimental findings.

W-PM-F6 X-RAY SCATTERING OF N-ACYL SPHINGOMYELIN VESICLES. DETERMINATION OF LIPID THICKNESS. P.R. Maulik, D. Atkinson and G.G. Shipley. Biophysics Institute, Boston University School of Medicine, Boston, MA 02118.

X-ray scattering data over the angular range $s=0.0015 - 0.1245 \text{ \AA}^{-1}$ were collected at $T > T_m$ from sonicated vesicles of a series of N-acyl sphingomyelins (SM) with chain lengths C-16, -18, -20, -22, and -24. Two scattering peaks were observed in each case, the positions of the maxima being dependent on the chain length of the sphingomyelin. The X-ray scattering data were buffer subtracted and corrected for Lorentz polarization. Fourier transformation of the corrected intensity data provides the Patterson function corresponding to the bilayer structure of the SM vesicle. A prominent peak in the Patterson function corresponds to the phosphate-phosphate distance (d_{pp}) across the bilayer, a measure of the bilayer thickness in the fluid chain state. For C-16 to C-24 SM, d_{pp} increases linearly from 36.5 to 47.5 Å. The linear plot of d_{pp} versus chain length gives an increment of 1.40 Å per CH_2 group and an intercept of 14 Å, the latter indicating a contribution of 7 Å per polar group to the bilayer thickness. The increment for the SM series, 1.40 Å per CH_2 group is significantly less than that observed for a series of phosphatidylcholines (PC) studied in a similar manner [B.A. Lewis and D. Engelman, *J. Mol. Biol.* (1983) 166, 211]. Since for the SM series only the N-acyl chain (and not the sphingosine chain) was varied, whereas both acyl chains were varied in the PC series, this difference in increment is expected.

W-PM-F7 THE KINETICS OF FORMATION AND STRUCTURE OF THE LOW TEMPERATURE PHASE OF 1-STEAROYL-LYSOPHOSPHATIDYLCHOLINE (18:0 LYSO PC). J. Mattai and G.G. Shipley. Biophysics Institute, Boston University School of Medicine, Boston, Massachusetts 02118.

A combination of differential scanning calorimetry (DSC) and x-ray diffraction have been used to study the kinetics of formation and structure of the low temperature phase of 18:0 lyso PC. For water contents >40%, DSC shows a sharp endothermic transition at 27°C ($\Delta H=6.75\text{Kcal/mol}$). This sharp transition is not reversible, but is regenerated in a time and temperature dependent manner. For example, with incubation at 0°C the maximum enthalpy ($\Delta H=6.75\text{Kcal/mol}$) is generated in ~45 minutes. The kinetics of formation of this low temperature phase is accelerated at much lower temperatures and may be related to the disruption of 18:0 lyso PC micelles by ice crystal formation.

For water contents >40%, x-ray diffraction patterns at 35°C show a diffuse 4.5Å reflection in the wide angle region, characteristic of melted hydrocarbon chains, and a single diffuse reflection in the low angle region indicating the presence of a micellar phase. X-ray diffraction patterns taken at 10°C over the hydration range, 20-80%, are characteristic of a lamellar bilayer gel phase with tilted hydrocarbon chains, with the bilayer repeat distance increasing from 47.6Å at 20% hydration to a maximum of 59.4Å at 40% hydration. Electron density profiles show a phosphate-phosphate distance of 30Å, indicating an interdigitated lamellar gel phase for 18:0 lyso PC at all hydration levels. For water contents >40%, this interdigitated lamellar phase switches to the micellar phase at 27°C in a kinetically fast process, while the reverse micellar-lamellar transition is a kinetically slower process (see also Wu, W., & Huang, C. (1983), *Biochemistry* 22, 5068).

W-PM-F8 EFFECTS OF ANESTHETIC ALCOHOLS ON PHOSPHATIDYLCHOLINE LIPOSOMES: IMPLICATIONS FOR THE MECHANISM OF THE PRETRANSITION. Timothy J. O'Leary, Philip D. Ross and Ira W. Levin, National Institutes of Health, Bethesda, MD 20892.

Previous studies have demonstrated that the clinical potencies of steroid anesthetics are correlated with their effects on the dipalmitoylphosphatidylcholine (DPPC) pretransition. To test the generality of this observation, we have studied the effects of the equipotent anesthetics, cis- and trans-9,10 tetradecenol on dimyristoylphosphatidylcholine (DMPC), dipalmitoylphosphatidylcholine (DPPC) and distearoylphosphatidylcholine (DSPC) multilayers using Raman spectroscopy and scanning calorimetry. Raman studies showed that these alcohols do not dramatically affect the structure of either gel or liquid crystalline phase at temperatures away from the gel to liquid crystalline phase transition. Calorimetric data demonstrate that the trans alcohol slightly lowers the midpoint (T_m) of the gel to liquid crystal phase transition, while the cis alcohol lowers it more dramatically. This difference is understood in terms of differences in the membrane void volume created when the alcohol is introduced into the bilayer. Both alcohols lower the pretransition temperature (T_p) for DMPC multilayers, and raise it for DSPC. Trans 9,10-tetradecenol raises T_p for DPPC multilayers, while cis-9,10-tetradecenol lowers T_p for this lipid. Both alcohols decrease the enthalpies of the pretransitions relative to those of the gel to liquid crystal transitions. These calorimetric results are interpreted in terms of a model for the pretransition in which unevenness of acyl chain termini within the bilayer center influences the relative stabilities of the gel and ripple phases.

W-PM-F9 MAGNETIC RESONANCE STUDIES OF THE EFFECTS OF RETINOIDS ON PHOSPHOLIPID MEMBRANES. Stephen R. Wassall* and William Stillwell†, Departments of Physics* and Biology†, Indiana University-Purdue University at Indianapolis, Indianapolis, IN 46223.

Retinoids (vitamin A and derivatives) - retinol (vitamin A), retinal (vitamin A aldehyde) and retinoic acid (vitamin A acid) - form a group of biologically important lipid soluble compounds which play an essential role in biological processes such as growth and vision. Their effects on phospholipid model membranes are of interest in understanding the interactions that occur in disk membranes where retinal, together with proteins and phospholipids, is a major component. Furthermore, the toxicity of retinoids at high concentration may be related to membrane disruption.

We have employed ESR of nitroxide spin labelled stearic acids incorporated at low concentration (1 mol%) into phospholipid bilayers and ^{13}C NMR of sonicated unilamellar phospholipid vesicles to observe the influence of up to 20 mol% retinoid. The data indicate that retinol and retinal affect the membrane interior in qualitatively similar manner, restricting acyl chain motion near the centre of the bilayer and having negligible effect towards the aqueous interface. Retinoic acid also restricts acyl chain motion approaching the centre of the bilayer but, in contrast to retinol and retinal, disorders the membrane in the upper portion of the chain. This difference in behaviour may be related to the greater increase in membrane permeability and larger reduction in temperature of the gel to liquid crystalline phase transition seen with retinoic acid.

W-PM-F10 FREQUENCY DEPENDENCE OF SPIN-LATTICE RELAXATION TIMES OF LIPID BILAYERS. Gerald D. Williams, Carl Trindle, Mohammad A. Khadim, Jeffrey F. Ellena, and Michael F. Brown. Department of Chemistry and Biophysics Program, University of Virginia, Charlottesville, VA 22901.

The measurement and interpretation of the nuclear spin-lattice (T_1) relaxation times of lipid bilayers have attracted much recent interest. Three classes of models which describe the influences of relatively slow fluctuations in the local bilayer ordering have been discussed. Such motions are referred to as order-director fluctuations (ODF). The first is a simple Lorentzian model, in which the slow motions fall into the long correlation time regime, leading to an ω_0 frequency dependence (1,2). In the second type of model, the director fluctuations are viewed as inherently long range in nature, resulting in an $\omega_0^{-1/2}$ dependence (1,3). Thirdly, Marqusee et al. (4) have proposed an interfacial collective model which predicts an ω_0 dependence. The presence of director fluctuations of significant amplitude in lipid bilayers has also been questioned (5,6). As a fourth alternative, Kimmich et al. (5) have suggested a one-dimensional kink diffusion model which predicts an ω_0 dependence in the MHz regime. The results of ^{13}C T_1 studies of phospholipid vesicles (7) will be discussed; an $\omega_0^{-1/2}$ dependence over an ω_0 or ω_0^{-1} dependence is favored. (1) M.F. Brown, *J. Chem. Phys.* **77**, 1576 (1982); *ibid* **80**, 2808 (1984). (2) N.O. Petersen and S.I. Chan, *Biochemistry* **16**, 2657 (1977). (3) R.J. Pace and S.I. Chan, *J. Chem. Phys.* **76**, 4228 (1982). (4) J.A. Marqusee et al., *J. Chem. Phys.* **81**, 6404 (1984). (5) R. Kimmich et al., *Chem. Phys. Lipids* **32**, 271 (1983). (6) D.W.R. Gruen, *J. Phys. Chem.* **89**, 146 (1985). (7) M.F. Brown et al., *PNAS* **80**, 4325 (1983). Work supported by NIH Grant EY03754, an NIH Postdoctoral Fellowship (J.F.E.), and by an RCDA from the NIH (M.F.B.). M.F.B. is an Alfred P. Sloan Research Fellow.

W-PM-F11 CONFORMATIONAL ANALYSIS OF PHOSPHATIDIC ACID-DIVALENT CATION COMPLEXES BY ^{31}P AND ^{13}C NMR. M.P. Murari and J.H. Prestegard, Department of Chemistry, Yale University, New Haven CT 06511

Membrane fusion induced by divalent cations binding to bilayers containing anionic phospholipids has stimulated considerable interest in the physical characterization of anionic phospholipid: divalent cation complexes. NMR spectra of spin $\frac{1}{2}$ nuclei in these strongly immobilized complexes frequently show chemical shift anisotropy (CSA) powder patterns that can be interpreted in terms of conformational preferences for the molecules. Accordingly, we have used ^{31}P and ^{13}C NMR to investigate the structural properties of phases formed as a result of Mg^{2+} and Ca^{2+} binding to dilaurylphosphatidic acid (DLPA). For the case of Mg^{2+} binding to DLPA, two distinct complexes, having the stoichiometries of 2:1 and 1:1 (PA: Mg^{2+}), can be formed depending on divalent ion concentration and other factors. For the 2:1 Mg complex, CSA powder patterns from acyl-chain carbonyls labeled specifically with ^{13}C in either both chains or only the 2 chain were combined with ^{31}P CSA powder patterns from the headgroup to fully characterize a previously proposed geometry for the complex. In the case of PA: Ca^{2+} complexes, phases are less well defined, with spectra showing considerable heterogeneity under most conditions. However, comparisons to the Mg^{2+} data suggest significant alterations of lipid geometry in response to the counter ion present.

W-PM-F12 ANIONS AFFECT ELECTROPHORETIC CHARGE REVERSAL OF CALCIUM BINDING TO PHOSPHATIDYL SERINE MEMBRANES. Joel A. Cohen, Dept. of Physiology, Univ. of the Pacific, San Francisco, CA.

Electrophoretic charge-reversal measurements provide fundamental information on the mechanisms of ion binding to charged membranes. A vesicle that is exactly neutralized by bound ions requires neither hydrodynamic analysis, since its electrophoretic mobility is zero, nor electrostatic analysis, since its net surface-charge density is zero. At charge neutrality the bare ion-binding isotherms of a phospholipid membrane are experimentally accessible, because (a) the (average) ion concentrations at the membrane/solution interface are known with certainty, and (b) the intrinsic plus adsorbed charge per phospholipid also is known with certainty. The aqueous concentration of Ca^{++} required to neutralize a phosphatidylserine membrane, $[\text{Ca}]_{\text{rev}}$, has been used in the past to determine the 1:1 Ca:PS intrinsic association constant, assuming (1) that Ca^{++} competes with monovalent cations for PS binding sites and (2) that anions do not affect $[\text{Ca}]_{\text{rev}}$. The binding constant then is $1/[\text{Ca}]_{\text{rev}}$. If the assumptions are correct, then $[\text{Ca}]_{\text{rev}}$ must be independent of monovalent cations and anions. $[\text{Ca}]_{\text{rev}}$ was measured in solutions of Na^+ and Cs^+ salts, at various concentrations, with Cl^- , NO_3^- , and Mops $^-$ anions. $[\text{Ca}]_{\text{rev}}$ was found to be an increasing function of monovalent salt concentration, to be weakly dependent on the monovalent-cation species, and to be sensitive to the anion species. The first effect is partially explainable in terms of ion pairing and ion activities in the aqueous phase. The last effect implies the existence of specific anion interactions with the membrane. The simple prescription for evaluating the Ca:PS association constant therefore requires modification. Analyses for the extraction of both anion and divalent-cation intrinsic association constants from charge-reversal data will be presented. (Supported by the Pacific Dental Research Foundation.)

W-PM-G1 FOLDING KINETICS OF BOVINE GROWTH HORMONE D. N. Brems and S. M. Plaisted, Control Research and Development, The Upjohn Company, Kalamazoo, MI 49001

Utilizing UV absorbance as a conformational probe and guanidine hydrochloride as a conformational perturbant, we have studied the unfolding and refolding kinetics of bovine growth hormone. At 11°C it is possible to observe all of the refolding reaction and 50% of the unfolding reaction by manual mixing experiments. Refolding occurs in two phases that are dependent on guanidine hydrochloride. The rate of the slower refolding phase is inversely dependent on protein concentration while the rate of the faster refolding reaction is independent of protein concentration. The observable unfolding reaction is protein concentration independent. Under identical final conditions, the refolding reaction is faster than the unfolding reaction. A model will be presented which accounts for the observed results.

W-PM-G2 THERMOSTABILITY OF THE SECONDARY STRUCTURE OF WILD TYPE AND MUTANT FORMS OF THE PHAGE P22 TAIL SPIKE PROTEIN. Betty Prescott⁺, Myeong-Hee Yu*, Jonathan King*, and George J. Thomas, Jr.⁺, ⁺Department of Chemistry, Southeastern Massachusetts University, No. Dartmouth, MA 02747 and *Department of Biology, M. I. T., Cambridge, MA 02139

The tail spike endorhamnosidase of the *S. typhimurium* phage P22 consists of a trimer of a 72-kD subunit (gp9) of known sequence which is extraordinarily thermostable.¹ Temperature-sensitive (ts) mutations in the gene for gp9 interfere with the folding and subunit association pathway at the restrictive temperature (40°C), but not with the activity or stability of the protein once matured at the permissive temperature. In order to understand the structural basis of the thermostability of the native protein, we have investigated the Raman spectra over the range 0 to 95°C of P22 tail spikes comprising mutant polypeptide chains for which the sites of point mutations were recently determined.² The results (i) confirm the high β -sheet content of wild-type gp9, (ii) demonstrate the equally high β -sheet content of several gp9 ts-folding mutants, (iii) indicate good agreement between experimental and predicted secondary structures for both wild-type and mutant subunits, (iv) indicate no major differences between wild-type and mutant chains in thermostability of secondary structure up to well above the restrictive temperature, and (v) reveal perturbations of secondary structure, as well as of specific side chain interactions, only at greatly elevated temperatures (>60°C). Supported by N. I. H. Grant AI11855.

1. Thomas, G. J., Jr. et al., *Biochemistry* (1982) 21, 3866-3878.
2. Yu, M.-H. & King, J., *Proc. Natl. Acad. Sci. USA* (1984) 81, 6584-6588.

W-PM-G3 THE X-RAY CRYSTAL STRUCTURE OF THE SWEET TASTING PROTEIN MONELLIN

Craig M. Ogata and Sung-Hou Kim, Department of Chemistry, University of Calif., Berkeley, CA 94720

Monellin belongs to the taste active class of proteins. The interest in this protein and the other sweet tasting protein, thaumatin¹, is in the search for common structural features. These structural features may serve as an active site region that interact with the surface of the tongue. The protein monellin is approximately 2000 times sweeter than sucrose when compared on a weight basis or 1×10^5 times on a molar basis. It consists of 94 amino acids in two different polypeptide chains. The conformation of these two polypeptide chains are important for its taste active ability. Monellin crystallizes at pH 7.2 with 4 molecules (8 polypeptide chains) in the asymmetric unit. The 4 molecules can be seen as 2 pairs of 2 molecules. There is a local dyad within each pair of molecules. Pairs of molecules were related by a screw-like axis consisting of a rotation of 160° and a translation of 29Å. These three local axes of symmetry and 5 isomorphous derivatives were used to make an electron density map. The resultant map revealed that the shorter, 44 amino acid chain, wraps around the 50 amino acid chain. The larger polypeptide chain consists entirely of $\frac{1}{2}$ long strands of β -sheet. Meanwhile, the shorter chain contains a stretch that forms a 5th strand of β -sheet, thus allowing strong hydrogen bonds between chains and a 4 turn α -helix that spans the 4 strands of the β -sheet.

¹de Vos, A.M., Hatada, M., van der Wel, H., Krabbendam, H., Peerdeman, A.F., and Kim, S.-H. *Proc. Natl. Acad. Sci. USA* 82, 1906-1409.

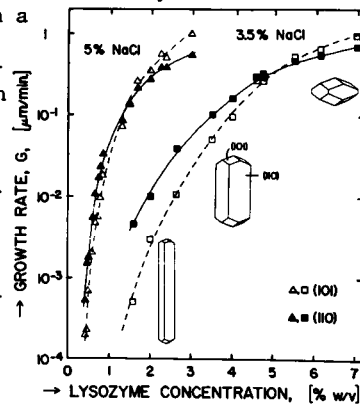
W-PM-G4 Effects of Amino Acid Substitution on the Folding of Tryptophan Synthase α -Subunit.

N. Tweedy and C.R. Matthews, Department of Chemistry, The Pennsylvania State University, University Park, PA. 16802.

The urea-induced folding of single amino acid substitution variants of *E. coli* tryptophan synthase α -subunit (E.C.4.2.1.20) has been studied to examine the role of specific residues in folding and to elucidate the folding pathway. Equilibrium studies show that the Gly 211 \rightarrow Arg 211 substitution decreases the stability of the native state and partially folded intermediates relative to completely unfolded forms. Kinetic studies reveal a novel pattern of relaxation times as urea concentration is varied. Simulation has been used to demonstrate that adjustment of the relative stability of intermediate species in the α -subunit folding model can account for this pattern. The first step in unfolding, $N \rightarrow I_2$, where I_2 is an intermediate species, is more than 10-fold faster for Arg 211. The Gly 211 \rightarrow Glu 211 mutant protein (Matthews et al. (1983) *Biochemistry* 22, 1445) shows stabilization of the protein and a 10-fold decrease in the $N \rightarrow I_2$ unfolding rate. Opposing effects from sidechains of opposite charge suggest that an electrostatic interaction near position 211 becomes important in the folding of the mutants. Mutations at other positions demonstrate less dramatic kinetic effects of substitution. These results will be discussed in terms of the utility of the mutants in probing the folding process.

W-PM-G5 STUDIES OF CRYSTAL GROWTH OF LYSOZYME AS A MODEL SYSTEM FOR PROTEIN CRYSTALLIZATION. S.D. Durbin and G. Feher, UCSD, La Jolla, CA 92093.*

The fundamentals of protein crystallization are poorly understood (1). In this study we focused on the post-nucleation growth of lysozyme. Growth rates were measured with a video camera attached to a microscope over a wide range of protein and salt concentrations. A flow system was used to eliminate protein depletion around the growing crystals. Comparison of the data (see Fig.) with theories of crystal growth (2) suggests that the growth cannot be explained by a single mechanism over the entire concentration range. At high supersaturation surface nucleation seems to predominate; at low concentration the observed rate is higher than predicted. In the latter regime, etch-revealed features correlating with variations of growth rate among equivalent faces indicate a defect-mediated growth mechanism. When crystals, grown for long times, were exposed to a highly supersaturated solution, new growth was observed only at isolated locations on the crystal surface. This phenomenon may be related to the cessation of growth problem (1). *Work supported by NIH.



Growth rate of tetragonal lysozyme crystals at 24°C, pH 4.6.

(1) For review, see G. Feher & Z. Kam (1985) *Methods in Enzymology*, vol. 114, chapter 4. Academic Press, N.Y.

(2) For review, see J.D. Weeks and G.H. Gilmer (1979) *Adv. Chem. Phys.* 40, 157.

W-PM-G6 GENETIC AND X-RAY STRUCTURAL ANALYSIS OF THE THERMAL STABILITY OF PHAGE T4 LYSOZYME Tom Alber, Sun Daopin, Keith Wilson, Jeffrey Bell, Joan Wozniak, Sean Cook and Brian W. Matthews, Institute of Molecular Biology, University of Oregon, Eugene, OR 97403

Bacteriophage T4 lysozyme provides an easily manipulated model system for understanding the contribution of specific non-covalent interactions to the thermal stability of proteins. Temperature sensitive (ts) and thermostable (st) mutants experimentally identify interactions that are essential for stability. Changes in stability can be correlated with differences in the X-ray crystal structures of the wild type and mutant proteins.

The best understood ts mutant is Thr 157 \rightarrow Ala. Using novel degenerate oligonucleotide primers, lysozymes with twelve different amino acids at position 157 — ser, gly, val, ile, leu, asn, asp, glu, arg, his, cys and phe — were constructed. The thermal stability of these mutants was measured, and the X-ray crystal structures of seven site-directed mutants were determined at high resolution. Comparisons with the wild type and Ala 157 mutant proteins lead to the following conclusions. 1) The methyl and hydroxyl groups of Thr 157 both contribute to stability. 2) The hydrogen bonds to the hydroxyl group are more important than the van der Waals contacts of the methyl group. 3) A bound water molecule stabilizes the protein by substituting for the Thr 157 hydroxyl in the Gly 157 mutant. 4) A new ion pair involving Arg 157 does not compensate for the loss of the hydrogen bonds to Thr 157. 5) Crystallographically observed hydrogen bonds make different contributions to protein stability. 6) Protein structures can readily adjust to changes in amino acid sequence.

W-PM-G7 TRYPTOPHAN INDOLE NH SOLVENT EXCHANGE IN WILD TYPE AND TEMPERATURE SENSITIVE MUTANTS OF BACTERIOPHAGE T4 LYSOZYME

L.P. McIntosh and F.W. Dahlquist, Inst. of Mol. Biol., Univ. of Oregon, Eugene, OR, 97403.

The roles that individual amino acids play in determining the structure and dynamics of a protein are not understood. A challenge is to establish how point mutations which alter the thermal stability of a protein influence its local and global fluctuations. To address this problem, we have measured the Trp indole NH solvent exchange kinetics of wild type and several temperature sensitive mutants of T4 lysozyme (T4L) by NMR as a function of temperature and pH*.

With WT T4L at 10°C and pH* 4.3, the H/D exchange rates of Trp126 and Trp158 (surface residues) are retarded by ca. 100 fold relative to free tryptophan, whereas the exchange of Trp138 (internal) is reduced by ca. 2000 fold. The exchange kinetics are consistent with an EX2 mechanism. The mutation Arg96→His reduces the thermal stability of T4L; however, identical Trp exchange rates with those of the wild type protein are observed from 10° to 30°C. In contrast, the destabilizing mutation Ala146→Thr enhances the exchange rate of Trp138 by 15 fold at 10°C and pH* 5.4 but does not alter the exchange kinetics of Trp126 or Trp158. Crystallographic studies (B.W. Matthews, *et al*) have shown that the Ala146→Thr mutation structurally perturbs only Trp138 and that the Arg96→His mutation does not alter the environment of any of the Trp residues in T4L.

These studies demonstrate that (i) the temperature sensitive mutation Ala146→Thr only locally perturbs the dynamics of the native conformation of T4L as measured by the H/D exchange of the proximal Trp138, and (ii) the influence of the two point mutations on the Trp indole solvent exchange correlate with the crystallographically observed structural changes.

W-PM-G8 CALCULATION OF HYDROGEN EXCHANGE RATES IN PROTEINS. Alexander A. Rashin, Department of Physiology and Biophysics, Mount Sinai School of Medicine, One Gustave L. Levy Place, New York, N.Y. 10029.

The recently developed method for calculation of protein stability based on measurements of the buried area [1] is applied to the "local unfolding" mechanism of hydrogen exchange in proteins. The free energy of local unfolding determines the differences in the exchange rates for surface amides and amides buried or hydrogen bonded in proteins. It is calculated as the difference between the stability of a protein structure with a short fragment (3 or 4 residues) unfolded to random coil, and the stability of the same protein in the native conformation. It is assumed that the proton of a particular amide exchanges when it becomes available for hydrogen bonding to water molecules due to such local unfolding. The hydrogen exchange rates calculated for individual amides of pancreatic trypsin inhibitor are in quantitative agreement with the experimental values [2], and reproduce the experimentally observed slower exchange in β-sheets compared to α-helices.

References.

1. A.A. Rashin, *Biopolymers*, 23, 1605-1620 (1984)
2. G. Wagner and K. Wuthrich, *J. Mol. Biol.*, 160, 343-361 (1982)

(Supported by a Fellowship from the Revson Foundation).

W-PM-G9 SIMPLIFICATIONS IN ANALYSIS OF LINKAGE SYSTEMS ARISING FROM THEIR ENTHALPY-ENTROPY COMPENSATION BEHAVIOR. Rufus Lumry, University of Minnesota, Minneapolis, MN 55455 and Roger Gregory, Kent State University, Kent, OH 44242.

The rapidly increasing number of reliable examples of "linear" enthalpy-entropy compensation behavior obtained from biological systems justifies investigation of the sources of the linearity since true linearity is possible only when compensation behavior rests on the second law. Most biological compensation behavior is due to weak, non-obligatory coupling of subprocesses of linkage systems trivial in origin but practically useful. In particular approximate linearity implies approximate underlying linear-free-energy relationships: $\Delta G^0_j = \Delta G^{00}_j + \sum p_i \Delta \Delta G^c_{ij}$ in which $\Delta G^0_j = -RT \ln K_j$; K_j is the equilibrium constant for any subprocess such as ligand binding which is directly measured; $\Delta \Delta G^c_{ij}$ is the total coupling free energy between sites i and j; and p_i is the probability of site i being in one of its macrostates not chosen as its reference state. This relationship occurs when subprocesses are indirectly coupled, that is, through one or more intervening subprocess, if $\Delta \Delta G^c_{ij}$ is sufficiently small. The observed near linearity of experimental compensation plots establishes that the weak-coupling approximation is frequently valid even with small experimental errors. This is fortunate since it greatly simplifies the analysis of linkage in complex systems. The next higher approximation is based on the Bragg-Williams mean-field. In the weak-coupling approximation it produces linkage equations of the same form. Its principal advantage lies in the fact that sets of identical sites can be treated as single sites with a mean linkage parameter so that detailed homotropic coupling, often the most difficult information to resolve, can be initially bypassed. Supported by NIH P0116833 and the Kent State Research Foundation.

- W-PM-G10 ASSOCIATION OF SLOW-EXCHANGING PROTONS WITH ENZYME FUNCTIONAL GROUPS. Roger B. Gregory, Kent State University, Kent, Ohio 44242 and Rufus Lumry, University of Minnesota, Minneapolis, Minnesota 55455.

Protein hydrogen-exchange rate distribution functions indicate the existence of several distinct classes of exchangeable protons (Gregory & Lumry, *Biopolymers*, 1985, 24, 301). The slowest exchanging protons are invariably located within regions of β -sheet and α -helix adjacent to non-polar groups. Their special exchange stability appears to be due entirely to cooperative electrostatic factors. Interactions of peptide dipoles, cooperative interactions among hydrogen bonds and between entire arrays of dipoles and adjacent non-polar groups are suggested to produce local regions ("knots") of very high strength and density. The list of proteins containing such regions includes lysozyme, ribonuclease A, BPTI, BUSI IIA and trypsin. Knots appear to serve an important role in controlling dynamic behavior critical for enzyme function. Among the enzymes studied so far knots are always found associated with catalytically essential residues. As rigid, cooperative domains, knots may enhance catalytic efficiency by reducing the number of fluctuating degrees of freedom that must be correlated for catalysis (Careri, 1982). Mechanically, knots can serve to limit local protein conformational relaxations and thus help to generate mechanical distortion within the substrate. Knots may also modify local electrostatic fields and through their very low local dielectric constant may enhance important charge and dipole interactions. Because of their great strength and H-bond cooperativity relatively large changes in electrostatic and conformational energy can be generated with only small adjustments in atomic coordinates. This feature of the knots provides interesting possibilities for coupling mechanical and electronic processes in enzyme mechanisms. Supported by NIH P0116833 and KSU Foundation.

- W-PM-G11 THE HYDROPHOBIC EFFECT AS A NONLINEAR COLLECTIVE PHENOMENON. Lyndon S. Hibbard, Departments of Radiology and Anesthesia, The M.S. Hershey Medical Center, The Pennsylvania State University, Hershey, Pennsylvania 17033 (Intr. by S. Goodman).

Protein structure formation is driven by the hydrophobic effect with free energy changes linear with respect to changes in side chain surface area measures like solvent accessibility (SA). To display the SA changes for all residues during folding, I devised a two-dimensional graph in which the value at each point (i,j) is the SA decrease of residue i due to each additional blocking residue j included in i's neighborhood. Though the total side chain SA lost on folding is path-invariant, the stepwise decreases in SA vary markedly depending on the order of the j's, suggesting that folding intermediates are strongly affected by the order in which specific i-j contacts are made. Further, contact graphs clearly subdivide into sets of features corresponding to specific secondary and tertiary interactions. Probing these contacts with interactive "unfolding" experiments using FRODO, I found that changes in SA with translation distance or bond dihedral angle were highly nonlinear. Model hard-sphere atom studies using Richmond's program ANAREA showed that SA changes for individual atom pairs are linear with respect to internuclear distance, but demonstrate collective nonlinear changes depending on the sizes and conformations of the opposing surfaces the atoms form. (Supported by NIH Grant R03 RR02274.)

- W-PM-G12 ROLE OF TOPOLOGICAL CONSTRAINTS IN THE HELIX-COIL TRANSITION OF TWO-CHAIN, COILED COILS. A MODEL FOR GLOBULAR PROTEINS. Jeffrey Skolnick, Department of Chemistry, Washington University, St. Louis, Missouri 63130

Employing a recently developed statistical mechanical theory of the helix-coil transition in two-chain, coiled coils (dimers), the effect of crosslinking on the stability of the native structure is examined and the helix-coil transition is shown to possess many of the essential qualitative features of the equilibrium globular protein folding process. By introducing single and double crosslinks into the dimer, we demonstrate how due to the influence of loop entropy an intrinsically continuous conformational transition evolves into one rather well approximated as an all-or-none type. In particular, due to the huge entropic cost engendered by the formation of constrained random coil loops, in singly crosslinked molecules, either the molecule lacks any interacting helices whatsoever or the pair of α -helical turns containing the crosslink is part of the interacting α -helical stretch. Introduction of a second crosslink is seen to further enhance the cooperativity of the transition. Either the molecule is fully helical and interacting between crosslinks or lacks any interacting helices. Thus, the present study points out the crucial role exerted by loop entropy on the conformational transition in coiled coils in particular and perhaps globular proteins in general. In the following paper, experimental data on the thermal denaturation profiles of the singly and doubly crosslinked coiled coil tropomyosin (tm) are presented and the theory is applied to a homopolymeric singly crosslinked analogue of tm to extract a molecular interpretation of the pretransition seen in singly crosslinked rabbit α -tropomyosin.

W-PM-G13 HELIX-COIL TRANSITION IN CROSSLINKED, TWO-CHAIN, COILED COILS. EXPERIMENTS ON AND A THEORETICAL MODEL FOR THE "PRE-TRANSITION". Jeffrey Skolnick and Alfred Holtzer, Department of Chemistry, Washington, University, St. Louis, MO 63130.

When α tropomyosin is disulfide crosslinked at C190, the thermal helix-coil transition becomes biphasic, the principal transition being shifted to higher T than in its noncrosslinked counterpart, but with the appearance of an additional transition ("pre-transition") at intermediate T. The latter has been ascribed to local destabilizing strains associated with steric effects of interchain disulfide formation. These strains are supposed to lead at intermediate T, to a conformation in which the coiled coil structure is intact except near C190 where a chain-separated "bubble" of random coil exists. To test this idea, a theoretical model of tropomyosin is developed which mimics the short- and long-range interactions in the actual protein. The theory includes loop entropy and out-of-register states. The latter turn out to be negligible. The calculations show that local destabilization near the crosslink does not produce a biphasic curve that mimics the experimental shape. Inhomogeneity in helix-helix interaction along the chain (which is known to exist) also does not yield experiment-like curves. The two in concert, however, do yield the required shape, i.e. they show a pre-transition. However, the nature of the pre-transition is not to form a "bubble", but rather to destroy the helix from the weakly-interacting end in to the crosslink. New experiments on doubly crosslinked (C190 and C36) $\beta\beta$ tropomyosin (by M. Holtzer, K. Askins and A. Holtzer) show that here there is no pre-transition. The doubly crosslinked molecules also are more stable than noncrosslinked counterparts and the transition is less steep. These results are discussed in terms of the entropy of the enormous loop that appears when the molecule unfolds between crosslinks.

W-PM-G14 INTERACTION OF CALMODULIN WITH CALMODULIN-BINDING PEPTIDES DERIVED FROM MYOSIN LIGHT CHAIN KINASE. Rachel E. Klevit, Donald K. Blumenthal, Harry Charbonneau, Koji Takio and Edwin G. Krebs. Howard Hughes Medical Institute and Departments of Chemistry, Biochemistry and Pharmacology, University of Washington, Seattle, WA 98195.

Synthetic peptides corresponding to the calmodulin-binding domain of myosin light chain kinase (MLCK) are useful models for studying the interaction of calmodulin (CaM) with this and other target enzymes. Peptides ranging in length from 17 to 40 residues bind CaM with high affinity ($K_D \sim 1$ nM) in a Ca^{2+} -dependent manner. Proton NMR and CD spectroscopy indicate that the MLCK peptides have little ordered structure when in free solution, but that they undergo major structural changes upon binding CaM. The data suggest that the peptides become α -helical when complexed to CaM and that they bind to CaM with high affinity in only one way. CaM also appears to undergo global conformational changes as the result of complex formation suggesting that these structural changes may be an important aspect of target enzyme activation. An MLCK peptide has been synthesized with an amino-terminal cysteine residue so that sulfhydryl-reactive probes can be coupled to the peptide. Carboxymethylation or attachment of the spin label, Iodoacetamido-PROXYL, to the N-terminal Cys had little effect on the affinity of the peptide for CaM, but coupling of the fluorescent probe, 1,5-I-AEDANS, reduced the affinity by a factor of more than 200. Presumably, the bulkiness of the AEDANS group prevents optimum interaction between the peptide and CaM. The spin-labelled peptide is being used to study the peptide-CaM complex and should be useful in mapping the position of the peptide on CaM and in determining the structure of the peptide and CaM in the complex.

W-Pos1 EXPRESSION OF AN EMBRYONIC FAST SKELETAL MUSCLE MHC mRNA DURING CHICK MUSCLE DEVELOPMENT.

R.R. Kulikowski*, R.M. Gubits*, and J. Robbins[†]. *Department of Anatomy, Mount Sinai School of Medicine, New York, NY 10029, and [†]Department of Pharmacology and Cell Biophysics, University of Cincinnati College of Medicine, Cincinnati, OH 45267.

The expressions of individual members of the myosin heavy chain multigene family appear to be restricted to a limited number of muscle tissues and developmental stages. In order to correlate the structure of a particular myosin heavy chain protein with the specific physiology of the muscle in which it is expressed, it is necessary to determine the structure and expression pattern of the individual myosin heavy chain genes. We have analyzed the expression of one of the MHC genes using the cDNA clone, pCM2, which represents the 3'-end of a MHC mRNA present in 13 d embryonic chick leg muscle. Northern blot analysis of embryonic cardiac RNAs at several stages of development showed hybridization of this probe to 2.5 d embryonic heart and 5.5 d embryonic atrium, as well as to the skeletal muscles examined. No significant hybridization to ventricular RNA was seen. Therefore, a series of S1 nuclease protection experiments was performed to determine more precisely the degree of homology of this probe to mRNAs expressed in cardiac and skeletal muscles at these stages of development. Our results indicate: (i) no sequence completely homologous to pCM2 is expressed in 2.5 d embryonic heart, 5.5 d embryonic atrium or ventricle, 5.5 d embryonic limb bud, adult red or white skeletal muscle, or adult atrium; (ii) MHC mRNAs with varying degrees of sequence homology to pCM2 are present at different abundance levels in 2.5 d heart, 5.5 d atrium, 5.5 d limb bud, and adult red and white skeletal muscles, but not in 5.5 d ventricle; and (iii) more than one MHC mRNA is detected in the embryonic and adult skeletal muscle. (Supported by USPHS HL30517 and HD13325.)

W-Pos2 IN VITRO MOVEMENT OF NONFILAMENTOUS MYOSIN AND HEAVY MEROMYOSIN (HMM). T.R. Hynes, S.M. Block, and J.A. Spudich (Intr. by C. Berlot). Department of Cell Biology, Stanford University School of Medicine, Stanford, CA 94305.

In previous work (Sheetz *et al.*, *J. Cell Biol.* 99:1867-1871, 1984), beads coated with skeletal myosin thick filaments were shown to move along actin bundles from *Nitella* at 2 to 5 μ /sec. We have now developed a variation of the assay in which a controlled number of individual myosin molecules are fixed with specific geometry to a bead surface. In this configuration, nonfilamentous chicken skeletal myosin, as well as preparations of rabbit 'long' HMM (tail \approx 600 Å) and 'short' HMM (tail \approx 400 Å) are capable of sustaining movement at speeds ranging from 0.5 to 2.5 μ /sec. Neither the light meromyosin (LMM) portion of myosin nor the ability to be organized into bipolar filaments are required. While it remains possible that small contaminating protein fractions are responsible for the movement of short HMM, it appears likely that force production is not dependent on the proteolytically-sensitive 'hinge region'. Myosins (or fragments) were linked through antibodies bound to protein A to the surface of formalin-fixed *Staph A* cells. Cells were washed in high salt to remove nonspecifically bound protein and to destabilize thick filaments. These cells moved smoothly along *Nitella* actin filaments in the presence of ATP. Movement was recorded on videotape and scored by a microcomputer. Protein components were quantified by SDS-PAGE. For myosin movement, a monoclonal antibody (a gift of S. Lowey) that recognizes the LMM portion of chicken skeletal myosin was used. For HMM movement, a polyclonal antibody (a gift of W. Harrington) for the S2 region of skeletal myosin was used.

W-Pos3 A NEW FLOURESCENT LABEL FOR SKELETAL MUSCLE HMM WHICH DOESN'T ALTER ITS ATPASE ACTIVITY
Marco Giordano, Reiji Takashi, and Toshio Ando. Cardiovascular Res. Inst., UCSF, San Francisco, CA 94143

Using a conjugate of a photoresistant flourophore, rhodamine, and 1,5-diaminopentane (cadaverine), together with transglutaminase we have been able to predominantly label the S2 region of heavy meromyosin. The rhodamine cadaverine conjugate was prepared by reacting lissamine rhodamine sulfonyl chloride with 1,5-diaminopentane in dry dimethyl formamide at 0°C under a nitrogen atmosphere. After completion of the reaction reverse phase HPLC was used to purify the rhodamine conjugate from the reaction mixture. Rhodamine cadaverine can be covalently attached to HMM with the use of transglutaminase. Transglutaminase, isolated from Guinea Pig liver, catalyzes a reaction in which -amide of glutamine residues is substitutes for a primary acyl amine. In the present case rhodamine cadaverine serves as the primary acyl amine. By comparing the electrophoretogram of labeled HMM and S1 we have been able to show that the transglutaminase-mediated-labeling occurs primarily in the S2 region of HMM. As a consequence of this fact the ATPase activity (which is localized in the S1 region) remains unaltered. This new labeling developed here enables us to optically observe the behavior of HMM that has an intact ATPase activity.

Supported by NIH Grant USPHS HL-16683

W-Pos4 X-RAY SCATTERING BY pPDM-CROSSLINKED MYOSIN SUBFRAGMENT 1 BEARING TRAPPED MgADP. D. B. Stone and R. A. Mendelson, Cardiovascular Research Institute and Department of Biochemistry and Biophysics, University of California, San Francisco, California 94143.

The existence of nucleotide-induced conformational changes in the cross-bridge or subfragment 1 (S1) portion of myosin is well documented. Because of their possible role in transduction it is important to define the magnitude and extent of the changes. MgADP was trapped at the active site of S1 by crosslinking two reactive thiols, SH1 and SH2, with the bifunctional thiol reagent N,N'-(p-phenylene)dimaldimide (pPDM) as described by Wells and Yount [PNAS 76, 4966 (1979)]. The pPDM-S1 had an average of 0.83 moles of ADP trapped per mole of pPDM-S1 and displayed an average of 3% of the K⁺(EDTA)-ATPase and 11% of the Ca⁺⁺-ATPase of control S1. Low-angle X-ray scattering by control S1 and pPDM-S1 yielded linear Guinier plots over the angular region 30-125 mr⁻². Comparison of the slopes of these plots indicated that the percent change in the radius of gyration (Rg) accompanying crosslinking and trapping of MgADP was -0.3 \pm 0.7%. We conclude that the trapping of MgADP at the active site of S1 is probably not accompanied by a gross deformation in S1 structure such as has been observed to accompany the binding of substrates to several kinases (where $\Delta Rg/Rg$ is -2.5 to -5%).

Supported by grants from NIH (HL-16683) and NSF (PCM-7922174).

W-Pos5 INTER-REGION UNION AND THE MYOSIN TRYPTOPHAN RESPONSE TO ATP. Andrzej A. Kasprzak, University of California, San Francisco, CVRI, San Francisco, CA 94143 (Intr. by J. Botts)

Dibromobimane, a bifunctional cross-linking reagent covalently joins the 20- and 50-kDa domains of myosin subfragment 1 (S1) [Mornet et. PNAS, 1985; 82, 1658]. This markedly reduces the fluorescence of the Trp residues and suppresses the MgATP-induced enhancement of the intrinsic protein fluorescence, suggesting that bound dibromobimane resides near the ATP-perturbable tryptophan. Alternatively, such effects could arise from a mechanical distortion of S1 tryptophan environments caused by the bulky dye. We have examined the modification with two non-chromophoric analogs of bimane, α -bromo- m -xylene and α, α' -dibromo- m -xylene. Both analogs are effective in reacting thiol groups of S1. Bifunctional dibromoxylene extensively crosslinks the 20- and 50-kDa fragments of S1. After the modification the fluorescence of S1 tryptophans remains unchanged, indicating that the large decrease in the Trp fluorescence of S1 Trp residues brought about by bimanes is probably due to resonance energy transfer from Trp to the dye. However, in the xylene-modified S1 the ATP-induced perturbation of Trp residues is reduced to approx. 15-20% of that for native protein. The suppression of the tryptophan response is not due to inability of the nucleotide to bind to the crosslinked protein. Nanosecond lifetime studies of bimane-labelled S1 have shown that Trp residues belonging to two lifetime classes (middle and long) are approx. 23 and 26 Å, respectively. (Supported by NSF PCM 8316007 and NIH HL-16683).

W-Pos6 ATTACHMENT OF MYOSIN CROSS-BRIDGES TO ACTIN IN THE PRESENCE OF AMPPNP. TRYPTIC DIGESTION STUDY OF MYOFIBRILS. T. Chen and E. Reisler, Department of Chemistry and Biochemistry, and the Molecular Biology Institute, University of California, Los Angeles, Los Angeles, CA 90024.

Myofibrils prepared from rabbit psoas muscle and frog sartorius muscle were digested with trypsin at a weight ratio of 1:250 under rigor and relaxed conditions and in the presence of MgAMPPNP. The relaxed state was achieved by incubating myofibrils with 3mM MgADP-V_i. The initial rates of tryptic cleavage of the myosin heavy chain were measured in these experiments and used to determine the fraction of myosin cross-bridges attached to actin in myofibrils in the presence of AMPPNP. At 24°C we detected between 10 to 15% cross-bridge dissociation by 3mM MgAMPPNP in both rabbit and frog muscle myofibrils. At 40°C, between 60 and 70% of rabbit muscle cross-bridges were dissociated by AMPPNP. Under the same conditions only about 20% of frog muscle cross-bridges were detached from actin. These results are consistent with the presence of an AMPPNP-induced cross-bridge conformation in frog muscle. This work was supported by grants from USPHS (AM 22031), NSF (PCM 8408507) and MDA postdoctoral fellowship.

W-Pos7 ACTO·pPDM S-1: AN ANALOG OF ACTO·S-1·ADP·P_i. D. Applegate and P. Flicker; Dept. of Chem. and Biochem., UCLA, L.A., CA.; Dept. of Cell Biol., Stanford Univ., Stanford, CA.

In order to form an analog of the A·M·ADP·P_i state, the carbodiimide crosslinked acto-S-1 complex was treated with pPDM. To eliminate competing reactions, Cys³⁷⁴ of actin was premodified. In the presence of MgATP, pPDM treatment results in inactivation of the MgATPase of the crosslinked complex, whereas in rigor little or no effect on the MgATPase is observed. The inactivation is accompanied by the incorporation of ¹⁴C-pPDM into the 20K peptide of S-1. Incubation of the crosslinked complex with monofunctional thiol reagents, IAEDANS or NEM, in the presence of MgATP does not inactivate the MgATPase activity. We conclude that treatment of the crosslinked complex with pPDM in the presence of MgATP results in bridging of SH₁ and SH₂, yielding the acto·pPDM S-1 complex. SH₁ and SH₂ are also bridged by pPDM in the presence of MgADP, but at a much slower rate and to a lesser extent than in the presence of MgATP. With uncrosslinked actin and S-1, with actin premodified, we observe no difference between the effects of ATP and ADP on the pPDM reaction with S-1. We suggest that in the crosslinked complex the pPDM reaction reflects differences between the A·S-1·ATP and A·S-1·ADP states. The appearance of the acto·pPDM S-1 complex observed by E.M. of negative stained or frozen hydrated unstained samples is very similar to negative stained images of crosslinked acto-S-1 in the presence of ATP (Craig, et al. (1985) PNAS USA 82, 3247). Crossbridges no longer assume the rigor 45° angle with the thin filament, but instead appear more disordered. Thus, the acto·pPDM S-1 structure may be a stable analog of the A·M·ADP·P_i state. Supported by grants from USPHS (AM 22031), NSF (PCM 8408507) and postdoctoral fellowships from A.H.A. to D.A. and from M.D.A. to P.F..

W-Pos8 PROTEOLYTIC RATE METHOD MEASURES THE BINDING OF MYOSIN TO ACTIN. A. Duong and E. Reisler, Department of Chemistry and Biochemistry, and the Molecular Biology Institute, University of California, Los Angeles, Los Angeles, CA 90024.

In order to validate the use of proteolytic rate method [Azarcon et al., *J. Biol. Chem.* 260, 6047 (1985)] in determinations of actomyosin binding in myofibrils we have carried out parallel measurements of acto-S-1 binding by airfuge centrifugation and by monitoring the initial rates of tryptic cleavage of S-1. Acto-S-1 binding was measured in the presence of 2 mM MgAMPPNP and 5 mM MgATP under different ionic strength conditions at 24°C. In the proteolytic rate approach the binding information was obtained by comparing the rates of tryptic cleavage of acto-S-1 in the presence of nucleotides with the rates of S-1 cleavage in acto-S-1 and free S-1. Trypsin to S-1 ratio was adjusted to permit proteolysis times of up to 10 minutes. Parallel MgATPase measurements monitored the consumption of ATP during these reactions. In general good agreement ($\pm 10\%$) was observed between acto-S-1 binding determinations made by airfuge centrifugation and proteolytic rate methods. This work was supported by grants from USPHS (AM 22031) and NSF (PCM 8408507).

W-Pos9 POLYMERIZATION OF G AND FITC LABELLED ACTIN BY MYOSIN SUBFRAGMENT 1. MgATPase OF THESE ACTO-S-1 COMPLEXES. Larry Miller and Emil Reisler, Dept. of Chemistry and Biochemistry and the Molecular Biology Institute. UCLA, Los Angeles, CA 90024.

Selective chemical modification at lysine 61 of rabbit skeletal actin by fluorescein isothiocyanate (FITC) has been shown to block the polymerization of G-actin by KCl and Mg^{2+} (Burtnick, L. *BBA* 791(1984) 57-62). We have studied the effect of myosin subfragment 1 (S-1) on the polymerization of such actin, as well as the ATPase properties of the FITC acto-S-1 system. Our results indicate that at stoichiometric acto-S-1 ratios, S-1 will induce the polymerization of FITC actin in G-actin buffer. Using light scattering and analytical ultracentrifuge techniques, we detect virtually no polymerization of FITC actin in G-actin buffer at low S-1/actin ratios which are normally used in ATPase assays. However, MgATPase assays run under the same conditions reveal that modified actin will activate S-1 ATPase to about 40-50% of the level of control actin. In order to evaluate these results, we have also studied the interaction of S-1 with native G-actin. We have observed differences in the time-dependent polymerization profiles between G-actin assembled by KCl and Mg^{2+} and that by S-1. S-1 causes rapid initial filament growth, unlike conventional polymerization patterns in which a slow nucleation step is thought to occur. We find that native actin incubated with S-1 for very short times (10-15 sec) can activate S-1 ATPase. Scattering data confirm that large actin filaments do not form during such short incubation times. Under similar conditions, we detect actin oligomers in the analytical ultracentrifuge. Supported by grants from USPHS (AM 22031), NSF (PCM 8408507), and a USPHS National Research Service Award (GM 07185).

W-Pos10 TWO PATHWAYS FOR OXYGEN EXCHANGE BY ACTO-HEAVY MEROMYOSIN. Kamal K. Shukla, Harvey M. Levy, Fausto Ramirez, James F. Marecek and Leonard A. Stein, Department of Physiology and Biophysics, School of Medicine, SUNY at Stony Brook, Stony Brook, N.Y. 11794.

Intermediate oxygen exchange has been measured for the MgATPase of heavy meromyosin (HMM) with actin at low ionic strength. Using $[\gamma\text{-}^{18}\text{O}]\text{MgATP}$ as substrate, the distribution of ^{18}O in the product P_i was determined by mass spectrometry. Computer analysis of the distributions, with no constraints on the kinetic variables, fits the data to a model with two pathways for hydrolysis. The extent of exchange, which occurs during reversible hydrolysis of enzyme-bound MgATP, is given by the ratio (R) of the rate of reverse-hydrolysis (k_{-3}) divided by the rate of the subsequent post-exchange reaction (k_4). From 1-100 μM actin, the apparent R (0.4-0.7) for a low exchange pathway (P1) was not significantly affected by the actin level. In contrast, the apparent R (20-2) for a high exchange pathway (P2) varied inversely with the actin level. Assuming that k_{-3} is the same for P1 and P2 and unaffected by actin, it appears that the post-exchange reaction, k_4 , differs markedly for the two pathways. For P1, k_4 appears fast and insensitive to actin at the levels tested. For P2, k_4 appears slow but markedly activated by actin. Thus the time available for exchange along P1 is always short, while the time available for exchange along P2 is relatively long but shortened to the degree that actin activates k_4 . The flux ratio for the production of P_i through P1 and P2 varied with the preparation of tryptic HMM but was usually between 30:70 (P1:P2) and 70:30. Significantly, this ratio appeared independent of the R values. It seems then that the overall flux is limited by a step in the reaction sequence other than the post-exchange step (k_4). These results with HMM add support to the suggestion that two pathways for hydrolysis are an intrinsic property of the actomyosin system. (Supported by NIH Grant AM 36701.)

W-Pos11 THE EFFECTS OF SPECIFIC ANTIBODIES AND NON-IMMUNE GLOBULINS ON THE ATPase ACTIVITY OF SMOOTH AND SKELETAL MUSCLE MYOSIN. K.D. Mazander, M. Weber and U. Gröschel-Stewart, Technische Hochschule, Darmstadt, West Germany and P.K. Ngai and M.P. Walsh, Department of Medical Biochemistry, University of Calgary, Alberta, Canada T2N 4N1.

We studied the effects of polyclonal antibodies to smooth and skeletal muscle contractile and regulatory proteins and non-immune globulins on the Ca^{2+} -ATPase and the actin-activated Mg^{2+} -ATPase of smooth and skeletal muscle myosins. All IgG fractions were rendered protease-free either by passage through DEAE-Affigel Blue or by heating to 56°C for 30-60 min. The Ca^{2+} -ATPases of both smooth and skeletal muscle myosin were only inhibited by their respective specific antibodies. The smooth muscle actin-activated myosin Mg^{2+} -ATPase was strongly inhibited by antibodies to myosin, tropomyosin, actin, myosin light chain kinase, as well as by the non-immune IgG. In contrast, smooth muscle myosin light chain phosphorylation was inhibited by antibodies to myosin and myosin light chain kinase, but not by anti-tropomyosin, anti-actin or non-immune IgG. On the other hand, the striated muscle actin-activated myosin Mg^{2+} -ATPase was stimulated by low concentrations of both specific antibodies and non-immune globulin and inhibited at higher concentrations. The stimulatory effect was only observed in the presence of tropomyosin. There was no measurable binding of immunoglobulins to either actin or actin/tropomyosin in cosedimentation experiments. The exact mechanism underlying the different effects of immunoglobulins on smooth and striated muscle actin-activated myosin Mg^{2+} -ATPases is not known. (Supported by Deutsche Forschungsgemeinschaft, MRC Canada and the Alberta Heritage Foundation for Medical Research).

W-Pos12 INTERMEDIATE $\text{Pi} \rightleftharpoons \text{HOH}$ EXCHANGE DURING ATP HYDROLYSIS BY ACTO-MYOSIN SUBFRAGMENT-1 (ACTO-S-1). John A. Evans and Evan Eisenberg, Laboratory of Cell Biology, NHLBI, NIH, Bethesda, MD 20892. (Intr. by Peter Lambooy).

The 6-state kinetic model we have proposed to account for the properties of the acto-S-1 ATPase activity predicts that ATP hydrolysis should be accompanied by considerable $\text{Pi} \rightleftharpoons \text{HOH}$ (^{18}O exchange) even when S-1 is completely bound to actin. However, Sleep and Boyer (Biochem. 17:5417) observed very little ^{18}O exchange at high actin concentration where S-1 is completely bound to actin. In the present study, we reinvestigated the effect of actin on ^{18}O exchange using both S-1 at high actin concentration and S-1 cross-linked to actin. First, we find that in all of our experiments the distribution of ^{18}O in the Pi fits a single pathway of ATP hydrolysis. Second, at very low ionic strength ($\mu=13$ mM), both with S-1 at high actin concentration and with S-1 cross-linked to actin, ^{18}O exchange is quite low (partition coefficient (P.C.) $\cong 0.15$). (P.C. varies from 0 at no exchange to 1.0 at complete exchange). Third, with cross-linked S-1 the P.C. increases markedly as the ionic strength is increased reaching a value of ~ 0.3 at $\mu=0.15$ M and ~ 0.4 at $\mu=0.5$ M. Interestingly, our measured P.C. value at $\mu=0.15$ M is nearly equal to the value observed for the dominant ATPase pathway in single rabbit muscle fibers in the isometric state (Hibberd et al., J.B.C. 260:3496). We conclude that fitting these data to the 6-state model requires that a process such as Pi rotation or H_2O accessibility rather than the back-rate of the ATP hydrolysis step determines the extent of ^{18}O exchange when S-1 is bound to actin. Second, it seems possible that the extent of ^{18}O exchange in crosslinked acto-S-1 and in single rabbit muscle fibers may be controlled by similar processes despite the very different ATP hydrolysis rate in these two systems.

W-Pos13 BINDING OF AMP-PNP TO RABBIT SKELETAL MYOFIBRILS. Jose A. Biosca, Lois E. Greene, and Evan Eisenberg, Laboratory of Cell Biology, NHLBI, NIH, Bethesda, MD 20892.

We previously studied the binding of AMP-PNP and P_i to acto-S-1 (Biophys. J. 97:308a) obtaining association constants of about $2-4 \times 10^2 \text{ M}^{-1}$ at 25 °C and $\mu=0.080$ M. We have now extended this binding study to rabbit skeletal myofibrils, directly measuring the amount of (^3H)-AMP-PNP bound at 25°, $\mu=0.12$ M using (^{14}C)-mannitol as a volume marker. With stretched myofibrils ($\sim 50\%$ out of overlap) the myosin cross-bridges bound AMP-PNP with two very different affinity constants. Forty percent of the myosin cross-bridges, presumably those out of overlap, bound AMP-PNP with a binding constant $> 5 \times 10^6 \text{ M}^{-1}$. The remaining myosin cross-bridges bound AMP-PNP very weakly; here the binding showed no evidence of leveling off even at 500 μM AMP-PNP. We also studied the binding of AMP-PNP to myofibrils in full overlap. Here only 6% of the cross-bridges bound AMP-PNP strongly. The remaining cross-bridges again bound AMP-PNP very weakly. Assuming a single population of cross-bridges and a binding stoichiometry of 1 mol of AMP-PNP per mol of myosin head, we could fit these data with a binding constant of about $1 \times 10^3 \text{ M}^{-1}$. At lower temperature and higher ionic strength (5°C, $\mu=0.17\text{M}$) the binding strength increased ~ 3 -fold, perhaps due to partial detachment of cross-bridges from actin. We conclude, first, that AMP-PNP binds to myosin cross-bridges out of overlap in myofibrils with the same affinity as to S-1 alone. Second, the binding of AMP-PNP to the actin-cross-bridge complex in myofibrils is almost as weak as to the acto-S-1 complex *in vitro*; this binding appears to be more than an order of magnitude weaker than the binding reported by Marston et al. (J. Mol. Biol. 104: 263) to rabbit skeletal muscle fibers at 8 °C, $\mu=0.1$ M, but agrees with the weak binding to myofibrils reported by Johnson (Biophys. J. 47: 62a).

W-Pos14 PHOSPHATE-WATER OXYGEN EXCHANGE PROBE OF Ca^{2+} -ACTIVATION OF ISOMETRIC CHEMICALLY SKINNED FIBERS FROM RABBIT SKELETAL MUSCLE. Martin R. Webb*, Mark G. Hibberd* and Yale E. Goldman* *National Institute for Medical Research, Mill Hill, London NW7 1AA, U.K. and †Department of Physiology, School of Medicine G4, University of Pennsylvania, Philadelphia, PA 19104. (Intr. by Robert J. Barsotti)

We have shown previously that isometric fiber-catalyzed ATP hydrolysis in (^{18}O)water is accompanied by oxygen exchange, so that the product P_i contains more than one oxygen from water. Relaxed fibers, in the absence of Ca^{2+} , show almost total exchange and Ca^{2+} -activated fibers show much less exchange, paralleling results obtained with subfragment 1 and actosubfragment 1 respectively. However, unlike isolated proteins, fibers consistently give distributions of ^{18}O in P_i that can be interpreted as two populations of P_i differing in extents of exchange, suggesting two mechanisms of hydrolysis. By varying the Ca^{2+} concentration to get different levels of fiber activation, we have followed the variation of the two pathways as the ATPase and tension increase. The ratio of the two populations varies only 2-fold while the k_{cat} increases 10-fold, showing both pathways are Ca^{2+} -activated. The population with low exchange varies from 35 to 65% of the total flux from no to full Ca^{2+} activation and its extent of exchange is almost independent of $[\text{Ca}^{2+}]$. The extent of exchange of the high exchange pathway decreases linearly with increasing k_{cat} for that pathway. The origin of the low exchange pathway is being investigated, but the higher exchange pathway probably represents ATP hydrolysis with Ca^{2+} modulating the breakdown of the $\text{ADP}\cdot\text{P}_i$ complex and so controlling both ATPase and exchange at the same point in the reaction. (Supported by NIH grant HL15835 to the Penn. Musc. Inst. and by the MRC, U.K.)

W-Pos15 EFFECT OF TRYPTIC CLEAVAGE OF S-1 ON THE RELATIVE ENERGIES OF THE APPARENT TWO STATES OF MYOSIN. Utpala Kamath and John W. Shriver. Department of Medical Biochemistry, School of Medicine; and Department of Chemistry and Biochemistry, College of Science; Southern Illinois University, Carbondale, Illinois 62901.

We have previously shown by NMR and UV difference spectroscopy that myosin S-1 experiences a non-denaturational, structural transition in the region of 0 to 30°C. The equilibrium data can be fit assuming a simple two-state transition. The midpoint of the transition is dependent on pH, ionic strength, and the form of the nucleotide bound. We present evidence here which demonstrates that the intactness of the heavy chain also affects the energetics of this transition. Trypsin hydrolysis of S-1 yields a functional S-1 which has been nicked at two locations to yield three fragments which remain associated (Balint et al. Arch. Biochem. Biophys. 190, 793 (1978)). AMPPNP induced UV difference spectra of tryptic S-1 show no structural change between 5° and 15°C with a slight change at 20°C. In contrast chymotryptic S-1 exhibits a significant change over this range. The tryptic S-1 data imply that cleavage of the heavy chain by trypsin increases the midpoint of the transition between the two apparent states of S-1.AMPPNP. Similarly, the region of SH_1 is also affected as indicated by the ^{19}F NMR spectra of an ^{19}F probe attached there. There is only a gradual increase in chemical shift with decreasing temperature with tryptic S-1. Chymotryptic S-1 shows a marked change over this temperature range, with a midpoint at 11°C. Thus nicking also affects the energetics of the free S-1. (Supported by the Muscular Dystrophy Association of America).

W-Pos16 COOPERATIVE DOMAIN STRUCTURE IN MYOSIN S-1 STUDIED BY DIFFERENTIAL SCANNING CALORIMETRY. John W. Shriver and Utpala Kamath, Department of Medical Biochemistry, School of Medicine, and Department of Chemistry and Biochemistry, College of Science; Southern Illinois University, Carbondale, Illinois 62901

We have initiated a differential scanning calorimetric (DSC) study of myosin S-1 structural transitions. We report here preliminary DSC results for denaturation of chymotryptic and tryptic rabbit skeletal S-1 in an attempt to delineate and characterize independent, cooperative units (domains) within S-1. The data were collected on a Microcal MC-2 at a scan rate of 60 °C/hour. The denaturation profile of both preparations shows a prominent endothermic peak at pH 8 at 48°C. An exothermic transition occurs at higher temperature and is assigned to protein aggregation. The shape of the endothermic peak does not indicate denaturation of a single domain, although this may be due to irreversibility. Upon mild oxidation of chymotryptic and tryptic S-1 two peaks are seen. The calorimetric heat of denaturation, ΔH° , for the first transition is roughly 90 kcal/mole. The van't Hoff heat of denaturation, ΔH_{vh} , is of comparable magnitude, so that the first transition probably represents the denaturation of a single cooperative domain. There is a significant difference between ΔH° and ΔH_{vh} for the second transition for tryptic S-1 which may indicate that the second transition represents the denaturation of at least two domains. The assignment of the denaturation of the associated alkali light chains to the observed transitions is in progress. (Supported by the Muscular Dystrophy Association).

W-Pos17 STUDIES IN THE COMPLEX S_1 -ADP-VANADATE USING FLUORESCENT PROBES. Raul Aguirre, Frances Gonsoulin and Herbert C. Cheung. Department of Biochemistry, University of Alabama at Birmingham, Birmingham, AL 35294

Myosin-ADP-Vi is believed to be a stable analog of the myosin-ADP-Pi intermediate. Based on observations of inhibition of ATPase activity it has been proposed that upon formation the ternary complex myosin-ADP-Vi undergoes a slow transition that stabilizes both bound ligands. We have examined this slow conformational change in isolated myosin heads (S_1) by following (a) changes in the fluorescence intensity of two fluorophores covalently attached to S_1 via SH₁ and (b) the quenching of the emission of ϵ ADP bound to S_1 by Co^{2+} . The fluorescence of 5-(iodoacetamide) fluorescein attached to S_1 increases upon addition of Vi to S_1 -ADP probably because internal quenching of the attached fluorophore is reduced. On the other hand, the fluorescence of S_1 modified by 5-iodoacetamidosalicylic acid decreases when the stable ternary complex is formed presumably due to an increased quenching of the fluorophore. With either modified S_1 , the slow fluorescence transition is characterized by rate constant of about $10^{-2}s^{-1}$ at 20°C in agreement with the rate of conformational change deduced from studies in enzymatic inhibition by Vi (Goodno, C.C., Proc. Natl. Acad. Sci. USA (1979) 76, 2620). The stabilization of the ternary complex S_1 - ϵ ADP-Vi produces a dramatic increase in the quenching of ϵ ADP fluorescence by Co^{2+} when compared with S_1 - ϵ ADP. This quenching is static as shown by lifetime measurements, suggesting that Co^{2+} forms a complex with ϵ ADP in the protein. (Supported in part by NIH AM 31239)

W-Pos18 Ca^{2+} -BINDING AND FLUORESCENCE MEASUREMENTS OF REGULATED COMPLEXES OF ACTIN WITH TnC_{DANZ}. Henry G. Zot and James D. Potter, Department of Pharmacology, University of Miami School of Medicine, Miami, Florida 33101.

The equilibrium binding of Ca^{2+} to two regulatory complexes was carried out at 25°C in the presence of 0.345 mM EDTA and no added Mg^{2+} (low Mg^{2+}) and at 2.0 mM Mg^{2+} . Both complexes were composed of actin, tropomyosin, and troponin (Tn) which was reconstituted from the Tn subunits TnT, TnI, and TnC or the fluorescent analogue TnC_{DANZ}. The binding to the two complexes, i.e. unlabeled (regulated actin) and labeled (regulated actin*) was measured by a centrifugation assay. The stoichiometry of binding and binding constants were determined for two classes of sites by interactive least squares Scatchard analysis. In comparing the regulated actin with regulated actin* there appears to be about a 30% decrease in affinity at the high affinity sites and the low affinity sites in 2 mM Mg^{2+} and about a 40% decrease in affinity at the low affinity sites and little difference at the high affinity sites in low Mg^{2+} . The Ca^{2+} -dependent fluorescence change of regulated actin* was also determined at the two [Mg^{2+}] and the midpoints of the titrations do not match the binding constants of either class of sites at either [Mg^{2+}]. The fluorescence midpoints correlate most closely with Ca^{2+} binding to low affinity sites with values greater than the binding constants for the low affinity sites at the two different [Mg^{2+}]. These results indicate that the fluorescent probe only slightly alters the affinity of TnC for Ca^{2+} at the low affinity sites in 2 mM Mg^{2+} , the TnC_{DANZ} fluorescence change is associated with Ca^{2+} binding at the low affinity sites in regulated actin, and the fluorescence change appears to be due, at least in part, to the binding of Ca^{2+} to either low affinity site. Supported by HL22619.

W-Pos19 HYDROGEN EXCHANGE AND TRANSIENT KINETIC ANALYSIS OF ATP HYDROLYSIS BY CARDIAC MYOSIN S1. J.H. Hazzard and M.A. Cusanovich, Dept. of Biochemistry, Univ. of Arizona, Tucson, AZ 85721.

The transient kinetics of ATP binding and hydrolysis by cardiac myosin subfragment 1 (S1) previously measured over a range of solvent parameters by fluorescence stopped-flow (Biophys. J. 47, 309a) have been analyzed using a consecutive, reversible three-step first-order mechanism. Values for the individual kinetic constants determined from this analysis demonstrate that the commonly used methods of graphical analysis overestimate the values for the binding and hydrolysis rate constants. The kinetic constants determined from the computer modeling procedure exhibit a pK of 7, consistent with the presence of one or more histidine residues in the active site. The initial ATP binding process is electrostatic in nature (active site charge = +1.5). The slower cleavage step which follows is driven thermodynamically by a large increase in entropy ($\Delta S^\circ = 183 J/^\circ K \text{ mol}$ at 15°C). To investigate the extent of protein conformational changes upon ATP hydrolysis the hydrogen-deuterium exchange profiles of S1 have been measured at 4°C by infrared spectroscopy both in the presence and absence of ADP-vanadate, which forms a stable complex with S1. The overall exchange rate with ADP-Vn is app. 7-fold greater than with S1 alone, indicating a significant difference in protein conformation which may contribute to the large increase in entropy observed upon hydrolysis. The infrared results are compared with similar measurements using hydrogen-tritium exchange techniques. Supported by NIH Grant HL28906 to M.A.C. and NIH postdoctoral fellowship and a Grant-in-Aid from the American Heart Association, Arizona Affiliate, to J.H.H.

W-Pos20 INTERACTIONS OF CARDIAC S1 WITH ACTIN

S.S. Margossian, A. Malhotra, J.W. Krueger, and W.F. Stafford, III, Albert Einstein College of Medicine and Montefiore Medical Center, Bronx, NY 10467 and Boston Biomedical Research Institute Boston, MA 02114.

The actin-activated ATPase of rat heart myosin is several fold higher than that of dog or rabbit heart myosins, reflecting the predominance of the V_1 isoform in the former. The difference in activity is maintained in the respective S1's. To explain the reason for this, binding of S1 from rat and dog heart myosins to actin was investigated. In these assays, increasing amounts of S1 were mixed with a constant amount of F-actin in 0.1 M KCl, 0.01 M imidazole (pH 7.0), 5 mM potassium phosphate, 1 mM $MgCl_2$, 0.3 mM EGTA and 1 mM DTT. The mixture was spun at 20° and at 40,000 rpm in a Model E analytical ultracentrifuge to sediment the acto-S1 complex and the concentration of free, unbound S1 determined from UV-traces scanned at 236 nm and 280 nm. S1's prepared by either α -chymotryptic digestion or papain digestion in the presence of $MgCl_2$ to preserve LC2, were analyzed by high speed equilibrium ultracentrifugation and the monomer molecular weight of S1 was calculated to be 94 KDa. Binding of such preparations gave a stoichiometry of association of one mole of S1 per mole of F-actin monomer with a K_a of $4 \times 10^6 M^{-1}$. No appreciable difference in association constant for rat or dog heart S1 could be detected. However, the V_{max} for rat heart S1 was significantly greater than that of dog heart S1. The presence of LC2 in papain S1 did not influence either the actin-binding affinity or the rate of ATP hydrolysis (Supported by NIH Grant HL 26569).

W-Pos21 PROPERTIES OF CARDIAC DOG AND RAT α -ACTININ. Ashwani Malhotra, Sarkis S. Margossian, Irving Listowsky and Henry S. Slayter. Depts. of Biochemistry, Medicine; Montefiore Medical Center, Albert Einstein College of Medicine, Bronx, NY 10467 and Dana Farber Cancer Institute, Boston, Mass. 02115.

A possible biochemical role was studied for the myocardial Z-line protein, α -actinin which was isolated and purified to electrophoretic purity by ion-exchange chromatography. Sedimentation velocity runs revealed a single boundary sedimenting with a $S_{20,w}$ of 6S. High speed equilibrium centrifugation using the model E analytical ultracentrifuge with a photoelectric UV scanner showed a single monodisperse component with a molecular weight of 195 KDa and 165 KDa for dog and rat heart α -actinin respectively. The difference in size was further corroborated by electron microscopic studies of tungston-shadowed preparations which appeared to be rod-like structures with a length of 480Å (dog) and 430Å (rat) for cardiac α -actinin. The α -helical content calculated from circular dichroism spectra was 72% and 63% for dog and rat heart α -actinins. Maximal activation (2-3 fold) of actomyosin ATPase was obtained by 0.35 - 0.40 μM of rat or dog cardiac α -actinin added and when the V_{max} of actin-activated ATPase of either dog or rat heart myosin was calculated in the presence of α -actinin, it was over two fold higher than the V_{max} obtained in its absence. The extent of actin-activation was reduced in the presence of increasing concentrations of KCl, but at the highest KCl (100 mM) concentration used, activation was about 50%. Although there is a clear difference in the size of rat and dog heart α -actinin, they appear to have similar activating effects on actomyosin ATPase. (Supported in part by NIH Grants HL-18824 James Scheuer and HL 26569 to Sarkis S. Margossian.

W-Pos22 ISOLATION OF A FACTOR THAT MODULATES THE CONTRACTILITY OF RAT HEART. L.-E. Lin and S. Winegrad, Department of Physiology, University of Pennsylvania, PA 19104

Treatment of hyperpermeable rat ventricular cells with cAMP, theophylline and 1% Triton X-100 increases maximum Ca-activated force (contractility) by about 150%. Sarcolemmal perforation can be produced by either perfusion of heart or soaking bundles in a solution containing 10mM EGTA or 0 ATP. The ability of cAMP to enhance force generation is lost when the intact heart is perfused through the coronary circulation with 10mM EGTA solution, but is retained in perforated cells produced by soaking in 10mM EGTA solution. When the heart is perfused with a small volume of 10mM EGTA recirculated solution, the cAMP regulatory system appears in the perfusate. When perforated bundles produced by soaking were immersed in perfusate overnight, subsequent exposure to 1% detergent in relaxing solution increased contractility by 195%. In control bundles, detergent increased contractility by only 35% and 1 μM cAMP, 5mM theophylline and detergent increased contractility by 91%. Ultrafiltration (10 or 15K dalton cut-off) did not alter the effect of the perfusate on contractility. Treating the perfusate with detergent for 10 mins. followed by SM-2 beads to remove detergent and ultrafiltration increased contractility by 250% without need for further detergent treatment. After gel filtration through a G75-40 column, all of the activity appeared in one peak. SDS electrophoresis of the solution in the peak produced one major band at about 21K daltons. The conclusions are: cAMP releases a factor that increases contractility; this factor is both membrane bound and has a high affinity for myofibrils. Its molecular weight is about 20K daltons. (Supported by NIH grant HL 16010)

W-Pos23 SEPARATION OF RAT CARDIAC MYOSIN ALPHA AND BETA HEAVY CHAINS ON SDS POLYACRYLAMIDE GELS. Gary G. Giulian, Cynthia Lord*, James M. Graham and Richard L. Moss, Department of Physiology, University of Wisconsin, Madison, WI 53706 and Department of Physiology & Biophysics*, University of Vermont, Burlington, VT 05405.

Rat cardiac myosin separates on pyrophosphate non-dissociating (Hoh, *et al.*, J. Mol. Cell Cardiol. 10, 1053-1076, 1978) gels to yield three major isoforms: V1, V2 and V3. The isoforms have been shown by ATPase activity, peptide mapping and immunological analysis to differ based on myosin heavy chain content. Myosin isoform V1 is thought to contain 2 alpha heavy chains; V2, 1 alpha and 1 beta heavy chain; and V3, 2 beta heavy chains. Using a high resolution SDS polyacrylamide gel system and a silver stain technique we have been able to separate rat cardiac myosin alpha and beta chains. The silver stain method is necessary in order to allow small sample size and assure resolution of the closely spaced alpha and beta bands. Interestingly, the beta heavy chain component of V3 has a greater electrophoretic mobility than the alpha heavy chain component of V1. This migration pattern is unexpected based on previous results found on pyrophosphate gels, in which V1 mobility is greater than V3. SDS gels were run using crude cardiac homogenates which were previously shown on Hoh gels to be predominately V1 or V3, or to contain V2. Quantitation of alpha and beta chain content agreed well with the isozyme content determined from the Hoh gels, and is consistent with the idea that the content of alpha and beta chains in V2 is equimolar. Picogram sensitivity in this SDS gel and staining system allows for the separation of myosin bands which heretofore have comigrated on SDS gels and has allowed for the quantitation of myosin heavy chains from single cardiac myocytes. (Supported by grants from NIH and the American Heart Association).

W-Pos24 CYCLING AND RIGOR CROSSBRIDGES ALTER THE STRUCTURE OF TnC IN THIN FILAMENTS. Anita S. Zot and J.D. Potter, Dept. of Pharmacology, Univ. of Miami School of Medicine, Miami, FL. Previous work by Bremel and Weber (Nature New Biol. 238:97, 1972) has shown that the attachment of rigor crossbridges increases the Ca^{2+} -affinity of troponin in myofibrils and thin filaments. In order to investigate if changes in troponin structure also occur due to rigor crossbridge attachment, we looked at the fluorescence response of dansylaziridine-labeled skeletal TnC, incorporated into reconstituted thin filaments (regulated actin), when rigor crossbridges formed. A 10% increase in fluorescence was observed when a saturating amount of HMM was added to regulated actin in the absence of ATP and Ca^{2+} . This result suggests that the attachment of rigor crossbridges changes the structure of TnC, probably in the N-terminal region, which could account for the increased Ca^{2+} -affinity produced by rigor crossbridges. When saturating Ca^{2+} was added to regulated actin with rigor crossbridges, an additional 10% fluorescence increase occurred, i.e. 20% over baseline, indicating a further conformational change due to Ca^{2+} -binding. Since Ca^{2+} -binding to TnC in the absence of HMM produced a 40% increase in fluorescence, this conformation of TnC must be different from either that produced by rigor crossbridges or that produced by Ca^{2+} -binding to TnC under rigor conditions. When MgATP was added to regulated acto-HMM in the presence of Ca^{2+} , a fluorescence level which is 30% above baseline resulted; we propose that this represents a mixture of TnC conformations that would be present in the contracting muscle. These fluorescence levels, or conformational states, are reversible and can be reached by different pathways; a model relating these states has been developed. Supported by NIH HL 22619-3A and a grant from the Lucille P. Markey Charitable Trust, Miami, Florida.

W-Pos25 THE EFFECTS OF ADP AND TROPOMYOSIN ON THE S-1-INDUCED ACTIN BUNDLING. Toshio ANDO Cardiovascular Res. Inst., UCSF, San Francisco, CA 94143

Rabbit skeletal myosin S-1 assembles actin filaments into bundles under physiological conditions (T. Ando & D. Scales, 1985, J. Biol. Chem. 260, 2321). The bundle formation results in an increase in light scattering (we call it "super-opalescence") of the acto-S-1 solutions. The rate of the initial process of bundle formation (i.e., side-by-side dimerization) can be estimated by measuring the initial rate of super-opalescence (V_0). V_0 has a maximum at a molar ratio of S-1 to actin of 1/6-1/7. We report here how V_0 is affected by ADP binding to S-1 and tropomyosin (TM) binding to F-actin. V_0 decreased nearly to zero (but never completely zero) with increasing ADP concentration. V_0 decreased by half at ca. 30 μ M ADP. When e-ADP was used instead of ADP, V_0 decreased by half at ca. 270 μ M e-ADP. Since these numbers are similar to the respective dissociation constants for acto-S-1, we can conclude that the acto-S-1-bound nucleotides reduced V_0 . An optimum S-1/actin remained constant (i.e., 1/6-1/7) regardless of the nucleotide concentration. On the other hand, when ADP was added to an acto-S-1 solution which had been showing super-opalescence, the light scattering intensity stayed at the same level as observed before adding ADP. It suggests that ADP binding does not disassemble actin bundles. V_0 sharply decreased to zero with increasing TM concentration. Only ca. 0.005 of TM/actin molar ratio was sufficient for reducing V_0 by half (this small number corresponds to two TM molecules per a 1 μ m long actin filament). While TM had such a strong inhibitory effect on actin bundling, TM could not disassemble actin bundles which had been formed before adding TM.

W-Pos26 INTRINSICALLY COOPERATIVE ACTIVATION OF THE RECONSTITUTED CARDIAC THIN FILAMENT AND THE ROLE OF TROPONIN T ISOFORMS. L.S. Tobacman, NHLBI, Bethesda, Md. 20892

The MgATPase rate of cardiac myosin S-1 was studied in the presence of regulated actin in order to investigate the mechanism by which Ca^{2+} cooperatively induces muscle contraction. The MgATPase rate increased cooperatively with Ca^{2+} , exhibiting a Hill coefficient of 1.8 and 50% activation at pCa 5.7. This cooperative response occurred despite an experimental design excluding three potential sources of cooperativity. First, to exclude spurious cooperativity due to erroneous calculation of pCa at low ionic strength, the affinities of EGTA for Mg^{2+} and Ca^{2+} were measured by a novel method using quin2. At pH 7.06, 25°C, and $u = 30$ mM, the K_{app} was 140 nM for EGTA- Ca^{2+} and 2.7 mM for EGTA- Mg^{2+} . Second, the cooperativity was not produced by actin-myosin S-1 binding: myosin S-1 was bound to only 1 of every 300 actin protomers and our earlier work has shown that cardiac myosin S-1 binds equally tightly to the thin filament at very low Ca^{2+} and at saturating Ca^{2+} . Finally, since cardiac troponin has only 1 regulatory Ca^{2+} -binding site, cooperative interactions between such sites did not occur. Also under study are the 2 major bovine cardiac troponin T isoforms, which differ near the amino terminus (Risnik, *et al.* *Biochem.J.* 225:549-552, 1985). Holo-troponin isoforms containing the larger T_nT_1 or the smaller T_nT_2 were separated by DEAE cellulose chromatography. Both troponin isoforms induced identical 30-fold Ca^{2+} sensitivity to the MgATPase rate of myosin S-1-actin-tropomyosin. However, substituting T_nT_2 for T_nT_1 produced a leftward shift in the Ca^{2+} activation curve. These results imply that the variable structure of troponin T near its amino terminus influences the response of the thin filament to Ca^{2+} , and that this response is intrinsically cooperative, presumably due to the interaction between adjoining troponin-tropomyosin complexes.

W-Pos27 INDUCTION OF NONPOLYMERIZABLE TROPOMYOSIN BINDING TO F-ACTIN BY TROPONIN AND ITS COMPONENTS AT LOW IONIC STRENGTH. D.H. Heeley and L.B. Smillie, MRC Group in Protein Structure and Function, Department of Biochemistry, University of Alberta, Edmonton, Canada T6G 2H7.

Removal of 11 residues from the C-terminus of rabbit cardiac $\alpha\alpha$ tropomyosin (TM) yields a non-polymerizable form of TM (designated NPTM), whose binding to F-actin has been markedly reduced at both physiological salt concentrations (0.1-0.15 M KCl) and at lower salt concentrations (0.01-0.05 M KCl). Previous work (J. Biol. Chem. (1983) 258, 14330) carried out in 0.15 M KCl has demonstrated the induction of NPTM binding to F-actin by troponin ($-\text{Ca}^{2+}$), TNI and TNT. By reducing the ionic strength to 0.01-0.05 M KCl, this binding can be made stoichiometric permitting the estimation of binding constants and cooperativity. These studies have demonstrated that troponin induced binding ($\pm\text{Ca}^{2+}$) retains a considerable degree of cooperativity. This cooperativity could arise either from the transmission of conformational changes through F-actin or by bridging the gaps between the N- and C-termini of NPTM by the TNT component of troponin or both.

To further investigate this question, the induction of NPTM binding by the troponin components and fragments thereof in various combinations is being tested under $\pm\text{Ca}^{2+}$ conditions. The failure of fragment T1 (residues 1-158) of TNT to promote NPTM binding suggests that at least part of this cooperativity is through the F-actin filament. However, T1 is observed to promote the binding of NPTM by TNI. This suggests either a direct interaction between TNI and T1 or an interdependence of the binding of these two components at separate sites on the NPTM molecule, such that TNI binding to NPTM leads to an increase in the strength of binding of T1, which in turn, further induces the interaction between NPTM and F-actin. (Supported by Alberta Heritage Foundation for Medical Research and MRC of Canada)

W-Pos28 THE KINETICS OF MYOSIN SUBFRAGMENT 1 INTERACTIONS WITH RECONSTITUTED THIN FILAMENTS. Michael A. Geeves & David J. Halsall Intr. by H. Gutfreund. Department of Biochemistry, University of Bristol, Bristol BS8 1TD, U.K.

The presence of troponin and tropomyosin on actin filaments has been shown, using an indirect method, to increase the affinity of actin for S1 by a factor of 6 (Greene J. Biol. Chem. (1982), 257, 13993-9). We have confirmed this result in the presence of calcium using fluorescence titration of S1 to thin filaments reconstituted with actin labelled at cys. 373 with N-(1-pyrenyl) iodoacetamide. This fluorescent label has minimal effect upon the equilibrium and dynamics of actin-S1 interactions (Criddle, A.H., Geeves, M.A. & Jeffries, T. (1985), *Biochem. J.* In press). The use of stopped flow methods to measure the rate of association of S1 with reconstituted thin filaments and with pure actin shows the rates to be indistinguishable over the [S1] range 10-40 μM (0.1 M KCl, 5 mM MgCl_2 , 0.5 mM CaCl_2 , 25 mM tris/imidazole pH 7.5 20°C).

Under the same experimental conditions displacement of pyrene labelled thin filaments from the complex with S1 by the addition of a 5 or 10 fold excess of native thin filaments allows the dissociation rate to be measured. The rate of dissociation was found to be 6-10 slower than that measured for pure actin.

| | Pure Actin | Thin filaments |
|---|--------------------|--------------------|
| Association constant ($\text{M}^{-1}\text{s}^{-1}$) | 2.15×10^6 | 2.09×10^6 |
| Dissociation constant (s^{-1}) | 0.39 | 0.035 |

This work was supported by the Royal Society and by the Medical Research Council U.K.

W-Pos29 ALTERATION OF ACTIN-TROPOMYOSIN (T_m) INTERACTION IN 2,4-PENTANEDIONE TREATED MYOFIBRILS. Saleh E. El-Saleh⁺⁺, R. John Solaro⁺⁺, and James D. Potter^Z. ⁺⁺Dept. of Physiol. & Biophys., Univ. Cinti. OH 45267 and ^ZDept. of Pharm., Univ. Miami School of Med., Miami, FL 33101.

Recently we have reported (El-Saleh et al., 1984, JBC 259, 11014) that the modification of Lys-237 in actin by 2,4-pentanedione (PD), producing an enamine, alters actin-T_m interaction forming a reconstituted thin filament (modified actin-T_m-troponin) that "potentiates" the actin-activated heavy meromyosin-Mg²⁺-ATPase activity in the presence of Ca²⁺ (+Ca²⁺) as well as in its absence (-Ca²⁺). In this investigation we tested whether modification of Lys-237 of actin in native thin filaments of myofibrils could produce a "potentiated" state of myofibrils (+Ca²⁺). Accordingly, myofibrils and desensitized myofibrils (free of T_m·T_n) (in 10 mM MOPS, pH 7.0, 2.0 mM EGTA, 0.4 mM DTT, 0.002% NaN₃) each were treated with PD at 100-fold molar ratio of PD to actin-lysine content. Enamines exhibiting characteristic maximal absorbance (λ_{max} = 310 nm) were the only spectrophotometrically detected products. PD-treated myofibrils (PD-M) measured ATPase levels of 100-106% (-Ca²⁺) and 110-120% (+Ca²⁺) compared to 100% levels in untreated myofibrils (+Ca²⁺) and in PD-treated and untreated desensitized myofibrils. Ca²⁺-sensitivity of PD-M was restored following hydrolysis of the enamine products by hydroxylamine. The modification of the T_m-troponin (T_n) complex in PDM did not contribute for their ATPase potentiation. This was confirmed by the ability of the PD-treated desensitized myofibrils to remain turned "on" (+Ca²⁺) upon reconstitution with PD-treated or untreated T_m·T_n complex. A similar argument could be stated for myosin modification-PD-treated myosin-Mg²⁺-ATPase was not activated by modified (or unmodified) actin alone or complexed with modified or unmodified T_m·T_n (+Ca²⁺). The above finding, therefore, argues that it is most likely that lysine modification in actin (probably at lys-237) "fixes" the actin-T_m interaction in the PD-M in a position (or conformation) that potentiates the ATPase level or at least keeps them turned on regardless of the presence of Ca²⁺. (Supported by MDA-Fellowship to S.E. El-Saleh, NIH HL22619-3a (J.D.P.) - 3b (R.J.S.)).

W-Pos30 CROSSLINKING STUDIES ON RECONSTITUTED THIN FILAMENTS USING SULFO-SANPAH AND SASD by T. William Houk and Sondra Karipedes, Department of Physics, Miami University, Oxford, Ohio 45056

The effects on the Ca⁺⁺ regulated ATPase of reconstituted thin filaments reacted with the heterobifunctional reagents sulfo-SANPAH [sulfosuccinimidyl 6-(4'-azido-2'-nitro phenylamino) hexanoate] and SASD [sulfosuccinimidyl 2(p-azidosalicyl-amido)-1,3'-dithiopro-pionate] have been studied. These reagents, which have a photoreactive moiety at one site and a chemically reactive moiety at another were bound at various labelling ratios to actin or tropomyosin. The crosslinking reagents do not affect the ability of reconstituted thin filaments formed using the chemically labelled proteins to activate the Mg⁺⁺ATPase of myosin. Gel electrophoresis indicates that these reagents, when reacted with the pure proteins before reconstitution, form inter and intramolecular crosslinks within actin and tropomyosin but not between the two proteins upon photo reaction in the reconstituted thin filaments. Crosslinks formed within actin decrease the Ca⁺⁺ activated ATPase of the filaments whereas those in tropomyosin do not. Cleavage of the disulfide bond in SASD crosslinked actin tends to reverse the effects of the crosslinking. These results indicate that flexibility of the actin polymer in the thin filament may be necessary for the normal functioning of the Ca⁺⁺ regulatory mechanism.

W-Pos31 STUDIES ON THE REGULATORY COMPLEX OF RABBIT SKELETAL MUSCLE: CONTRIBUTIONS OF TROPONIN SUBUNITS AND TROPOMYOSIN IN THE PRESENCE AND ABSENCE OF Ca²⁺ AND Mg²⁺ ON THE ACTO-S1 ATPase ACTIVITY. J.E. Van Eyk, P.J. Cachia, R.H. Ingraham and R.S. Hodges, Department of Biochemistry and MRC Group in Protein Structure and Function, University of Alberta, Edmonton, Alberta Canada T6G 2H7.

We have re-examined the regulatory roles of the components of the troponin-tropomyosin complex on the acto-S1 ATPase. In the absence of TM, a free Mg²⁺ concentration of 2.5 mM (5.0 mM Mg²⁺ - 2.5 mM ATP) produces an additional 38% (1:1 S1 to actin ratio) or 37% (2:1) decrease in the ATPase activity of T_n compared to no free Mg²⁺ (2.5 mM Mg²⁺ - 2.5 mM ATP). Similarly, in the presence of TM and T_n, Mg²⁺ exerts its effect at both S1 to actin ratios. Inhibition by the IT complex in the presence of TM is unaffected by free Mg²⁺ and we conclude that Mg²⁺ and, by analogy, Ca²⁺ binding to the Ca²⁺ - Mg²⁺ sites of T_nC promotes muscle relaxation by inducing inhibition of the actomyosin ATPase; whereas Ca²⁺ binding to the Ca²⁺-specific sites promotes contraction by potentiating the ATPase. Examination of the inhibition of acto-S1-TM ATPase by T_nT indicated that, in the presence of TM, T_nT exerts the same level of inhibition upon the ATPase as do T_nI or T_n. In the presence of TM, the IT complex is a more effective inhibitor than T_nI, T_nT or T_n. These observations support growing evidence that the role of T_nT involves more than anchoring T_n to the thin filament. (Supported by the Medical Research Council of Canada and the Alberta Heritage Foundation for Medical Research)

W-Pos32 CATION CONSIDERATIONS IN THE PREPARATION AND CHARACTERIZATION OF MONOMERIC ADP-ACTIN
Lynn A. Selden, Lewis C. Gershman and James E. Estes, Research and Medical Services, Veterans Administration Medical Center, Albany, and Departments of Physiology and Medicine, Albany Medical College, Albany, New York 12208

As usually prepared and purified in most laboratories, monomeric actin contains one mole of ATP and one mole of tightly-bound Ca^{++} per mole protein. To exchange the ATP for ADP, we have used hexokinase and glucose to remove all free ATP, and then allowed the bound ATP to exchange with free ADP. However, the exchange process is very slow and results in significant amounts of denaturation. We have found that replacement of the actin-bound Ca^{++} for Mg^{++} greatly accelerates the rate of release of actin-bound nucleotide from monomeric actin. At 20°C the rate of release of ATP from Ca-actin is $1.65 \times 10^{-7} \text{ s}^{-1}$, similar to that measured by Hitchcock (JBC 255:5668-5673, 1980) and Frieden (JBC 257:2882-2886, 1982), while the ATP release rate for Mg-actin was measured to be $7.7 \times 10^{-4} \text{ s}^{-1}$. Thus, replacement of the actin-bound Ca^{++} by Mg^{++} allows the more rapid (1½ hr) preparation of ADP-actin with less denaturation. Monomeric Mg-ADP actin thus prepared displayed kinetic properties similar to those reported by Lal et al. (JBC 259:13061-13066, 1984). Initial experiments with Ca-ADP actin indicate its properties are similar to those of Mg-ADP actin, while the kinetic properties of Mg-ATP actin and Ca-ATP actin, as we have reported previously, are quite different (BBRC 116:478-485, 1983). Frieden & Patane (Biochemistry 24:4192-4196, 1985) reported that the conformation of monomeric ATP-actin is different than that of ADP-actin, and our results suggest these conformational differences may be reflected as differences in polymerization kinetics. Supported by the Veterans Administration and NIH 1R01 GM-32007-01A1

W-Pos33 THE MOLECULAR DYNAMICS OF ACTIN MEASURED BY A SPIN PROBE ATTACHED TO LYSINE. A. J. Waring K. Franks and R. Cooke. Department of Biochemistry & Biophysics, and the CVRI, University of California, San Francisco, CA 94143-0448.

Rabbit skeletal muscle G-actin was labeled with a spin probe, 3-(5-fluoro-2,4-dinitro-anilino)-PROXYL. Tryptic digestion of the labeled actin followed by ultrafiltration and ion exchange column chromatography indicated the label was attached to residue Lys-61. This residue is found within a 9 kD N-terminal segment that is easily degraded by proteolytic enzymes. Ascorbate quenched the signal of the bound label at a rate that was 20 times less than that for free label, showing that the label was buried within the protein structure. Replacing bound Ca with Mn decreased the observed intensity of the EPR signal, indicating the spin label is about 2 nm distant from the metal binding site on the actin molecule. Labels attached to G-actin displayed an absorption spectrum characteristic of rotational motion with a correlation time (τ) of approximately 10 nsec, which is faster than that for the whole molecule. Using saturation transfer electron paramagnetic resonance labels attached to F-actin had a value for τ of 10 μsec , which again indicates a greater mobility than that of the filament. The binding of heavy meromyosin or troponin-tropomyosin to labeled F-actin resulted in a further decrease in the rotational correlation times, with the greatest decrease in mobility, $\tau = 100 * 10 \mu\text{sec}$., observed when both were bound. Together the above results suggest that the 9 kD segment of actin is mobile relative to the rest of the molecule and that this mobility can be influenced by the binding of heavy meromyosin and troponin-tropomyosin. Supported by a grant from the USPHS: AM30868.

W-Pos34 PHOTOAFFINITY LABELING OF SKELETAL MUSCLE ACTIN BY 2-N₃ADP. Hideto Kuwayama and Ralph G. Yount, Biochemistry/Biophysics Program and Dept. of Chemistry, Washington State University, Pullman, WA, 99164. (Sponsored by L. Kirschner)

The photoaffinity analogue 2-N₃ATP has been used to label the single nucleotide-binding site in F-actin. 2-N₃ATP displaces ADP from G-actin and binds with an apparent dissociation of 25 μM . Addition of ATP prevents 2-N₃ATP binding. Dual treatment of G-actin with 40 μM [³H] 2-N₃ADP resulted in incorporation of 0.6 mol 2-N₃ADP/mol G-actin. Addition of MgCl_2 promoted the G-to-F-actin transition with concomitant hydrolysis of [³H]2-N₃ATP to [³H]2-N₃ADP. F-actin was collected by centrifugation and washed to remove excess [³H]2-N₃ATP. Photolysis of the [³H]2-N₃ADP F-actin complex (0.6 mol 2-N₃ADP/mol actin subunit) resulted in 70% covalent incorporation. Trypsin digestion of the [³H]2-N₃ADP labeled actin and subsequent HPLC separation yielded one major labeled peptide (80% of the covalent incorporation). Amino acid composition and N-terminal analysis gave Lys-(Asx₄, Thr₂, Ser, Pro, Gly₃, Ala₂, Val, Met₂, Ile, Leu, Tyr) Arg, corresponding to residues 291-312 in the actin sequence of Elzinga, M., Collins, J. H., Kuehl, W. M., and Adelstein, A. S. (1973) Proc. Natl. Acad. Sci. USA 70, 2687-2691 except an Ile replaced Thr₃₀₉ and one Tyr was missing. Thermolysin digestion of the isolated labeled tryptic peptide yielded a major labeled peptide with an N-terminal Val and a composition Val(Thr₂, Ser, Pro, Gly₃, Met₂). More extensive thermolysin digestion gave a single [³H] labeled peptide of composition Met (Pro, Gly). These peptides correspond to residues 298-308 and 305-308 and indicate the only amino acid labeled is Tyrosine 306. Supported by NIH grant AM-05195 to R.G.Y.

W-Pos35 VOLTAGE DEPENDENCE OF SLOW INWARD CURRENT AND SHORTENING IN CARDIAC MYOCYTES

A. Bahinski and S.R. Houser, Department of Physiology, Temple University
School of Medicine, Philadelphia, Pennsylvania 19140.

Transsarcolemmal entry of calcium via slow inward current (I_{Si}) is believed to initiate contraction in cardiac muscle via either; i) direct activation of the contractile filaments or ii) by triggering calcium release from the sarcoplasmic reticulum. The present study sought to elucidate the relationship between I_{Si} and contraction in isolated feline ventricular myocytes. A single microelectrode voltage clamp technique was utilized to control membrane potential and to measure membrane current while extent of myocyte shortening was monitored via a linear photodiode array. Depolarizing voltage clamp steps (500 msec. duration) from a holding potential (H.P.) of -40 to -50 mV elicited an inward current and a contraction. The activation curves of I_{Si} and of contraction were nearly identical with a peak around +5 to +15 mV. Depolarizing clamp steps to more positive potentials caused I_{Si} and contraction magnitude (CM) to decrease. In separate protocols myocytes were subjected to drives of depolarizing clamp pulses (0.5Hz; H.P. = -40 to -50 mV). In these studies CM and I_{Si} showed a marked beat dependence. In this regard CM showed a positive staircase. In contrast I_{Si} was largest in Beat 1 and diminished over time to a steady state value. During drive protocols the activation curves of I_{Si} and CM were identical in the first beat post rest. However in the steady state the activation curves for I_{Si} and CM diverge at clamp potentials positive to +20 mV with I_{Si} decreasing and CM continuing to increase to a maximum. These results support the idea that in cat ventricular myocytes the first contraction post rest is dependent upon the amount of calcium entering with I_{Si} while the steady state CM is more dependent on intracellular calcium stores. (Supported by NIH grants: HL33921 and HL33648)

W-Pos36 EFFECT OF OUABAIN ON K INTRACELLULAR IONIC ACTIVITY IN COLON CIRCULAR SMOOTH MUSCLE.

N.L. Shearin, Univ. Utah Medical Center, Dept. Surgery, Salt Lake City, Utah

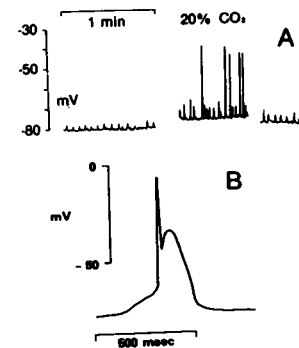
Isolated, whole-mount preparations of transverse cat colon superfused with modified kreb's solution ($[K]_o=5.9$) was used to study the effect of ouabain (1×10^{-6} - 10^{-8} M) on motility membrane potential (EM), intracellular K ionic activity (a_K^i) and K equilibrium potential (EP_K). Simultaneous measurements of EM and a_K^i were obtained with a double-barreled microelectrode. The following table of results was obtained:

| | EM | a_K^i | EP_K | $[K]_o$ |
|-----------------------|------|---------|--------|---------|
| control | 64±5 | 113±24 | 86±7 | 5.9 mM |
| ouabain | 32±3 | 20±2 | 40±2 | 5.9 mM |
| control: post ouabain | 67±6 | 75±17 | 76±6 | 5.9 mM |

Following a 20 min exposure to ouabain, the cell membrane was depolarized and a_K^i decreased. After ouabain removal (20 min superfusion of control media), the MP was elevated, but a_K^i did not return to control levels. Spike activity of the slow wave cycle was not altered, but frequency increased upon exposure to ouabain. Motility was increased during ouabain exposure and did not return to control levels when ouabain was removed. Conclusion: an inhibitory effect by ouabain on the Na-K pump is suggested.

W-Pos37 SPONTANEOUS Ca^{2+} OSCILLATIONS DURING ACIDOSIS CAN PRODUCE ACTION POTENTIALS IN UNSTIMULATED CARDIAC MYOCYTES. S. R. Houser, C. H. Orchard, M. C. Capogrossi, A. A. Kort, A. Bahinski and E. G. Lakatta. Temple University, Philadelphia, PA and Gerontology Research Center, National Institute on Aging, Baltimore, MD.

Increases of Ca_i can produce spontaneous Ca^{2+} oscillations (CaOS) from the sarcoplasmic reticulum (SR) in heart cells. While acidosis can increase Ca_i it also suppresses SR Ca pumping and thus its effect on CaOS is unknown. Spontaneous Ca^{2+} release during CaOS is manifested as a contractile wave and accompanied by a small depolarization of the cell membrane. We have investigated the effect of acidosis on these responses. Fig. A shows membrane potential in an isolated rat myocyte ($Ca_o = 4$ mM, $37^\circ C$) before, during and after acidosis produced by increasing perfusate $[CO_2]$ from 5% to 20% ($[HCO_3^-] = 20$ mM). Within 10 minutes of exposure to the acid solution: i) membrane potential had depolarized significantly from -79.3 ± 0.5 mV to -75.8 ± 2.0 mV (mean + S.E.M., $n = 4$). ii) The frequency of contractile waves and accompanying transient membrane depolarizations had increased by $50 \pm 22\%$ iii) the amplitude of the membrane depolarizations had increased by $31 \pm 6\%$ and became large enough to frequently trigger an action potential (Fig. B). These changes were reversible. The results suggest that the increased Ca_i during acidosis overrides the H^+ suppression of SR function and may be important in the genesis of acidosis-induced arrhythmias.



W-Pos38 **VOLTAGE FLUCTUATIONS IN SMOOTH MUSCLE CELLS ISOLATED FROM HOG CAROTID ARTERIES: INTRACELLULAR Ca RELEASE ALTERS K CONDUCTANCE.** M. Desilets, C.M. Baumgarten and S.P. Driska. Dept. of Physiology and Biophysics, Medical College of Virginia, Richmond, VA 23298

Smooth muscle cells were enzymatically isolated from the hog carotid artery and were superfused at 37°C with a HEPES-buffered Tyrodes solution containing 1.8 mM Ca. Membrane potential (E_m) was monitored with fine suction electrodes (30–50 M Ω) filled with (in mM): 100 K aspartate (or glutamate), 20 KCl, 5 Na₂ATP, 5 KH₂PO₄, 10 taurine and 5 HEPES (pH 7.3). Relaxed cells usually underwent partial but sustained shortening upon impalement, suggesting an increase in intracellular Ca. Under these conditions, an action potential could not be elicited. E_m was not stable but underwent voltage fluctuations characterized by hyperpolarizing "spikes" of less than 100 msec duration. Spike amplitude in cells with a E_m negative to -50 mV was < 3 mV, but increased to as much as 30 mV during constant current depolarization to near 0 mV. The spectral distribution obtained from noise analysis demonstrated a maximum power between 1 and 5 Hz, depending on the preparation. Similarly, bursts of outward currents were observed with voltage clamp. At -50 mV, current fluctuations were < 10 pA, and at 0 mV were \approx 60 pA. These depolarization-induced voltage and current fluctuations were reversibly inhibited by 10 mM TEA. These observations argue that K conductance fluctuations are directly responsible for the voltage variations observed at depolarized E_m . To test if oscillatory release and uptake of Ca from internal stores gates the K conductance, cells were exposed to 10 mM caffeine or 10 μ M ryanodine. In both cases, the voltage and current spikes were inhibited. The results suggest that: 1) a Ca-dependent K conductance can markedly affect the electrical behavior of arterial smooth muscle cells, and 2) internal Ca stores, probably the sarcoplasmic reticulum, can give a very rapid and frequent release of Ca. Supported by NIH HL-24827 (CMB), HL-24881 (SPD), MRC Fellowship (MD), AHA EI (CMB), and RCDA (SPD).

W-Pos39 **TEMPERATURE-DEPENDENCE OF THE ACTION OF RYANODINE ON ISOLATED RABBIT VENTRICULAR MUSCLE.** Michael J. Shattock, Youngjee Kim and Donald M. Bers. Division of Biomedical Sciences, University of California, Riverside, CA 92521.

Many experimental studies describing EC coupling have been conducted at subphysiological temperatures and many have used the neutral plant alkaloid, ryanodine, as a probe of sarcoplasmic reticular (SR) function. There is evidence to suggest that hypothermia may alter cellular calcium handling and it is also likely that the pharmacological properties of ryanodine may be temperature dependent. The influence of temperature on the ability of ryanodine to reduce tension development was therefore investigated in isolated superfused rabbit ventricular muscle. Cumulative ryanodine dose-response curves were constructed over the range 10⁻¹⁰M to 10⁻⁶M at either 37, 29 or 23°C. Temperature shifted these dose-response curves such that at 37°C, a half-maximal effect ($K_{1/2}$) was induced by 5 x 10⁻¹⁰M ryanodine, at 29°C the $K_{1/2}$ was shifted to 5 x 10⁻⁹M and at 23°C the $K_{1/2}$ was further elevated to 3 x 10⁻⁸M. The maximal reduction of tension induced by ryanodine was also greater at 37°C than at the lower temperatures. This implies that ryanodine is either less effective at blocking SR function at lower temperatures or that the SR plays a decreasing role in EC coupling as the myocardial temperature is reduced. This temperature-dependence, may in part explain the apparent differences in maximally effective ryanodine concentrations reported under different experimental conditions. These results may also provide some insight into the influence of temperature on cardiac EC coupling. (Supported by NIH HL30077 and AHA Calif. Affiliate).

W-Pos40 **REST REMOVES RYANODINE INHIBITION OF POST-REST CONTRACTION.** C.O. Malecot and B.G. Katzung. Pharmacology Dept, Univ California, San Francisco, CA 94143.

We studied the effects of low concentrations of ryanodine on the post-rest potentiation (PRP) of tension in ferret papillary muscle. Under control conditions, maximal PRP occurred after 30 sec of rest, and was not affected by a long conditioning rest of up to 20 min preceding the PRP test. In the absence of conditioning rests, 100 pM ryanodine depressed steady-state contraction amplitude only slightly (4.2%) but strongly inhibited the first contraction elicited upon restimulation of the preparation after rest periods of 1 sec to 20 min. 100 pM ryanodine reduced the 30 sec PRP (relative to the pre-rest steady-state tension) from 200% to 68%. In the presence of 100 pM ryanodine, application of a conditioning rest caused PRP to increase as the conditioning rest increased, and PRP recovered exponentially towards control (drug-free) PRP amplitude with a time constant of 582 sec. Block of PRP could be reinduced by stimulating the muscle and occurred faster when higher rates were used (107 sec time constant at 3 Hz). Since rest potentiation of the twitch is believed to be mostly dependent upon Ca release from the sarcoplasmic reticulum, the results suggest that the ryanodine-induced blockade of PRP reflects a use-dependent block of Ca release from the sarcoplasmic reticulum. This effect might be caused by voltage-, state-, or calcium-dependent binding of the drug to its receptor.

W-Pos41 DECAY OF Ca^{2+} TRANSIENTS FROM FROG SKELETAL MUSCLE COMPARED WITH INTRINSIC DECAY KINETICS OF AEQUORIN. P.A. Iaizzo*, E.D.W. Moore*, D.G. Clark* and S. Taylor. Dept. Pharmacology, Mayo Foundation, Rochester, MN 55905.

Decay rates of Ca^{2+} transients in frog muscle are described fairly well by mono-exponentials but the fits are not exact (Blinks et al., 1978). We studied a single batch of aequorins with a Gibson stopped-flow rapid mixing apparatus, confirmed that it had mono-exponential decay kinetics (k3 in Hastings et al., 1969) and used only this batch in the following experiments. EGTA quenching of Ca^{2+} -activated luminescence (Ca/K/Na/Mg-EGTA; pCa = 6.0) was compared with quenching by frog parvalbumins. Aliquot parts of these aequorins were injected into isolated intact tibialis anterior frog muscle fibers. Ca^{2+} transients in tetanic contractions usually decayed as mono-exponentials at 5°C; quenched luminescence always decayed this way. But Ca^{2+} transients at 15°C had fast initial and slow delayed components to their decline. Quenching rates and fast initial decay rates after fused tetani are listed below. These data are consistent with the idea that the fast initial decay of a Ca^{2+} transient at warm temperatures is influenced by SR reuptake. But the slow delayed component and the entire decay at low temperatures may be dominated by binding to parvalbumins. (Supported by NS 14268 and HL 12186).

| Temp. | EGTA (5 mM) | Parvalbumins (0.3 mM) | Tetani (0.5 s) |
|-------|-------------|-----------------------|----------------|
| 15°C | 83.5/s | 33.1/s | 33.0 ± 6.4/s |
| 5°C | 41.7/s | 15.9/s | 10.4 ± 2.5/s |
| Q10 | 2.00 | 2.08 | 3.17 |

W-Pos42 IN VITRO CALIBRATION OF THE METALLOCHROMIC INDICATOR DYE ANTIPYRYLAZO III (ApIII).

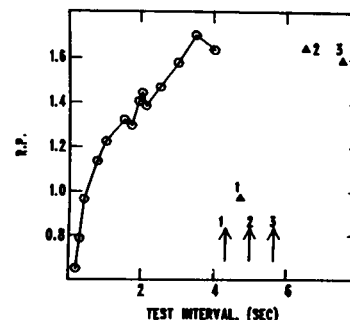
S. Hollingworth, R. W. Aldrich* and S. M. Baylor, Department of Physiology, University of Pennsylvania, PA 19104 and *Department of Neurobiology, Stanford University, CA 94305.

In vitro calibrations of the steady-state reactions of ApIII with Ca and Mg were performed, primarily to measure properties of the 1:2 Ca:ApIII complex (Rios and Schneider, 1981; Biophys. J. 36:607), the principle complex observed when ApIII is used to monitor intracellular Ca transients. Absorbance spectra were measured between 400 and 850nm at 20°C with 140mM KCl, no Mg, and total dye and Ca concentrations up to 2mM and 12.5mM, respectively. These spectra were analysed with least squares fits of equations describing the equilibrium reactions of the complexes considered.

In the absence of divalent cations ApIII forms a higher order complex, probably a dimer with a dissociation constant (K_D) of about 4mM. At pH 6.90 three Ca-ApIII complexes were identified with 1:1, 1:2 and probably 2:2 Ca:ApIII stoichiometry. Interference from divalent-free dimers and 2:2 complex was negligible at low concentrations of ApIII (<40 μ M) and spectra were well fitted assuming that only 1:1 and 1:2 complexes formed with K_D 's of 2.2mM and 35,000 μ M², respectively. The change in extinction coefficient on forming the 1:2 complex, estimated per dye molecule at 720nm, $\Delta\epsilon_2(720)$, was $1.49 \times 10^4 \text{ M}^{-1}\text{cm}^{-1}$. At pH 4.0 formation of the 1:1 and 2:2 complexes was suppressed and a large fraction of ApIII could be driven into the 1:2 form; $\Delta\epsilon_2(720)$ estimated from these data, $1.46 \times 10^4 \text{ M}^{-1}\text{cm}^{-1}$, was closely similar to that obtained at pH 6.90. These values for $\Delta\epsilon_2(720)$ are about 1.8 times that reported by Rios and Schneider who analysed calibrations over a smaller range of Ca concentrations (<1mM) and assumed that only a 1:2 complex formed. Calibrations with Mg at pH 6.90 revealed in addition to the expected 1:1 complex, a second complex, probably 1:2 Mg:ApIII, which absorbed at 720nm, a wavelength at which ApIII has usually been assumed to respond only to Ca.

W-Pos43 SPONTANEOUS SARCOPLASMIC RETICULUM Ca^{++} RELEASE LIMITS THE EXTENT OF TWITCH REST POTENTIATION IN RAT CARDIAC MYOCYTES. M. C. Capogrossi, H. A. Spurgeon, D. J. Pelto, and E. G. Lakatta, Gerontology Research Center, NIA, Baltimore, MD

When spontaneous sarcoplasmic reticulum Ca^{++} release (manifest mechanically as a contractile wave) (W) occurs during the period between twitches, it interferes with Ca^{++} release in the subsequent twitch (T) evoked by an action potential. We measured the extent of rest potentiation (RP), measured as extent of shortening in the test T normalized to that at steady state during stimulation (S), and the occurrence of W following S at 2 Hz in single rat cardiac myocytes bathed in HEPES buffer (37°C, pH 7.4, $\text{Ca}^{++} = 4.0 \text{ mM}$). Following an S train T was measured in a test interval and the sequence repeated at varying test intervals. The extent of RP of T that was achieved did not plateau but was limited to about 1.7 by the occurrence of a W. Arrows 1-3 in fig. represent W occurrence in 3 separate S-test cycles; Δ 1, 2, 3, are the corresponding RP of a subsequent test T. At the short W-T interval (arrow 1- Δ 1) note the fall in RP; even at longer times following W, RP did not exceed that prior to occurrence of first W. We conclude that the occurrence of W's limit the extent of RP of T that can be achieved but that under these conditions the first W following S is sufficiently delayed (> 4 sec) to permit substantial RP of T.



W-Pos44 EFFECT OF DANTROLENE ON $[Ca^{2+}]_i$ IN HUMAN MALIGNANT HYPERTHERMIA SKELETAL MUSCLE. J.R. López, P. Medina, L. Alamo. Centro de Biofísica y Bioquímica IVIC, Caracas, Venezuela. Departamento de Anestesiología, Hospital J.M. Vargas, Caracas, Venezuela.

Malignant hyperthermia (MH) is a hereditary myopathy, triggered when susceptible patients are exposed to depolarizing muscle relaxant, and/or potent volatile anesthetics. We have studied the effects of dantrolene on the free $[Ca^{2+}]_i$ on intercostal muscle biopsies obtained from two MH susceptible patients before and after administration of dantrolene orally (2.5 mg/Kg for 3 days) and endovenous (1.0 mg x Kg two hours before the biopsy). The free $[Ca^{2+}]_i$ was measured by Ca^{2+} selective microelectrodes prepared and calibrated as previously described (Lopez et al *Biophys J.* 43:1-4 1983). The mean resting free $[Ca^{2+}]_i$ in the MH susceptible muscle before dantrolene treatment was $0.42 \pm 0.05 \mu M$ ($M \pm SEM$, $n=12$). The administration of dantrolene reduced this value to $0.27 \pm 0.03 \mu M$ ($M \pm SEM$, $n=14$). There was no detectable difference in the resting membrane potential after dantrolene. These results represent the first direct demonstration that dantrolene is able to reduce the resting free $[Ca^{2+}]_i$ in skeletal muscle of MH susceptible patients. (Supported by CONICIT Grant S1-1277, Muscular Dystrophy Association).

W-Pos45 MYOPLASMIC FREE $[Ca^{2+}]_i$ AND CALCIUM UPTAKE IN HUMAN SKELETAL MUSCLE WITH CARNITINE DEFICIENCY. J.R. LOPEZ¹, L.E. BRICEÑO², M. CONDRESCU¹, G. CORDOVEZ¹, L. ALAMO¹. Centro de Biofísica y Bioquímica. Apartado 1827, Caracas 1010A, Venezuela.² Departamento de Neurología, Hospital Infantil J.M. de los Ríos, Caracas, Venezuela.

The main physiologic role of carnitine is related to the transport of long chain fatty acid into mitochondria in skeletal muscle. We have measured the $[Ca^{2+}]_i$ and the sarcoplasmic reticulum Ca^{2+} uptake in skeletal muscle biopsies obtained from three patients in which a myopathic carnitine deficiency was detected. Intercostal muscle biopsies were carried out under local anesthesia and then splitted for electron microscope study, electrophysiological measurements, biochemical study, and carnitine determinations. For the electron microscopy study, the muscle biopsies were fixed in 1% glutaraldehyde mammalian Ringer and then processed by standard methods for E.M. The $[Ca^{2+}]_i$ was measured by means of Ca^{2+} selective microelectrodes which were prepared and calibrated as previously described (López et al, *Biophys. J.* 43:1,1983). The ^{45}Ca uptake by the sarcoplasmic reticulum vesicles was measured using a protocol similar to that described by Meissner and Fleischer (BBA 241:356 1971). Longitudinal sections of muscle fiber showed excessive accumulation of lipid droplets between the myofibrills adjacent to mitochondria. The $[Ca^{2+}]_i$ was $0.42 \pm 0.02 \mu M$ ($M \pm SEM$) while the calcium uptake was $0.46 \pm 0.11 \mu M/mg.min.$ ($M \pm SEM$). These results suggest that in patients with myopathic carnitine deficiency there is a significant increase in the resting myoplasmic calcium concentration (3.8 times higher than the resting value in control subjects) and also a considerably lower calcium uptake by sarcoplasmic reticulum vesicles (2.4 times lower than control values). Supported by CONICIT S1-1277, M.D.A. and Laboratorios Elmor.

W-Pos46 CONTRACTILE INACTIVATION IN MUSCLE FIBERS. THE EFFECTS OF LOW CALCIUM, TETRACAINE, DANTROLENE, D-600 AND NIFEDIPINE. Carlo Caputo and Pura Bolaños. Laboratorio de Biofísica del Músculo. Centro de Biofísica y Bioquímica. IVIC. Apdo. 1827 Caracas 1010A Venezuela.

Contractile inactivation without previous activation can be induced in voltage clamped short muscle fibers of the frog, by conditioning depolarizing ramps of slopes slower than 0.1 mV/s. The sensitivity to depolarizing ramps can be increased by D-600, 50 μM , to 1mV/s; dantrolene, 50 μM , to 0.8 mV/s; tetracaine, 100 μM , to 0.4 mV/S; and low calcium, $10^{-8} M$, to 0.2mV/s. Nifedipine has also been found to increase this sensitivity but to lesser extent. In the presence of D-600, after inactivation had been induced, no repriming could be attained by membrane repolarization to -100 mV, and only a partial recovery was observed 10 to 20 min after washing out the drug. In the presence of the other agents repriming could be achieved after membrane repolarization to -100 mV. For the case of low calcium, tetracaine and nifedipine, the tension voltage relationship (activation curve) was not affected, while the steady state inactivation curve (contractile repriming) was shifted by 10-25 mV toward more negative potentials. For the case of D-600 the activation curve was not modified, while the inactivation curve could not be obtained due to repriming failure (paralysis; Eisenberg, McCarthy and Milton, 1983). For the case of Dantrolene the inactivation curve was not affected, while the activation curve was shifted toward less negative potentials, and peak tension diminished depending on the pulse duration. These results indicate that it is possible to pharmacologically differentiate activation and inactivation parameters related to Depolarization-Contraction Coupling, suggesting that activation and inactivation might be two separate processes (Supported by MDA and CONICIT, S1-1148).

W-Pos47 CALCIUM AND THE VOLTAGE SENSOR OF SKELETAL MUSCLE EXCITATION-CONTRACTION COUPLING.

G. Brum and E. Rios, (introduced by M. Chuman). Department of Physiology, Rush Medical School, Chicago.

Rios et al. (Biophys. J. 47, 1985) showed that extracellular Ca (Ca_e) modulates Ca release from the sarcoplasmic reticulum (SR) and that this effect is not mediated by the slow Ca current. Consequently the agonist site must be accessible from the extracellular medium. The voltage sensor of E-C coupling seems a candidate for mediator of this action of Ca_e .

We measured the effect of $[Ca^{2+}]_e$ on intramembrane charge movement, in cut skeletal fibers of the frog, voltage-clamped in a vaseline gap. We simultaneously monitored Ca transients with Antipyrylazo III and derived SR Ca release (Melzer et al., 1984). In low $[Ca^{2+}]_e$ conventionally measured charge movement was substantially reduced and charge immobilization by maintained depolarization occurred at more negative holding potentials. Ca release was likewise diminished and its inactivation occurred at more negative holding potentials. The disappearance of charge mobile in the -80 mV to 0 mV range (charge 1) was accompanied by appearance of charge mobile between -80 mV and -160 mV, analogous to 'charge 2', that appears in fibers under sustained depolarization (Brum and Rios, this meeting).

All observations may be explained as follows: the voltage sensor of E-C coupling has at least 4 states: resting, active (inducing Ca release) and 2 inactivated states; Ca binds preferentially to resting and active states. Voltage drives resting \rightarrow active transitions in which charge 1 moves. Sustained depolarization and/or Ca deprivation put the sensor in the inactivated states. Charge still moves between these states (charge 2) but no Ca release is induced. Supported by NIH grant AM32808.

W-Pos48 DEPRESSION OF SR CALCIUM RELEASE DUE TO SR CALCIUM DEPLETION IN FROG SKELETAL MUSCLE.

B.J. Simon, M.F. Schneider and G. Szucs, Cardiovascular Section, Gerontology Research Center, Baltimore, Maryland

Myoplasmic free calcium transients ($\Delta[Ca]$) and rate of release of calcium (RREL) were determined in cut segments of single frog twitch fibers at 8° C. using a double vaseline gap voltage clamp (Melzer et al., Biophys. J. 45:637). During 200 ms depolarizing steps to membrane potentials from -20 to +60 mV RREL rose to a peak and then declined to a final level of ~.3 of the peak amplitude. The basis for the decline of RREL during the pulse was investigated with a double pulse protocol. Using a given pre- and test pulse combination to study recovery of RREL as a function of time after a prepulse, the recovery exhibited a fast and slow phase. During the fast phase, which was completed within about the first sec of recovery, the peak RREL was relatively more depressed than the final level. During the slow phase of recovery, which required as much as 60 sec, RREL followed the same wave form as the control but was simply scaled down. Using the slowing of the decay of $\Delta[Ca]$ after the test pulse to estimate the increased calcium occupancy of myoplasmic binding sites (Melzer et al., 1985, J. Physiol. in press) we found that the slow recovery paralleled the loss of calcium from these sites. Varying the prepulse amplitude and duration but using a set 1 to 2 sec recovery period, the depression of RREL was proportional to the amount of calcium released during the prepulse. These observations are as expected if the slow recovery represents recovery from SR calcium depletion. The depression of calcium release that recovers rapidly appears to be due to a calcium-dependent inactivation of the SR calcium channel (Simon et al., J. Gen. Physiol. 86:abstract in press).

W-Pos49 THYROID HORMONE ALTERS THE INTRACELLULAR CALCIUM TRANSIENT IN CARDIAC MUSCLE.

Roderick MacKinnon and James P. Morgan, Harvard Medical School, Beth Israel Hospital, Boston, Massachusetts, 02215.

Thyroid hormone has a profound effect on the mechanical behavior of cardiac muscle. Because intracellular calcium plays a key role in the activation of muscle contraction, the calcium sensitive bioluminescent protein aequorin was used to investigate whether the intracellular calcium transient during excitation-contraction coupling in cardiac muscle is influenced by changes in the thyroid state. Aequorin was chemically loaded into cells of ferret papillary muscles from hyperthyroid ($+T_4$) n=6, control (C) n=6, and hypothyroid ($-T_4$) n=5, age-matched ferrets. Isometric tension and the aequorin signal were simultaneously recorded. The time to peak tension and time to an 80% relaxation of tension were reduced by 23% and 26% respectively in $+T_4$ as compared to C, while these measures were prolonged by 18% and 16% respectively in $-T_4$ as compared to C. Following a brief latency, the aequorin signal rose rapidly to a maximum in approximately 40 msec in the three groups, followed by a slower monotonic decline back to baseline. The time from the maximum to an 80% decline in msec (\pm S.D.) was 68 ± 5 , 95 ± 8 and 114 ± 17 for $+T_4$, C and $-T_4$ respectively. These results indicate that the decay of myoplasmic calcium during excitation-contraction coupling in cardiac muscle is altered by changes in the thyroid state and are consistent with the findings of altered sarcoplasmic reticulum function (Suko, J. Physiol. 1973, 228). The basis of the altered calcium transient and its relationship to the changes in the mechanical properties are presently under investigation (Support: HL07044, HL3117 and HL01611).

W-Pos50 CAN K DEPOLARIZATION STIMULATE Ca ENTRY VIA Na/Ca EXCHANGE IN HEART MUSCLE? John H.B. Bridge*, (Intr. by K.W. Spitzer) Cardiovasc. Res. & Training Institute, Univ. of Utah, Salt Lake City, UT 84112

Ca might enter heart cells upon K depolarization via a) Na/Ca exchange or b) via a gated channel. Following a period of rest in 144mMNa and 2.7mMCA (which depletes SR Ca) extracellular Na reduction to 2.0mM replenished SR Ca in rabbit papillary muscles. This was concluded from increased cooling contractures which appear to reflect SR Ca replenishment (Biophys J 47:459a, 1985). This SR replenishment is not blocked by 10 μ M verapamil and is attributable to reverse Na/Ca exchange. If Na and Ca are simultaneously reduced during rest (44.0mM Na, 78 μ MCA) Na/Ca exchange reversal is prevented and the SR does not replenish. Muscles rested in 44.0mMNa and 78 μ MCA and then depolarized to approximately zero mV in 100mMK for 2 minutes exhibit significant SR replenishment. This replenishment was completely blocked by 10 μ M verapamil. It is concluded that this SR replenishment is due to Ca entry via a verapamil sensitive pathway (presumably a Ca channel) that was activated by depolarization. Calculations suggest that, under these circumstances (44mMNa, 78 μ MCA), the reversal potential of the Na/Ca exchange is unlikely to be exceeded by K depolarization. Following a period of rest (Na=144mM, Ca=2.7mM) Na was reduced to 24.0mMCA (in the presence of 10 μ M verapamil) which replenished the SR. However, simultaneous Na reduction (24.0mM) and K elevation (100mM) produced additional SR replenishment in the presence of 10 μ M verapamil. Calculations suggest that under the circumstances of this experiment (24.0mMNa, 2.7mMCA, 100mMK) the reversal potential of the Na/Ca exchange would be exceeded. This suggests that this additional verapamil insensitive component of SR replenishment (Ca entry) occurring during K depolarization might be attributed to depolarization sensitive Na/Ca exchange.

W-Pos51 EMBRYONIC ACETYLCHOLINE RECEPTORS ON CHICKEN MYOBLASTS ARE FUNCTIONALLY LINKED TO MECHANISMS INVOKING CHANGES IN $[Ca^{2+}]_i$. M. James-Kracke and J. Chai. (Intr. by R.L.Cross). SUNY Upstate Medical Center, Syracuse, N.Y., 13210.

Acetylcholine (ACh) receptors labeled with alpha-bungarotoxin have been reported to appear on the surface of chicken myoblasts by the 8th to 9th day of development. Are these receptors functionally linked to Ca^{2+} release mechanisms for excitation-contraction coupling at the time of first appearance, or are they linked at a later stage of development? Attempts to prepare suspensions of Fura-2 loaded myoblasts from pectoralis muscle which would respond to ACh were unsuccessful. Although isolation of single cells with purified collagenase in the presence of trypsin inhibitor yielded cells responsive to other stimuli, ACh invoked no Ca^{2+} increase. Since myoblasts isolated from more advanced embryos also did not respond, the isolation of the cells was thought to deactivate the receptors. To circumvent the isolation procedure, a thin sheet of muscle (M. transverse abdominis) from the abdominal wall was dissected and stretched across a plexiglass frame with a central window and inserted diagonally in a cuvette. ACh-induced increases in $[Ca^{2+}]_i$ have been observed in these embryonic muscles ranging in age from 10 to 19 days. The dependence of this response on extracellular Ca^{2+} or sarcoplasmic reticulum release over this interesting stage of differentiation will be correlated with ultrastructural changes to attempt to obtain information about intermediate steps of excitation-contraction coupling as they develop. Supported by the Muscular Dystrophy Association.

W-Pos52 EFFECTS OF VERAPAMIL, MUSCLE LENGTH, AND POST-EXTRASYSTOLIC POTENTIATION ON TENSION INDEPENDENT HEAT OF RABBIT PAPILLARY MUSCLES. Edward M. Blanchard, Louis A. Mulieri, Norman R. Alpert. University of Vermont, Dept. Physiology & Biophysics, Burlington, VT 05405.

Right ventricular papillary muscles of rabbits mounted on thermopiles produce 1.50 mcal/g of activity-related initial heat per twitch when contracting isometrically at 0.2 Hz and L. After twitch tension is eliminated by a 2.1X hyperosmotic Krebs solution (2.1XN) containing 2,3-butanedione monoxime (BDM), the muscles produce 0.20 mcal/g heat (tension independent heat, TIH). Our working hypothesis is that the TIH signal represents the thermal equivalent of calcium cycling during the twitch; thus, interventions known to alter the inotropic state of cardiac muscle should produce predictable changes in TIH. The following data partially support the hypothesis. The calcium channel blocker verapamil at 14×10^{-6} M reduced twitch tension to 12% ($\pm 2\%$) of control and reduced TIH to 43% ($\pm 7\%$) of control. Decreasing papillary muscle length from L to 0.8L reduced twitch tension and TIH to 23% ($\pm 5\%$) and 63% ($\pm 6\%$) of control, respectively. When an extra stimulus was interposed 1800 msec after a regular stimulus, twitch tension of the next regular response was 35% ($\pm 3\%$) greater than control at 0.2 Hz and 58% ($\pm 12\%$) greater than control at 0.017 Hz. TIH was not potentiated by the extra stimulus at either pacing frequency. In summary, inhibition of TIH by verapamil and muscle shortening are consistent with our working hypothesis and current concepts about the dependence of cardiac excitation-contraction coupling on the slow inward calcium current and on muscle length. The reason for the absence of post-extrasystolic potentiation (PESP) of TIH is not yet determined but may be related to the increased intracellular ionic strength caused by the (2.1XN) Krebs solution since PESP is also absent when the muscle is in (2.1XN) Krebs alone.

W-Pos53 THE EFFECTS OF Ca^{2+} , Mg^{2+} , ADENINE NUCLEOTIDES AND CALMODULIN ON THE Ca^{2+} RELEASE CHANNEL IN CARDIAC SARCOPLASMIC RETICULUM VESICLES. Gerhard Meissner and Julia S. Henderson, Department of Biochemistry, University of North Carolina, Chapel Hill, NC 27514

A subpopulation of canine cardiac sarcoplasmic reticulum (SR) vesicles was found to contain a " Ca^{2+} release channel" which mediates the rapid release of intravesicular Ca^{2+} stores. $^{45}\text{Ca}^{2+}$ efflux rates from vesicles passively loaded with 1 - 10 mM $^{45}\text{Ca}^{2+}$ were determined with the use of a rapid quench apparatus and by Millipore filtration. At pH 7 and 5 - 50 μM external Ca^{2+} , vesicles released $^{45}\text{Ca}^{2+}$ with a first order rate constant of 20 - 50 s^{-1} , as compared to 1 - 2 s^{-1} for rabbit skeletal muscle SR Ca^{2+} release vesicles when analyzed under identical conditions. Ca^{2+} -induced Ca^{2+} release from cardiac SR Ca^{2+} release vesicles was half-maximally inhibited at about 10^{-6} and 5×10^{-4} M Ca^{2+} , by the addition of $\sim 3 \times 10^{-4}$ M Mg^{2+} , or by decreasing the pH from 7 to 6.7. Ruthenium red, ryanodine, La^{3+} , tetracaine and neomycin inhibited Ca^{2+} -induced Ca^{2+} release. Addition of the nonhydrolyzable ATP analog AMP-PCP to a release medium containing 5 μM Ca^{2+} and 0.6 mM free Mg^{2+} increased the rate constant of Ca^{2+} release from about 5 to 30 s^{-1} . Calmodulin inhibited Ca^{2+} - and nucleotide-induced $^{45}\text{Ca}^{2+}$ release rates by a factor of 4 - 10 in a reaction that did not seem to involve a calmodulin-dependent protein kinase. These studies suggest that cardiac SR vesicles contain a Ca^{2+} channel which is capable of releasing Ca^{2+} with rates comparable with those expected to occur during excitation-contraction coupling in cardiac muscle. The channel is activated by micromolar concentrations of external Ca^{2+} and by adenine nucleotides, and inhibited by Mg^{2+} and calmodulin. Supported by USPHS Grants HL27430 and AM18687.

W-Pos54 Ba^{2+} INDUCES STRESS DEVELOPMENT IN SWINE CAROTID ARTERY BY MOBILIZING INTRACELLULAR Ca^{2+} Chi-Ming Hai and Richard A. Murphy. Department of Physiology, University of Virginia, Charlottesville, VA 22908

We investigated whether Ba^{2+} could substitute for some actions of Ca^{2+} on the regulatory systems in intact and Triton X-100 skinned swine carotid medial strips. Ba^{2+} induced dose-dependent contractions in the absence of extracellular calcium. The maximum stress averaged $90.9 \pm 15.8\%$ of that produced by K^{+} depolarization with an EC_{50} of approximately 4 mM Ba^{2+} . The Ba^{2+} induced contraction was associated with gradual increases in myosin light chain phosphorylation from a basal level of about 5% to a sustained level of $30.0 \pm 0.8\%$. This observation suggested the involvement of Ca^{2+} since Ba^{2+} does not activate Ca-calmodulin dependent enzymes. Partial intracellular calcium depletion with 100 μM histamine and 25 mM caffeine in addition to extracellular calcium depletion failed to abolish Ba^{2+} induced contractions. However, repeated contractions with Ba^{2+} in Ca-free solutions followed by relaxation in zero Ca^{2+} (5 mM ECTA) solutions led to decreases in stress development. Repeated contractions with high potassium (1.6 mM Ca^{2+}) followed by relaxations in zero Ca^{2+} (5 mM ECTA) solutions showed no significant changes in stress development. Ba^{2+} did not induce significant stress development in skinned fibers even at high concentrations. Ba^{2+} also failed to maintain stress in fibers previously contracted with 4 mM Ca^{2+} . These observations suggested that Ba^{2+} induced stress development is not due to a direct effect on the contractile protein system as previously suggested. Ba^{2+} appears to mobilize Ca^{2+} from an intracellular store that was not released by histamine or caffeine. (Supported by 2-P01-HL19242 and a fellowship from American Heart Association, Virginia Affiliate)

W-Pos55 REACTION OF THE TRANSVERSE TUBULE MEMBRANE Mg -ATPASE WITH NUCLEOTIDE-MIMETIC INHIBITORS. Kurt C. Norton, Michael P. Moulton, Shannon M. Rose, Roger A. Sabbadini, and A. Stephen Dahms, Molecular Biology Institute, San Diego State Univ., San Diego, CA 92182.

Several nucleotide-mimetic agents have been used to explore catalytic and regulatory mechanisms of the chicken skeletal muscle transverse tubule Mg -ATPase (TT-ATPase). 7-Chloro-4-nitrobenzo-2-oxa-1,3-diazole (NBD) and 5'-fluorosulfonylbenzoyladenine (FSBA) are putative structural analogues of adenine and adenine nucleotides, respectively, and have been shown to covalently modify and inhibit ATPases from a number of sources. Kinetics of inhibition of the TT-ATPase by NBD (pH 7.3, 25C) indicate both the presence of 2 classes of reactive residues with quite different reactivities and the presence of a saturation phenomenon with regard to NBD; no protection against inactivation was afforded by ATP, Mg -ATP, or Mg over the 0.01-15 mM concentration range. The lectin Con-A, which completely abolishes the complex, non-Michaelis-Menton kinetics manifested by the TT-ATPase, totally protects against inactivation by NBD. Mercaptoethanol does not reverse the inactivation, suggesting the absence of sulfhydryl involvement or of stable tyrosyl modification. The data are consistent with the modification of lysyl residues (or tyrosyl residues with a subsequent O \rightarrow N transfer) in a Con-A sensitive/reactive putative regulatory site. The TT-ATPase was shown to be fully insensitive to FSBA under conditions which substantially inhibit $\text{F}_1\text{-ATPase}$, pyruvate kinase and the Na, K-ATPase. Tetraiodofluorescein (TIF) is a strong, linear competitive inhibitor (K_i , 0.3 μM) of the TT-ATPase with regard to ATP. The nature of the interaction between these nucleotide site probes and the TT-ATPase is compared with the plasma membrane Na,K-ATPase and the closely-related sarcoplasmic reticulum Ca-ATPase. Supported in part by NSF PCM 8405007.

W-Pos56 SINGLE CHANNEL MEASUREMENTS OF THE CALCIUM RELEASE CHANNEL FROM SARCOPLASMIC RETICULUM: ACTIVATION BY Ca^{2+} , ATP AND MODULATION BY Mg^{2+} . Jeffrey Smith, Roberto Coronado, and Gerhard Meissner, (Intr. by Kenneth Jacobson) Depts. of Biochemistry and Pharmacology, University of North Carolina, Chapel Hill, NC 27514

In a recent report (*Nature* 316:446, 1985) we identified a large conductance (125 pS in 50 mM Ca^{2+}), adenine nucleotide activated calcium channel present in heavy sarcoplasmic reticulum fractions. Here we report on bilayer experiments which indicate the channel is activated by cis Ca^{2+} . Cis Ca^{2+} increased open probability (P_o) in single channel records without affecting open event lifetimes. P_o increased 10-fold in the range of 2 μM to 950 μM after which inhibition was observed. Millimolar ATP was found to be as good or better than Ca^{2+} for activation, however, neither Ca^{2+} nor ATP alone was sufficient to bring the P_o vs. concentration curve to $P_o = 1$. Based on exponential fits of the single channel lifetimes we propose a preliminary kinetic scheme to explain the effects of Ca^{2+} and nucleotide on the gating of the channel. In this model both Ca^{2+} and nucleotide interact with the closed state to decrease its duration and increase the frequency of open events. Nucleotide and possibly Ca^{2+} in the presence of nucleotide have an additional interaction with the open channel which increases the duration of open events. Mg^{2+} was found to permeate the SR calcium channel in a trans to cis direction such that $i_{\text{Mg}^{2+}}/i_{\text{Ca}^{2+}} = .40$. Cis Mg^{2+} was inhibitory and in single channel recordings produced an unresolvable flickering of nucleotide activated channels. Nucleotide activated macroscopic barium conductance was inhibited by cis Mg^{2+} with an $\text{IC}_{50} = 1.5$ mM. Supported by NIH Grants AM18687, HL27430, GM32824.

W-Pos57 PRECOOLING: ITS MAGNITUDE DURING QUICK-FREEZING WITH A LIQUID HE-COOLED COPPER BLOCK. R. Nasser, N.R. Wallace, I. Taylor, and J.R. Sommer. Depts. of Pathol. and Physiol., Duke University and VA Medical Centers, Durham, N.C. 27710

We are studying the ultrastructure in thin sections and freeze-fracture preparations, and the local microchemistry in ultra-cryosections from quick-frozen single intact frog skeletal muscle fibers after known time intervals following electrical stimulation. Our superb cryopreservation (Sommer et al., *Proc. EMSA* 1983, pp. 464, 526, 648) indicates very high freezing rates, ruling out significant "pre-cooling". Nevertheless, the success of these investigations during the first msec of excitation-contraction-coupling requires us to rule out the possibility that the single muscle fiber was frozen between the time of electrical stimulation and that of impact on the cold copper block. We measured the temperature as a function of time during the descent toward the cold copper block of a thermocouple (25- μm Copper-Constantan, or 12- μm Chromel-Constantan) mounted on a specimen holder in place of the single fiber. In most experiments, the temperature just before impact was between 4 and 15°C making premature freezing of the muscle fibers unlikely even when stimulated microseconds before impact. The notable absence of cryo-artefacts in our fibers as an independent measure of pre-cooling is borne out by the present results, confirming the validity of our approach in the study of quick-freezing during the first msec following electrical stimulation.

(Supported by the VA Research Service, and NIH grants #HL-12486 and HL-33680).

W-Pos58 THE EFFECT OF FREQUENCY DEPENDENT CONDUCTIVITIES IN A VOLUME CONDUCTOR MODEL OF SKELETAL MUSCLE. B. Roth, F. Gielen and J. Wikswo, Department of Physics & Astr., Vanderbilt University, Nashville, TN 37235.

A volume conductor model has been developed to calculate the electric potential and the magnetic field of a single active skeletal muscle fiber in a muscle bundle¹. The bundle is considered to be homogeneous, so that we use space averaged effective conductivities to describe the electrical properties of the tissue, and anisotropic, so that the effective conductivities transverse and longitudinal to the fiber axis are different. By space averaged we mean that we calculate an effective conductivity, which incorporates the structure of the tissue at a cellular level; this includes the size and electrical properties of the muscle cells and their packing². The effective conductivity depends on the spatial length of the depolarizing phase of the action potential (spatial frequency) as related to the length constant of the inactive fibers around the active fiber. The temporal frequency will also play a role because of the membrane capacitance, making the effective conductivities complex. We have incorporated these frequency-dependent conductivities into the volume conductor model, so that we can investigate the effect of the bundle conductivities on the electrical potential and magnetic field produced by skeletal muscle.

¹Roth, B. and J. Wikswo, *Math. Biosci.*, (in press) 1985.

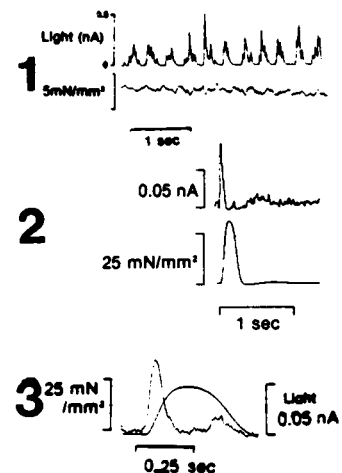
²Gielen, F. L. H., *Med. & Biol. Eng. & Comp.*, (in press) 1985.

W-Pos59 MEASUREMENT OF INTRACELLULAR IONIZED Mg AND K IN SINGLE BARNACLE MUSCLE CELLS. David Van Wagoner, Jose Whittembury and Antonio Scarpa, Intr. by Meredith Bond, Dept. Biochem/Biophysics and Biomedical Instrumentation Group, University of Pennsylvania, Philadelphia, PA 19104.

Measurements of cellular ionic activity with liquid sensors have thus far been accomplished with microelectrodes containing either free liquid sensor, or with the sensor incorporated in a PVC matrix. These electrodes have extremely high DC resistances, short lifespan, and low stability. We have designed a mini-electrode which overcomes these problems and may be used with any of the liquid cation sensors. The body of the electrode consists of a 5 cm long 100 μm (o.d.) quartz capillary with a 1 mm long ceramic plug at the tip. The plug serves as a stable matrix for the sensor without increasing its resistance. These electrodes may be used with a standard p(H or ion) meter, and have a life expectancy of several days, with low drift. Using the appropriate Fluka sensor cocktails, we have measured the Mg and K activities in single barnacle muscle cells. The K electrode is nerstian over the range 1-200 mM in solutions of constant ionic strength (Na and K). The free K in freshly dissected fibers averaged 135-140 mM. The Mg electrode is sub-nerstian (an inherent property of the sensor), with a slope of 18 mV/decade, and a detection limit of 0.1 mM free Mg in calibrating solutions containing 140 mM KCl, 15 mM NaCl, and 0-10 mM MgCl_2 . In preliminary experiments the Mg activity ranged from 0.5-2.0 mM, lower than the 4.2 mM concentration estimate using the Eriochrome B null point technique in barnacle (Brinley et al., J. Physiol. 266:545-565), but similar to the 1.7 mM activity measured in frog skeletal muscle with the same liquid sensor (Alvarez-Leefmans et al., Biophys. J. 47:458a). A scaled up version of this electrode could be used with cell suspensions. Supported by NIH grant HL-15835.

W-Pos60 SPONTANEOUS Ca^{2+} RELEASE CAN OCCUR DURING AN ISOMETRIC TWITCH IN CARDIAC MUSCLE. M. E. McIvor, E. G. Lakatta and C. H. Orchard (Intr. by David Bickar). Gerontology Research Center, National Institute on Aging, Baltimore, MD.

Oscillations of myoplasmic $[\text{Ca}^{2+}]$ associated with oscillations of tension can be demonstrated under conditions of Ca^{2+} overload in resting cardiac muscle. Figure 1 shows such oscillations in an unstimulated ferret papillary muscle produced by substituting K for external Na in the presence of 10 μM ouabain and 5 mM Ca^{2+} . A single cell was injected with the photoprotein aequorin, which emits light as a function of $[\text{Ca}^{2+}]$. The traces show aequorin light (top) and tension (below). The oscillations had a frequency of 3 Hz and peak $[\text{Ca}^{2+}]$ was estimated to be 6-7 μM . Figure 2 is the averaged record of a beating preparation in which a single cell was injected with aequorin. In the presence of 1 μM isoproterenol and 5 mM Ca^{2+} , when the muscle was stimulated at 0.3 Hz, there was spontaneous Ca^{2+} release following the twitch associated with an aftercontraction. We now show that spontaneous Ca^{2+} release can occur during the twitch itself. (Figure 3) in an averaged record from a muscle in which several cells were injected with aequorin. The functional implications of spontaneous Ca^{2+} release during a twitch, when the sarcolemma may be partially depolarized, might be expected to differ from a release occurring between twitches.



W-Pos61 MAXIMUM UNLOADED SHORTENING VELOCITY (V_{max}) IN SINGLE ISOLATED SMOOTH MUSCLE CELLS: EFFECTS OF $[\text{Ca}]$ AND ISOPROTERENOL (ISO) ON V_{max} . Shinobu Yagi, Kevin E. Fogarty, Michael B. Ryherd and Fredric S. Fay. Dept. of Physiol. Univ. of Mass. Med. Ctr., Worcester, MA.

The kinetics of most aspects of smooth muscle contraction are believed to be slower than striated muscle. While V_{max} and actomyosin (AM) ATPase are depressed in smooth muscle, V_{max} is depressed to a greater extent. To determine if this difference indicates a fundamental difference in the limiting factor(s) for AM interaction and cross-bridge turnover between smooth and striated muscles, we investigated the contractile kinetics of unloaded shortening of single isolated smooth muscle cells (SMC's). SMC's were mounted for isometric measurement of force (Warshaw and Fay: J.G.P. 82:157, '83) and subjected to rapid releases to varying extents. Maximum unloaded shortening velocity was determined using the slack test method. We reported previously that V_{max} was 0.92 cell lengths/sec (Biophys. J. 47:296a, '85), several times greater than previously reported in tissue strips. The slowing of this V_{max} relative to skeletal muscle is similar to the slowing of the AM-ATPase. This may well reflect the fact that the steps limiting AM-ATPase and V_{max} are probably quite similar in both muscle types. However, even lower values (0.19 cell lengths/sec) for V_{max} have been reported in these SMC's (Warshaw: Biophys. J. 47:299a, '85). In order to ascertain the cause for this difference we investigated the effects of low $[\text{Ca}^{++}]_0$ (0.18 mM) and ISO (1-10 μM) on V_{max} - the principle difference between the two studies. Our results showed that ISO (10 μM) decreased V_{max} to 1/3-1/2 especially in low Ca, although low Ca itself did not remarkably affect it. These results may be explained by a direct effect of the cAMP-protein kinase system on cross-bridge turnover. Grant support: NIH (HL14523) and MDA.

W-Pos62 **CONTRACTION OF SKINNED SINGLE SMOOTH MUSCLE CELLS.** Gary J. Kargacin and Fredric S. Fay, Dept. of Physiology, Univ. of Mass. Med. Ctr., Worcester, MA.

Single smooth muscle cells isolated from intact tissue continue to be the subject of much experimental interest. To investigate more completely the fundamental events in excitation-contraction coupling and force generation in such cells, we have developed techniques for chemically permeabilizing, or "skinning" them. Suspensions of single smooth muscle cells isolated enzymatically from the stomach of the toad *Bufo marinus* are resuspended in high K^+ rigor solution (0 ATP, 5 mM EGTA) and exposed briefly to saponin. Trypan blue uptake and SDS gel electrophoresis indicate that at saponin concentrations between 20 and 50 $\mu\text{g}/\text{ml}$ virtually all cells in a suspension are skinned and that they retain all of their major high molecular weight proteins. Under the electron microscope, skinned cells in rigor solution are seen to have a fragmented loosely attached surface membrane but retain numerous thin (actin) filaments arranged in tight rosetts around thick (myosin) filaments. Those fixed after ATP is added show a more diffuse arrangement of thin filaments around the thick filaments producing a more uniform distribution of actin throughout the cell cross section. We have begun to study control of shortening in skinned cells and find that they shorten in the presence of ATP and Ca^{++} to $<1/3$ their resting length at a rate dependent on $[free\ Ca^{++}]$ and approximately half maximal at $pCa\ 6.2$. Shortening rate at a given $[Ca^{++}]$ is reduced in the presence of trifluoperazine and increased when cells are preincubated in ATPyS indicating that the Ca^{++} control mechanism thought to be responsible for regulation of contraction of intact smooth muscle is retained after saponin treatment. Supported by NIH grants HL14523 and AM07341 and by a MDA grant in aid.

W-Pos63 **HIGH TIME RESOLUTION MEASUREMENTS OF $[Ca^{++}]$ IN SINGLE SMOOTH MUSCLE CELLS USING FURA-2 AND AN ULTRA-FAST DIGITAL MICROFLUORIMETER.** J.F. Hatch, D.A. Williams, K.E. Fogarty and F.S. Fay. Dept. of Physiology, Univ. of Mass. Med. Ctr., Worcester, MA.

In order to obtain insights into excitation-contraction coupling in smooth muscle, we have developed a high time resolution microfluorimeter to measure $[Ca^{++}]$ in Fura-2 loaded single cells with 4 msec time resolution with the goal of relating msec changes in $[Ca^{++}]$ with changes in electrical and contractile activity in the same cell. The microfluorimeter fits onto a standard microscope and consists of transmissive sectors peaking at 340 and 380 nm separated by two smaller opaque sectors. Wheel geometry has been optimized for maximum fluorescence data collection per revolution without cross-talk between the two spectral channels. Optical disc position and rotational speed is detected via an infrared optoelectronic sensor focused onto a reflective/absorptive index attached to the optical disc. Fluorescence emission at 500 nm is detected during 340 and 380 excitation by a digital photomultiplier/photon counter gated from signals derived from the index. Cytoplasmic $[Ca^{++}]$ is calculated once per revolution by comparing the ratio of fluorescence at 340:380 to similar ratios obtained with Fura-2 \pm saturating levels of Ca^{++} . Utilizing this approach, resting $[Ca^{++}]$ in Fura-2 loaded isolated relaxed smooth muscle cells was found to average 134 nM; in fully contracted cells it was typically $\sim 1\ \mu\text{M}$. A rise in free cytoplasmic $[Ca^{++}]$ was found to always precede the onset of contractions as determined as the beginning of cell shortening. The precise kinetic relation of changes in membrane potential, cytoplasmic $[Ca^{++}]$ and contraction are presently being investigated using this approach. Supported in part by grants from the NIH (HL14523) and the MDA.

W-Pos64 **MAXIMAL CELL SHORTENING IN INTACT SMOOTH MUSCLE REQUIRES RELATIVELY SMALL CHANGES IN CYTOPLASMIC Ca^{++} : MEASUREMENTS OF FURA-2 FLUORESCENCE IN SINGLE CELLS.**

David A. Williams, Kevin E. Fogarty and Fredric S. Fay, Physiol. U. Mass. Med. Sch. Worcester, MA.

The digital imaging fluorescence microscope, coupled with the Ca^{++} -sensitive fluorescent probe Fura-2, has been used to investigate the changes which occur in free cytoplasmic $[Ca^{++}]$ accompanying activation of single isolated smooth muscle cells. A series of fluorescent images (10-30 frames) were automatically collected at alternating wavelengths (340 nm and 380 nm excitation: 500 nm emission) from a single dye loaded cell (internal dye concentration 10-30 μM). During this period the cell was stimulated by application of a depolarizing stimulus, (brief electrical stimulus or localized application of an isosmotic K^+ based ringer solution). Total cell fluorescence and cell length were determined in each image using interactive graphics software. Half times for the contraction and relaxation of single cells were 3-6 and 20-50 sec ($n=10$) respectively. The $[Ca^{++}]$ increased significantly before (1-2 sec) any change in cell length was noted, peaked at a relatively low value of between 600-700 nM before maximal cell shortening had occurred, and returned to prestimulus levels (140 nM) while the cell had reextended only $\sim 20\%$. Preliminary results obtained with cholinergic stimuli (e.g. ACh) show quantitative similarities. Localized contractions (with localized $[Ca^{++}]$ elevations), and larger elevations ($>1\ \mu\text{M}$) of cytosolic $[Ca^{++}]$ were achieved through stimuli such as mechanical agitation of the cells or by passage of supra-maximal electrical stimuli. The results point to a direct, primary role for Ca^{++} in smooth muscle contraction and to the involvement of powerful regulatory mechanisms for limiting increases in cytoplasmic $[Ca^{++}]$ during contractile activity. Supported by grants from the NIH (HL14523) and the MDA. D.A.W is an Australian National Heart Foundation Research Fellow.

W-Pos65 3-D DISTRIBUTION OF Ca^{++} IN SINGLE CELLS DETERMINED USING FURA-2 WITH THE DIGITAL IMAGING MICROSCOPE. K.E. Fogarty, D.A. Williams and F.S. Fay. Dept. of Physiology, Univ. of Mass. Med. Ctr., Worcester, MA. Intr. by James G. Dobson, Jr.

Ca^{++} is believed to control a variety of cellular processes often with a high degree of spatial and temporal precision. Ca^{++} in single living smooth muscle cells has been measured in two dimensions utilizing a digital imaging microscope equipped for epi-fluorescence and the highly fluorescent Ca^{++} sensitive dye Fura-2. In a single image obtained when focused midway through the cell, free Ca^{++} levels over the cytoplasm (137 nM), nucleus (220 nM), and sarcoplasmic reticulum (500 nM), can be clearly distinguished. An uncertainty arises in such images because the cellular compartments are 3-D in nature and the fluorescence microscope, even using the highest magnification and numerical aperture lenses, has a large depth of field. Thus, the 2-D image of the 3-D cell structure accesses contributions of Ca^{++} in structures above and below the image plane. We modeled the entire imaging process with assumed cell geometry based upon our biological data: nuclear and SR Ca^{++} greater than that in the cytoplasm. We found that the cytoplasmic $[\text{Ca}^{++}]$ measured in an image plane midway through the model image exceeded its true concentration by 30%, due to a mixture of signal from the nucleus and the SR; that nuclear $[\text{Ca}^{++}]$ was underestimated by 10% due principally to mixture with the cytoplasmic signal; and that SR $[\text{Ca}^{++}]$ was underestimated by at least 20%. In response to this problem, we have developed a 3-D iterative image restoration algorithm reversing distortion due to the image formation process and yielding an even more accurate measure of localized $[\text{Ca}^{++}]$. Supported in part by grants from the NIH (H114523) and the MDA.

W-Pos66 CELL VOLUME MEASUREMENT USING THE DIGITAL IMAGING FLUORESCENCE MICROSCOPE (DIFM).

Peter L. Becker & Fredric S. Fay, Dept. Physiol., U. Mass. Med. Ctr., Worcester, MA.

In order to accurately determine the intracellular concentration of any fluorescent indicator, it is essential to be able to accurately determine cell volume. A method was devised to accomplish this. Single toad-stomach smooth-muscle cells in Ringers containing 2.0 mg/ml of rhodamine labeled dextran (60-90,000 mw) were placed in a 100 μm deep chamber and viewed with the DIFM (40x, 0.66 N.A. obj.). Images were taken of the cell (cell image) and when the cell was out of view (non-cell). Since cells displace dye proportional to their volume, they appear dark. A crude estimate of volume is the IOD (integrated optical density) of the image resulting from a subtraction of the cell image from the non-cell image. However, IOD's of difference images from repetitive cell and non-cell images showed unacceptable variability. Sources of variability are: (1) temporal variations (bleaching and variations in illumination); (2) spatial variation in system gain (non-uniform illumination, optical imperfections, etc.); and (3) pixel noise of the measurement system. Type 3 errors were minimized by only processing pixels within $\sim 4 \mu\text{m}$ of the cell. To correct type 1 errors, the IOD of a region surrounding the cell was divided by the IOD of that region in the non-cell image, yielding a scaling factor used to adjust the non-cell image before subtraction. To correct for type 2 errors, the difference image was divided (pixel by pixel) by the non-cell image, under the assumption that spatial variations in the non-cell image intensity are mainly due to spatial variations in system gain. Using these corrections, relative volume measurements of the same cell have a S.D. of $<4\%$, and are independent of focal plane, at least within 8 μm of the cell's center plane. Absolute volume can be determined by calibrating with objects of known volume. Support: NIH (H114523) and MDA.

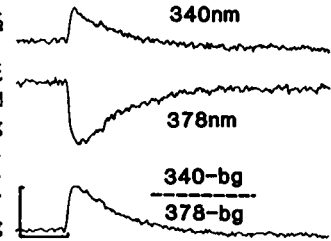
W-Pos67 USE OF FURA-2 AND DIGITAL IMAGING METHODS TO DETERMINE CYTOSOLIC FREE Ca^{2+} IN LIVING SINGLE ARTERIAL SMOOTH MUSCLE CELLS. W.F. Goldman, W.G. Wier and M.P. Blaustein (SPON: R.J. French), Dept. of Physiol., Univ. of Maryland Sch. Med., Baltimore MD, 21201

A rise in cytosolic free Ca^{2+} , $[\text{Ca}^{2+}]_{in}$, is the immediate trigger for contraction in arterial smooth muscle (ASM). However, it has not previously been possible to measure $[\text{Ca}^{2+}]_{in}$ in single living ASM cells because of their small size. In the present study we employed the Ca -sensitive fluorochrome, fura-2, to measure $[\text{Ca}^{2+}]_{in}$ in single ASM cells with low light level digital imaging microscopy. Viable ASM cells were obtained from bovine tail arteries by enzymatic digestion. Fura-2 loading was accomplished by adding 5 μM fura-2/AM, the acetoxymethyl ester, to the digestion medium 30 min before the end of the digestion period. The dissociated, fura-2 loaded ASM cells were spindle shaped when relaxed in normal Krebs' solution containing 1.0 mM Ca ; they contracted rapidly in response to a pulse of norepinephrine (NE), and then slowly relaxed as the NE diffused away. Fluorescent images (at 510 nm) of single ASM cells were recorded on video tape during excitation with 340 nm and 378 nm light. Digital processing of the video taped images was used to obtain 340/378 nm image ratios; data from several video frames were usually averaged before obtaining the image ratios. In some instances we also employed a photomultiplier tube to measure the emitted light directly. The system was calibrated directly through the microscope using the fluorescence ratios of solutions containing fura-2 and known $[\text{Ca}^{2+}]$. Preliminary data indicate that resting $[\text{Ca}^{2+}]_{in}$ is $\sim 100-150$ nM; $[\text{Ca}^{2+}]_{in}$ is increased in contracting and damaged cells. We conclude that digital imaging methods will enable direct analysis of the distribution of $[\text{Ca}^{2+}]_{in}$ in the cytosol, and the role of changing $[\text{Ca}^{2+}]_{in}$ in mammalian vascular smooth muscle. Supported by AHA & NIH.

W-Pos68 **[Ca²⁺]_i IN RESTING AND CONTRACTING SINGLE HEART CELLS: SPATIALLY AVERAGED FURA-2 SIGNALS, AND SPATIALLY RESOLVED FURA-2 SIGNALS FROM DIGITAL IMAGING MICROSCOPY**

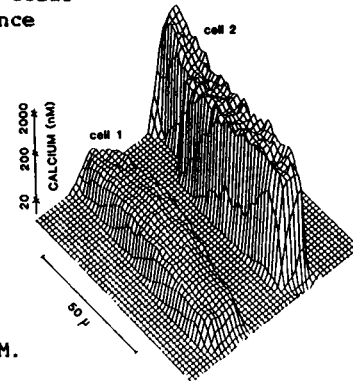
W.G. Wier and E. Marban, Department of Physiology, University of Maryland School of Medicine and Department of Medicine, The Johns Hopkins Medical Institutions, Baltimore, MD

Single, fura-2 loaded rat ventricular cells were studied using an inverted microscope equipped with epifluorescence illumination, an intensified silicon intensifier target camera video system (v.s.) and a photomultiplier tube (p.m.t.). The p.m.t. system is linear, fast, and has a large dynamic range, but provides a spatially averaged measure of fura-2 fluorescence. When combined with digitization of single frames, the v.s. provides spatial information on fura-2 fluorescence in the cell (340/380 fluorescence ratios at each pixel) but is non-linear and has poor temporal resolution. Quantitative agreement between the two systems provides important tests of methodology. The v.s. measurements indicate a uniform distribution of [Ca²⁺]_i in resting cells, a prerequisite for using the fura-2 ratio method with spatially averaged signals (p.m.t.). In individual resting cells, [Ca²⁺]_i calculated using p.m.t. and v.s. agree closely: 61 ± 21 nM in 6 cells at 37°C in 1 mM [Ca]_o; 518 ± 99 nM in 4 cells exposed to .3 mM ouabain and 10 mM [Ca]_o. Averaged records of fura-2 fluorescence, and the corresponding fluorescence ratio signal recorded with p.m.t. from a stimulated cell contracting under physiological conditions, are shown in the inset (calibration: 0.2 ratio units, 0.2 sec.). From a level indicating [Ca²⁺]_i of 60 nM, the ratio signal rises to a peak within 30 msec before declining with a t_{1/2} of 160 msec. Comparable data from v.s. is being sought.



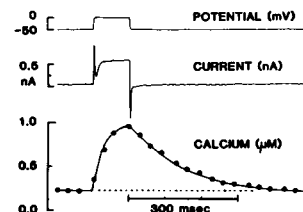
W-Pos69 **FREE INTRACELLULAR CALCIUM IN NORMAL AND CALCIUM-OVERLOADED RAT HEART CELLS: DIGITAL IMAGING FLUORESCENT MICROSCOPY USING FURA-2.** M.B. Cannell, W.G. Wier, J.R. Berlin, E. Marban and W.J. Lederer. Dept. Physiol., Univ. Maryland Med. Sch. and Dept. Med., Johns Hopkins Univ., Baltimore, MD.

Enzymatically dissociated adult rat heart muscle cells were exposed to 5 μM fura-2 AM for 10 minutes and then incubated in fura-free media for one hour. The cells were illuminated sequentially at 340 nm and 380 nm and fluorescence was observed at 510 nm using either an ISIT video camera or a photomultiplier tube. After background subtractions, the image obtained with 340 nm illumination was divided pixel-by-pixel by the 380 nm image to yield a "ratio image", the values of which reflect free intracellular calcium activity. The figure is a surface plot of intracellular calcium of two neighboring cells. Cell 1 (left) was a normal quiescent cell which had a mean calcium of about 100 nM. Cell 2 (right) was typical of a "calcium-overloaded" cell which had spontaneous fluctuations of calcium and had propagating fluctuations ("waves") of increased subcellular calcium and of shortening. This calcium-overloaded cell had a mean calcium of more than 1 μM.



W-Pos70 **Ca²⁺ TRANSIENTS ELICITED BY VOLTAGE-CLAMP DEPOLARIZATIONS IN SINGLE RAT VENTRICULAR MUSCLE CELLS CALCULATED FROM FURA-2 FLUORESCENCE IMAGES.** M.B. Cannell, J.R. Berlin and W.J. Lederer. Dept. Physiology, Univ. of Maryland Sch. of Med., Baltimore, MD 21201

Enzymatically-dissociated single rat heart muscle cells were viewed through a dual-excitation-wavelength fluorescence microscope and voltage-clamped with a single microelectrode technique. Fura-2 was loaded into the cells by diffusion from the microelectrode (containing 0.2 mM fura-2 in 140 mM potassium glutamate) after gigaseal formation and breaking into the cell. Fluorescence at 510 nm was recorded using an ISIT camera and video recorder. Video frames were digitized and images (formed by dividing images obtained with 340 nm illumination by those obtained at 380 nm) were calculated on a frame-by-frame basis after correction for nonlinearities in the recording system. The ratio was converted to free Ca²⁺ with an in-vitro calibration curve. By calculating free Ca²⁺ from images of the cells, artifacts associated with cell movement and the light emission from the electrode were eliminated. Figure 1 shows the changes in free Ca²⁺ associated with 100 msec depolarizations from -50 mV to 0 mV that were applied at 1 Hz. In this experiment a resting calcium level of 230 nM is observed at -50 mV which rises on depolarization with good spatial uniformity to a peak value of 950 nM. On repolarization, calcium declines slowly and remains elevated for more than 300 msec following the repolarization.



W-Pos71 QUASI-ELASTIC LIGHT SCATTERING MICROSCOPE SPECTROMETER. Paul S. Blank, Roy B. Tishler, Francis D. Carlson, Jenkins Dept. of Biophysics, The Johns Hopkins University, Baltimore MD. 21218

We have developed a high performance quasi-elastic light scattering (QELS) microscope spectrometer by suitably modifying a commercially available instrument, the Nikon Diaphot. The coherence requirements of microscope spectrometers have been developed and our system performs in agreement with theory. Microscopic scattering volumes can be studied with a minimum of spatial averaging effects on the measured intensity autocorrelation function. Spatial averaging effects were examined as a function of the ratio of detector area to coherence area over the range .004 to 10.0. The measured amplitudes of the intensity autocorrelation function, $g^2(\tau=0) - 1$, from light scattered through 90 degrees from .109 μm diameter polystyrene latex spheres were in agreement with theory. The measured diffusion coefficient of .357 μm diameter polystyrene latex spheres, $1.21 \pm .01 \times 10^{-8} \text{ cm}^2/\text{sec}$, from scattered light collected over a range of angles from 30 to 90 degrees, was in agreement with the calculated value of $1.203 \pm .018 \times 10^{-8} \text{ cm}^2/\text{sec}$. The instrument is now being used to examine transport and membrane phenomena in isolated cells. This work was supported by U.S.P.H./N.I.H. grant 5R01AM12803-25,26 (F.D.C.), 5T32GM07231 (P.S.B.), and 5T32GM07309 (R.B.T.).

W-Pos72 ANALYSIS OF MULTI-COMPONENT EMISSIONS BY PHASE SENSITIVE DETECTION OF FLUORESCENCE, by S. Keating-Nakamoto, H. Cherek and J.R. Lakowicz, University of Maryland, School of Medicine, Department of Biological Chemistry, Baltimore, Maryland 21201.

We describe the resolution of the lifetimes and steady state fractional intensities of each component in multi-component fluorescence emissions, using phase sensitive data collected at one or more modulation frequencies. While the analysis of data from one frequency requires knowledge of the individual steady state spectra of each component, fits of phase sensitive data recorded at more than one frequency do not require knowledge of the component spectral distributions. Analysis of the data using a non linear least squares routine reveals the component lifetimes and wavelength dependent fractional intensities, thus reconstructing the steady state spectra of each component. Two and three component mixtures of the fluorophores, N-acetyl-L-tyrosinimide, N-acetyl-L-tryptophanimide, indole and 2,3-dimethylindole were resolved using data collected at only 30 MHz. These probes have closely spaced lifetimes of 1.5, 2.9, 4.5 and 4.3 nsec respectively and display a large amount of spectral overlap. The analysis of simulated and experimental phase sensitive variable frequency data will be presented to illustrate how the spectral resolution is affected by increasing spectral overlap and lifetime separation. These simulations indicate that phase sensitive detection can be used to resolve multi-component emissions of closely spaced fluorophores even when the steady state spectra of the component probes are unknown.

W-Pos73 WIDEBAND ACOUSTO-OPTIC MODULATOR FOR FREQUENCY DOMAIN FLUOROMETRY. D. W. Piston and E. Gratton, Department of Physics, University of Illinois, Urbana, IL 61801.

The new technique of multifrequency phase fluorometry allows for accurate analysis of fluorescent activity using frequency domain measurements. So far, techniques for wideband modulation of light have been restricted to the Pockel's cell or intrinsically modulated sources such as the mode-locked laser and synchrotron radiation. A Pockel's cell modulator requires both a very well collimated beam and very high voltages for efficient modulation. We have developed an acousto-optic modulator which can be used with either CW laser sources and highly collimated arc lamps. The novelty of this new modulation scheme is that quasi-continuous modulation frequencies can be produced from DC to above 40 MHz and also from 80 MHz up to 200 MHz. The modulation efficiency is about 50% and the RF power required to drive the modulator is only a few watts. In this new design, two acoustic standing waves are generated simultaneously in the same medium and modulation is achieved by proper combination of the two standing wave frequencies. The propagation medium of the acoustic wave is a fused quartz bar in which the faces are optically flat and parallel. A standing wave at any given frequency may be obtained by varying the temperature of the modulator. In our system, one frequency is fixed for optimum efficiency of modulation at 80 MHz, while the other can be set quasi-continuously between 50 MHz and 110 MHz. By varying this second frequency we can obtain modulation at the sum and difference of the two frequencies, as well as excite other modes of the modulator. Supported in part by the National Science Foundation grant NSF PCMB4-03107 and the Department of Navy grant MDA903-85-K-0027.

W-Pos74 MATHEMATICAL MODELS FOR PHOTON DIFFUSION IN BIOLOGICAL TISSUE. R. F. Bonner, R. Nossal and G. H. Weiss. National Institutes of Health, Bethesda, MD 20982.

Various characteristics of photon diffusion in turbid biological media are examined. Incident radiation is assumed to be applied at an interface between a turbid tissue and transparent medium, and the reemission of photons from that interface is analyzed. Making use of a discrete lattice model, we derive a mathematical expression for the joint probability $P(n, \underline{r}) d^2 \underline{r}$ that a photon will be emitted in the infinitesimal area centered at surface point $\underline{r}=(x,y)$, after having made n collisions with the tissue. Other expressions are obtained for: 1) the intensity distribution of diffuse surface emission, 2) the probability of photon absorption as a function of depth, and 3) the mean path length of detected photons as a function of the distance between the site of the incident radiation and the location of the detector. The theory has general applicability to the diagnostic and therapeutic uses of light on tissues. We show that the depth dependence of the distribution of photon absorptions can be inferred directly from measurements of the surface emission profile. Once the characteristic scattering and absorption parameters for a given living tissue have been obtained, the analytical expressions can be used to provide other relevant information. Results of pertinent computer simulations also are presented. We illustrate use of the theory by interpreting data acquired with Laser Doppler blood flow monitors.

W-Pos75 THE CONTRIBUTION OF LINEAR DICHROISM AND BIREFRINGENCE TO THE APPARENT CIRCULAR DICHROISM OF GELS AND SUSPENSIONS. Rex P. Hjelm, Jr.*, Pappan Thiyagarajan and Michael E. Johnson, Department of Medicinal Chemistry and Pharmacognosy, University of Illinois at Chicago, Chicago, IL 60680.

The circular dichroism (CD) of oriented systems is known to be strongly affected by the presence of net linear dichroism (LD) and birefringence (LB) in the sample. The presence of such effects can easily be detected by a strong dependence of the CD on sample orientation. Systems, such as liquid crystals, consisting of plates with optical axes related by a helical screw also show strong influences in the CD from the LB and LD of the plates and the screw angle between them, even though no net LB and LD is apparent, and the spectra are, as a result, invariant with orientation. We show here, using Stokes-Mueller formalism, that in any gel or suspension, consisting of randomly oriented domains or particles, there is a contribution to the CD from the LB or LD of the individual domain or particles. The spectra are orientation invariant. The effects of LB and LD are significant when the domains or particles are of sufficient absorbance that second order terms in LB and LD are significant in the elements of the Mueller matrix representing the optical properties. Thus when aggregates of molecules show significant changes in the CD compared to the solution spectrum, then the interpretation of such changes as molecular CD is problematic unless it can be shown that the individual domains or particles have no LD or LB or that second order effects can be neglected. We show how significant such effects can be in the CD in the so-called region of sickle hemoglobin gels. Gels formed at 25°C show strongly orientation dependent CD that are radically different from the CD of the molecule in solution. Gels formed at 35°C show an orientationally invariant CD that appears to be a linear combination of the orientation dependent spectra of 24°C gels. These effects are understandable in terms of this theory and the domain structure of the gels.

W-Pos76 ^{35}Cl AND ^2H NMR MEASUREMENT OF INTRACELLULAR WATER VOLUME. David Hoffman and Raj K. Gupta
Dept. Physiology & Biophysics, Albert Einstein College of Medicine, Bronx, N.Y. 10461

Knowledge of cell water volume is essential for the calculation of concentrations of intracellular ions and metabolites. We have developed a method which utilizes $^{35}\text{Cl}^-$ NMR as a measure of extracellular volume and ^2H NMR as a measure of the ratio of intra- and extracellular water volumes. Measurement of extracellular volume by $^{35}\text{Cl}^-$ NMR is possible since intracellular $^{35}\text{Cl}^-$ resonance is broadened beyond detection in most cells. The ^2H NMR measurements exploit the fact that only extracellular water is in direct contact with a membrane-impermeant shift reagent. However, rapid exchange of water across the cell membrane results in only a single $^2\text{H}_2\text{O}$ resonance at a chemical shift which is a weighted average of the shifted extra- and unshifted intracellular water resonances and is therefore a direct measure of the fractional intracellular water volume. We find $[\text{Dy}(\text{citrate})_2]^{3-}$ and $[\text{DyEDTA}]^-$ to be useful as stable chemical reagents for shifting the water resonance. Both ^{35}Cl and ^2H measurements can be performed using the same sample and NMR probe configurations, thus eliminating errors due to variations in the ratio of extra- to intracellular spaces throughout the sample volume. Denoting the extracellular volume as a fraction of the total volume by S_0 , and the extracellular water volume as a fraction of the total water volume by H_0 , the fractional cell water content $W = [(1/H_0)-1]/[(1/S_0)-1]$. The average water content of 8 red blood cell samples was found to be $67.8 \pm 5.2\%$. A somewhat similar approach based on ^1H NMR has been suggested by Cowan et al (FEBS Lett. 184, 130). However, the paramagnetic broadening of the ^1H resonance is about 40-fold greater than that of the ^2H resonance and the use of different NMR samples and probe configurations for the ^1H and ^{23}Na measurements may introduce additional errors. (Supported by NIH Grant AM32030. D.H. is a fellow supported by NIH Training Grant HD07053).

W-Pos77 A ^{13}C NMR STUDY OF GLUCONEOGENESIS IN ISOLATED PERFUSED LIVERS FROM NORMAL MICE AND MICE IN REMISSION FROM MALARIA. Yves Geoffrion, Thérèse Kroft, Keith Butler, Ian C.P. Smith and Roxanne Deslauriers. Division of Biological Sciences, National Research Council of Canada, 100 Sussex Drive, Ottawa, Canada K1A 0R6.

One dose of Cyclosporin-A (CY) causes a 4-5 day remission from the rapid and fatal *Plasmodium berghei* infection in CF-1 male mice. The gluconeogenic rates of perfused livers isolated from starved control (C) and CY-treated control mice (C+CY) were identical with 10 mM unlabeled or $[2-^{13}\text{C}]$ pyruvate. ^{13}C NMR spectra from HClO_4 extracts of freeze-clamped livers perfused with $[2-^{13}\text{C}]$ pyruvate showed identical labeling patterns of all metabolites in both C+CY and C livers. Isolated perfused livers from starved, 48h-malarial animals (M) were used when they showed a 30% level of parasitemia. The gluconeogenic rate of the liver of M mice was 75% of that found in C or C+CY livers. When M mice were used 2 days after treatment with CY (M+CY), they showed a 0% parasitemia but produced glucose from pyruvate at a rate identical to that of the M livers. The liver extracts showed a similar labeling pattern of metabolites in all control and malarial groups, with lactate, pyruvate, alanine, glutamate, glutamine, citrate, serine and aspartate being labelled in the same positions and to similar extents. However, the labeling patterns of glucose and glycogen were different in the M and M+CY livers relative to those of the C and C+CY livers. Our results indicate that the reduced gluconeogenic rate found in M mice is not restored to that of control mice on treatment with cyclosporin (M+CY), even though the treated animals show no apparent signs of the malarial infection.

W-Pos78 MEASUREMENT OF ROTATIONAL MOLECULAR MOTION BY SATURATION RECOVERY EPR.

P. Fajer, J. Feix, J. Hyde and D. Thomas, Dept. of Biochem., Univ. of Minnesota, Minneapolis and National Biomedical ESR Center, Medical College of Wisconsin, Milwaukee.

Saturation-recovery EPR utilizes an intense microwave pulse to saturate the spin population with one particular orientation with respect to the magnetic field. Time evolution of the signal is then observed. The signal increases in time as saturation is relieved by spin-lattice relaxation (T_1) as well as by rotational diffusion (τ_r) bringing non-saturated spins into the resonant position. In the presence of both events the recovery is characterized by a double exponential, with the initial phase related to τ_r and the second phase determined by T_1 . We have measured the saturation recoveries of spin labelled haemoglobin tumbling in media of known viscosities, as a function of τ_r and pulse duration (t_p). For rates between 0.2 and 20 μs , biexponential deconvolution of the signal response to short pulses gives reliable estimates of τ_r . The rates estimated from the initial phase of recovery were 0.7 ± 0.3 , 1.2 ± 0.6 , 4.3 ± 1.3 and 15.6 ± 4.7 μs for haemoglobin tumbling with $\tau_r = 0.24$, 2.0, 5.0, and 20.0 μs , respectively. Long pulses quenched the motional effects and recovery times were in good agreement with T_1 determined from the tail of recoveries following the short pulses. Variation of the pulse time can also be used to determine τ_r . The recovery is a single exponential when $t_p \leq \tau_r$ and a double exponential when $t_p \gg \tau_r$. For faster diffusion, recoveries are determined by T_1 as the saturation is equilibrated by the motion between resonant and non-resonant spins during the pulse. For much slower motion, rotation is ineffective in transferring non-saturated spins into resonance and the recovery is again determined solely by T_1 .

W-Pos79 1H NMR METHOD FOR INDIRECT DETECTION OF 13C IN THE PERFUSED LIVER MOUSE LIVER SPECTRUM

T. Jue, F. Arias-Mendoza, and R.G. Shulman

Dept. of Mol. Biophys. and Biochem., Yale University, New Haven, CT 06511

The potential sensitivity gain of 1H over 13C NMR holds a distinct promise that low concentration metabolites in in vivo systems can be detected. We have directed our attention to refining indirect detection methods in order to follow dynamic processes in the perfused mouse liver system. By using a heteronuclear editing scheme involving a 1H semi-selective spin-echo pulse sequence (1331) and a 13C 0/180 pulse applied synchronously with the 180 1H pulse, we have avoided the attendant problems of the intense water signal and the 1H-1H homonuclear Jmodulation effects. The spin-echo evolution time is 50 ms, $t = n/2J$, where J is the 13C-1H coupling constant of about 125 Hz. Only the 13C protons are edited from the 1H spectrum.

1H: 90 (1331)----t----180 (2662)----t----ACQ (+/-)

13C: 0/180

We have applied the technique in following ethanol oxidation via both the alcohol dehydrogenase and aldehyde dehydrogenase enzyme reactions. 13C labeled C2 ethanol was infused into the perfusion medium and the time course of acetate formation was followed. No acetaldehyde signal was detected in either the 13C or 1H spectra. The time resolution of the 1H NMR experiment was about 1.5 minutes. Sensitivity enhancement of 1H over 13C was clearly noticeable. Such kinetics would be difficult to observe by conventional 13C NMR. Consequently, our experimental results underscore the applicability of indirect detection methods in monitoring dynamic processes in vivo.

W-Pos80 FURTHER STUDIES ON THE APPLICATION OF METHYLPHOSPHONATE AS AN INDICATOR OF INTRACELLULAR PH BY ^{31}P -NMR. M. De Fronzo, R. J. Gillies and N. Didier; Dept. Biochem.; Colorado State University; Fort Collins, CO 80523.

In whole-cell or *in vivo* ^{31}P NMR experiments, intracellular pH (pH^{in}) has been monitored using the chemical shifts of inorganic phosphate or 2-deoxyglucose-6-phosphate (1). There are numerous disadvantages in the application of these indicators (1,2). Because of these limitations, methylphosphonate (MP) has been proposed as an alternative indicator of pH^{in} (1-3).

We have recently been investigating the application of this compound to Ehrlich ascites tumor cells in more detail. *In vitro*, we have observed that the pK_a of MP is extremely insensitive to ionic strength, the presence or absence of specific ions and to temperature. All of these observations support the use of MP as a pH^{in} indicator. However, we have also obtained data which might limit its applicability.

The T_1 of MP is anomalously long, being about 8.5 seconds in buffer at 37°C . There is also apparently contradictory data regarding its permeability characteristics. Assuming equimolar equilibrium distribution, MP does not enter cells to a significant degree within 4 hours under NMR conditions. Under similar conditions, MP has been observed to escape from pre-loaded cells within 15 minutes. There are a number of possible explanations for this behavior which are currently being explored.

- 1) Gillies et al. (1982) in "Intracellular pH" Alan R. Liss
- 2) Slonczewski et al. (1982) Proc. Nat. Acad. Sci. USA 78, 6271-6275
- 3) Gillies et al. (1985) 4th Mtg. Soc. Mag. Reson. Med., p. 465

W-Pos81 NMR IMAGING AT 400 MHZ. Ronald A. Meyer, Charles B. Mulhern and Truman R. Brown. NMR Lab, Fox Chase Cancer Center, Philadelphia, PA 19111

In order to examine the potential for NMR imaging of small biological samples at very high fields, we have interfaced a Bruker AM 400 spectrometer (7.3 cm clear bore) with the waveform memories and gradient power supplies of a Biospec. Our prototype imaging probe includes dedicated gradient coils (each 4 turns, 22g) which generate maximum gradients of 5 Gauss/cm (at 10 amp), and interchangeable parallel-loop saddle-shaped transceiver coils with diameters of 3.2, 1.6, or 0.6 cm. Proton images of the brains of live adult and newborn mice were obtained by the 2DFT spin-echo technique ($\text{TR}=1-2$ sec, $\text{TE} = 30-70$ msec), with pixel size ranging from 80×80 to 150×150 microns (500 micron slice thickness). Thus, gross anatomical features of the mouse brain (ventricles, optic and olfactory tracts, etc.) could easily be resolved using the device. Using the smaller coils, images of excised rat and mouse tissues were obtained with pixel size down to $30 \times 30 \times 200$ microns. These results suggest that high field proton imaging will prove useful for monitoring development of embryos, as well as non-invasive imaging of, for example, experimental tumor growth in mice. (Supported by NIH AM-36146-01.)

W-Pos82 NORMALIZED INTEGRAL ST-EPR, AN EASIER METHOD OF ST-EPR ON BIOLOGICAL SAMPLES.

Arnt Inge Vistnes, Inst. of Physics, University of Oslo, Blindern, Oslo, Norway.

Saturation transfer EPR is a powerful technique in the study of dynamical behavior of biological systems. However, biological samples have poor S/N which make phase adjustment difficult. Also the spectrum is often composite of narrow line resonances superimposed on the slow motion spectrum.

MH-PER and M-ST-EPR can be modified to minimize these problems, but integration procedures seems to be more promising because of their higher S/N. This technique was first introduced by Evans (J. Magn. Res. 44(1981)109) and later modified by Horvath and Marsh (J. Magn. Res. 54(1983)363). The latter procedure is not very practical since it requires that various spectra be recorded successively to get enough data for the complete analysis. Also the phase problem still remains. The method introduced here utilizes a digital phase sensitive detector* to minimize these problems. Two spectra are recorded simultaneously from a single sweep. The digital data is manipulated to produce a normalized integral that increases monotonically with the rotational correlation time. Furthermore, it is independent of the phase setting and depends only on the rapid motion component when this component is very strong. The algorithm for calculation of such a normalized integral will be given. The analysis is automated and the computer output yields, beside of the normalized integral value, the corresponding rotational correlation time estimated from isotopic tumbling data (spin-labelled hemoglobin in glycerol/water). In summary, the method offers no new concepts, but it certainly makes life easier for the experimentalist.

* Vistnes et al. Rev. Sci. Instrum. 55 (1984) 527.

W-Pos83 PHOSPHORUS-31 NMR OF ALCOHOLIC CARDIOMYOPATHY IN HAMSTERS

R. White, J. Wikman-Coffelt, S. Wu, R. Sievers, M. Wendland, C. Higgins, T. James and W. Parmley, Depts. of Radiology and Medicine, University of California, San Francisco, CA.

Alcoholic cardiomyopathy is characterized by biochemical and functional abnormalities. Recently, protective and therapeutic effects from the use of agents causing calcium channel blockage have been proposed. In the present study, high-energy phosphate metabolism associated with alcoholic cardiomyopathy in the Syrian hamster (6 months of 50% ethanol) was studied both with and without concurrent treatment with a calcium channel blocker (verapamil, 1.2 mg/ml). Phosphorus-31 spectra were obtained to demonstrate relative changes in inorganic phosphate (Pi), phosphocreatine (PCr), and adenosine triphosphate (ATP), as compared to spectra in controls. These energy profiles were compared with indicators of cardiac performance. Findings were as follows:

| | Measured Mole Fraction | | | Developed Pres. (mmHg) | Coronary Flow (ml/min) |
|-------------------|------------------------|------------|------------|---------------------------|---------------------------|
| | Pi | PCr | ATP | | |
| Control | 0.18 ± .05 | 0.37 ± .03 | 0.44 ± .05 | 88.0 ± 1.1 | 8.6 ± 3.1 |
| Alcohol | 0.35 ± .06 | 0.34 ± .11 | 0.31 ± .06 | 39.0 ± 15.9 | 4.7 ± 1.4 |
| Alcohol+Verapamil | 0.10 ± .04 | 0.45 ± .06 | 0.45 ± .03 | 86.0 ± 8.4 | 5.0 ± 1.2 |

Body and heart weights were significantly greater in the control group than in the other two. There were marked biochemical alterations associated with alcoholic cardiomyopathy in the hamster, including a relative increase in Pi and decrease in ATP levels, consistent with diminished energy stores. Biochemical changes were manifested functionally in depressed cardiac performances.

W-Pos84 AN NMR STUDY OF THE EFFECTS OF METABOLIC ACIDOSIS ON PHOSPHORUS METABOLITE LEVELS IN LANGENDORFF PERFUSED RAT HEARTS IN THE PRESENCE AND ABSENCE OF VASODILATORS

M. F. Wendland, S. T. Wu, J. Wikman-Coffelt, T. Watters, R. Sievers, E. H. Botvinick, T. L. James, and W. W. Parmley (Introduced by: Jolinda A. Traugh), Departments of Pharmaceutical Chemistry and Medicine, Cardiovascular Division, University of California, San Francisco, CA.

Sprague-Dawley rat hearts were perfused for 30 min with a Krebs-Henseleit solution (pH 7.4). NMR spectra, intraventricular pressure and coronary flow rates were measured. Metabolic acidosis was induced by changing to a perfusate containing a reduced concentration of Na bicarbonate (6 mM compared to 25 mM), reducing pH to 6.5. Measurements were taken at 5 min intervals. After 30 min the hearts were re-equilibrated with the starting solution and measurements were continued for 15 min. With 4 mM Ca⁺⁺ in the perfusate, significant changes were observed in NMR spectra and physiologic measurements within 5-10 min of acidic perfusion. By 30 min, internal pH fell to 6.5, phosphocreatine (PCr) and ATP fell to 35% and 70% respectively of their original values, and coronary flow and developed pressure respectively fell to 50% and 30% of starting values. With re-equilibration at pH 7.4, further declines were observed and hearts died within 5-10 min. Reducing cardiac work, either by lowering Ca⁺⁺ or by apex puncture, protected the heart during acidosis. When the acidic perfusate contained a vasodilator (hydralazine, nitroglycerin or nitroprusside), internal pH fell to 6.8, and there were variable modest declines in PCr, ATP and developed pressure, while coronary flow remained above baseline values. When re-equilibrated at pH 7.4, all measured parameters returned to basal values within 15 min. The data were consistent with the idea that metabolic acidosis does not lead to permanent cellular damage when sufficient oxygen is present.

W-Pos85 SPATIALLY RESOLVED HIGH RESOLUTION ¹H NMR RELAXATION MEASUREMENTS OF HUMAN TISSUES IN SITU

P.R. Luyten, and J.A. den Hollander, Philips Medical Systems, P.O.Box 218, 5600 MD Eindhoven, The Netherlands.

Spatially Resolved Spectroscopy (SPARS) is a method to obtain high resolution NMR spectra of localized volumes in intact biological systems. The method is based upon a combination of selective and non-selective rf pulses such that the magnetization is dephased in the entire sample, except for the volume of interest (VOI) where longitudinal magnetization has been preserved. After these selection pulses a single non-selective 90 degree observation pulse generates a signal from the VOI. SPARS is a modification of VSE (1) in order to allow for implementation on a whole body MRI instrument.

SPARS is easily extended to spatially resolved NMR relaxation measurements. For T₁ measurements the SPARS sequence is preceded by a single 180 degree inversion pulse followed by a relaxation delay period; for T₂ measurements the observation pulse is replaced by a 90-180 degree spin echo sequence. In this way it is possible to measure T₁ and T₂ values for each of the resolved spectral lines. This information is not easily obtained in MRI measurements.

The method was used to measure relaxation times of human tissues *in situ*. Experiments were done on a 1.5 Tesla Philips Gyroscan, using the regular head and body coils. We measured ¹H NMR relaxation in a localized volume in the human bone marrow of the tibia, the calf muscle, and the liver. This approach provides a reliable way to measure multiple relaxation times in various human tissues, information which is crucial in the interpretation of T₁ and T₂ weighted MRI images.

(1) W.P. Aue *et al.*, J. Magn. Reson., 56, 350 (1984).

W-Pos86 A SIMPLE PROCEDURE FOR NMR MEASUREMENTS OF INTRA- AND EXTRACELLULAR SODIUM IN INTACT TISSUES. M. Bárány, C. Arús, R. Barmada, E. Abraham, J.A. Anderson, and S.F. Marotta. Departments of Biological Chemistry and Orthopaedics, and Research Resources Center, University of Illinois at Chicago, IL 60612

^{23}Na -NMR spectra were recorded with a 12 mm probe at 52.92 MHz in a Nicolet NMC-200 spectrometer, with 90° pulse angle, sweep width of ± 1302 Hz, 8 K data points, under fully relaxed conditions. A coaxial capillary containing 20 mM DyCl_3 and 40 mM $\text{Na}_5\text{P}_3\text{O}_{10}$ in $^2\text{H}_2\text{O}$ was inserted into the samples to serve as a chemical shift reference of -30.79 ppm, relative to the 0.00 ppm value of the 150 mM NaCl standard. The capillary was calibrated against a wide concentration range of pure NaCl solutions, for measurement of intracellular Na at the 0 ppm range, and against the same concentrations of NaCl solutions containing 2.5 mM DyCl_3 and 5 mM $\text{K}_5\text{P}_3\text{O}_{10}$ in 100 mM choline-Cl and 50 mM histidine-Cl, for measurement of extracellular Na between -10 and -13 ppm. Tissues (frog muscle, liver and skin, and human muscle biopsies) of known weight were placed into the 12 mm NMR tubes and a known volume of the shift reagent solution, 5 mM DyCl_3 , 10 mM $\text{K}_5\text{P}_3\text{O}_{10}$, 100 mM choline-Cl, and 50 mM histidine-Cl was added to the samples, followed by inserting the calibrated coaxial capillary. The area of the tissue-Na peak, from 0 to 0.6 ppm for the intracellular Na and from -4.3 to -12.7 ppm for the extracellular Na, and the area of the capillary-Na peak were integrated. From these areas, the calibration factor of the capillary, and from the weight of the tissue, the intra- and extracellular Na concentration of the tissue could be calculated. The sum of the intra- and extracellular Na was in agreement with the total Na content of the tissue, determined either by NMR or atomic absorption spectroscopy after trichloroacetic acid liberation of the total tissue Na. (Supported by MDA).

W-Pos87 NMR SPIN-LATTICE RELAXATION TIME STUDY OF HORMONE TREATED RAT BREAST TISSUES. H.S. Sandhu and G.B. Friedmann, Physics Department, University of Victoria, Victoria, B.C., Canada, V8W 2Y2

NMR spin-lattice relaxation, T_1 , was measured in normal and hormone treated (estradiol and clomiphene) rat breast tissues at room temperature ($\sim 21^\circ\text{C}$). These measurements were carried out at frequencies of 4 and 20 MHz using standard NMR pulse techniques. Estradiol was administered by subcutaneous pellets containing about 50 mg implanted in 9 month old virginal rats. Clomiphene was administered orally to 9 months and 3 months old virginal rats at 4 mg/kg live weight. T_1 was measured in the treated breast tissues over a period of time after which the rats were sacrificed. Breast tissue gave two T_1 values: one long [$(T_1)_L$] and the other short [$(T_1)_S$] contrary to previously reported single T_1 values ^{1,2}. The short T_1 at both 4 and 20 MHz showed no significant variations between the normal and the hormone treated samples. For Estradiol treated rats, the long T_1 was elevated after 5-6 days by $\sim 25\%$ at 20 MHz and $\sim 15\%$ at 4 MHz. The elevated value persisted till sacrifice. For clomiphene treated rats, the long T_1 values fluctuated with a 4 or 5 day period - perhaps reflecting the ovulating cycle.

¹) Beall, P.T. *Physiol. Chem. and Phys. and NMR*, 1984, 16, 129.

²) Beall, P.T. et al. *Mag. Res. Imaging*, 1984, 2, 83.

W-Pos88 VALIDATION OF NMR KINETIC MEASUREMENTS. E.W. McFarland and M.J. Kushmerick, Francis Bitter Magnet Lab, MIT, Cambridge, MA 02139; Dept. of Radiology, Brigham & Women's Hospital, Boston, MA 02115.

Unambiguous interpretation of NMR spin transfer experiments in terms of chemical reaction rates *in vitro* and *in vivo* require the assumption that the modified Bloch equations exactly describe the actual biochemical reaction scheme. Other typical complications encountered in living systems are cellular heterogeneity, overlapping resonances from nuclei in kinetically distinguishable compartments, and interactions not due to chemical exchange, such as nuclear overhauser effects (NOE). Our analysis of several NMR kinetic models accounting for heterogeneity and compartmentalization showed that, *in vivo*, significant differences between the actual and NMR-derived rates may arise. We extended the use of binomial-selective excitation to a transient kinetic experiment that involved monitoring the relaxation of all exchanging species following excitation of specific resonances. This technique and conventional steady-state saturation transfer were applied *in vitro* to the hydration of $^{13}\text{CO}_2$ and the ^1H exchange of valium isomerization. Both systems have well defined reaction mechanisms and rate constants. The ^{13}C exchange rates for the hydration reaction agreed with those measured chemically over a range of values from $.03$ - $.5$ s^{-1} . The rate constants determined using saturation transfer underestimated the ^1H exchange rate by more than 20% due to a strong NOE. The transient method can correctly account for these non-exchange processes. This study is the first comparison of NMR-derived rate constants to rate constants derived by non-NMR methods when the appropriate NMR techniques and all interactions are accounted for.

Supported by NIH grant AM-14485.

W-Pos89 A NEW PHOTON-COUNTING, 2-D X-RAY DETECTOR FOR MUSCLE DIFFRACTION. Brian Collett*, Keith Gorlen[§] and Richard J. Podolsky*, *NIADDK and [§]DCRT, NIH, Bethesda 20892

We have had a detector constructed for us by Instrument Technology Limited (29 Castleham Rd., St. Leonards-on-Sea, East Sussex, TN38 9NS, England) which consists of an imaging photon detector (Rees, D, et. al. J. Phys. E. 13,763,1980) fiber-optically coupled to a 40 mm gadolinium oxy-sulphide phosphor. X-ray photons falling on the phosphor are converted to light, which is then converted to electrons by a bi-alkali photocathode. The electrons are amplified by a micro-channel plate stack and fall upon a resistive anode. This produces two voltage pulses proportional to the position of the incident photon relative to the detector. These pulses are digitized and sent to a computer which builds a 512x512 pixel map representing the intensity of the incoming X-ray signal. We have made a preliminary characterization of the detector using 6 keV (Fe⁵⁵) X-rays. It has a very high quantum efficiency (~90%, limited by the Be window) and low noise level (~20 counts/sec at 20°C over the entire face of the tube). The efficiency is not uniform over the active area but falls as low as 50% in some regions; however the nonuniformity is a smooth, slowly varying function of position and is stable over a period of months, allowing us to correct the collected data. The point resolution is ~.1 mm at the centre of the active area but is degraded by coma distortion to 1 mm at the edge: the azimuthal resolution remains excellent. We have used the detector to collect 2-D diffraction patterns from small bundles (1 mmx0.8 mm) of skinned rabbit psoas fibers using an Elliot GX-13 X-ray generator and Huxley-Holmes camera. The first and seventh actin layer lines in rigor muscle can be recorded in as little as 20 minutes and the tropomyosin reflection on the second actin layer line obtained in only 100 minutes, at least ten times as fast as on film.

W-Pos90 A NEW LOW Q DIFFRACTOMETER AT THE LOS ALAMOS NEUTRON SCATTERING CENTER

Philip A. Seeger and Jill Trehwella
Los Alamos National Laboratory, Los Alamos, NM 87545

The Los Alamos Neutron Scattering Center (LANSCE), scheduled to come into full operation in the fall of 1986, will be one of the highest intensity pulsed neutron sources in the world. We have designed and begun construction on a novel low-Q neutron diffractometer which is expected to be operational at the same time, and which will be used for small angle scattering and low resolution diffraction. Biophysical applications were important in establishing the design criteria for this instrument. The spectrometer utilizes time of flight methods with a white neutron beam to maximize flux on sample, and multiple pinhole apertures to increase total intensity (for large samples). The concept of "dynamic gravity focussing" is introduced in order to center all wavelengths on a two dimensional position sensitive detector that is at a fixed distance from the source, at the point of convergence of the multiple aperture system. The spectrometer will measure over a wide Q range, from 0.003 to 1.0 Å⁻¹, with good resolution. This will be suitable for the study of objects from 10 to 1000 Å in diameter.

W-Pos91 NORMALIZATION OF FIBER AREA TO SARCOMERE LENGTH BY OPTICAL DIFFRACTION OF FREEZE-SUBSTITUTED WHOLE SKELETAL MUSCLE. R.L. Lieber, J.L. Boakes, L.R. Kitabayashi, A.R. Hargens, R.R. Roy, and V.R. Edgerton. Division of Orthopaedics and Rehabilitation, Department of Surgery, University of California, San Diego, and Brain Research Institute, University of California, Los Angeles.

Skeletal muscle fiber areas vary in response to changing levels of muscle use. Quantification of fiber area distributions within muscle thus provides insights into the nature of muscular adaptation to exercise or disease. However, fiber area also varies as a function of muscle length as the individual fibers retain a constant volume. We have therefore implemented a simple technique to normalize muscle fiber areas to sarcomere length, enabling quantification of muscle fiber areas from frozen muscle without variability due to the different lengths at which the muscles were fixed.

Using the stereometric point counting technique of Weibel (*Stereological Methods*, Acad. Press, 1980), areas of specific fiber types are measured from histochemically-stained frozen sections. The frozen block of tissue is then freeze-substituted according to a modification of the methods of Pease (*J. Ultr. Res.* 21:75, 1967) and Eisenberg and Kuda (*J. Histo. Cyto.* 10:1169, 1977), and embedded in Epon for longitudinal sectioning. Unstained longitudinal sections are transilluminated by a low power HeNe laser enabling sarcomere length measurement from the resulting diffraction pattern. The entire longitudinal section may also be scanned to produce a two-dimensional sarcomere length distribution map.

W-Pos92 MOLECULAR DYNAMICS IN RED AND PURPLE MEMBRANE FRAGMENTS OF THE HALOBACTERIUM HALOBIUM.

J. Herzfeld and C.M. Mulliken, Department of Physiology & Biophysics, Harvard Medical School, Boston, MA 02115; D.J. Siminovich and R.R. Griffin, Francis Bitter National Magnet Laboratory, Massachusetts Institute of Technology, Cambridge, MA 02139.

^2H NMR has been used to study the dynamics of amino acid residues in purple membranes of the *Halobacterium halobium*. In general, most of the intensity in the spectrum resides in a broad powder pattern indicative of rigid or anisotropically moving groups on the ^2H NMR time scale. A much smaller intensity resides in a narrow line representing an isotropically moving component. The intensity of this line has been found to depend on the method of preparation of the sample. Using electron microscopy and gel electrophoresis we find that the samples are not significantly aggregated or proteolyzed. Differences between the samples are seen in the residual red membrane content as judged by the intensities of the carotenoid lines in the first derivatives of the visible spectra. In ^2H -leucine labelled samples, these differences correlate with differences in the ^2H NMR spectrum: the cleaner the sample, the smaller the intensity of the narrow ^2H NMR line. We conclude that most, if not all, of the isotropic signal derives from residual red membrane proteins and that there are few, if any, leucine residues in bacteriorhodopsin moving isotropically on the ^2H NMR timescale. The loss of the isotropic NMR signal on proteolysis may be explained by preferential loss of the contaminating protein. (Supported by NIH grants GM-23316, GM-23289, and RR00995).

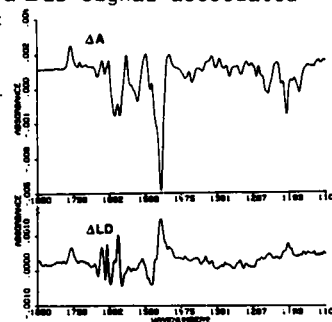
W-Pos93 DIFFERENTIAL SCANNING CALORIMETRY OF THE PURPLE MEMBRANE. C. G. Brouillette¹, D. D. Muccio² and J. S. Barton¹, Department of ¹Pathology and ²Chemistry, University of Alabama at Birmingham, 35294.

Differential scanning calorimetry as well as other spectroscopic techniques, has been utilized to study conformational changes in bacteriorhodopsin within the purple membrane of *H. halobium*. Three major, pH-dependent, structural transitions observed by all techniques are associated with the single protein component, bacteriorhodopsin. The low temperature transition is reversible and highly cooperative, involving as many as 10-20 protein molecules. Non-covalent interactions between the retinal moiety and protein are implicated in this low temperature transition, however, the transition still exists in retinal-depleted purple membrane, suggesting more than one process occurs in this temperature region. The removal of the retinal moiety also significantly lowers the temperature of the denaturation transition for the protein. Proteolysis experiments on bacteriorhodopsin suggest that denaturation may be accompanied by a gross disruption of the membrane which results in exposure of the intramembranous portions of the protein to the aqueous environment.

W-Pos94 POLARIZED FOURIER TRANSFORM INFRARED SPECTROSCOPY OF BACTERIORHODOPSIN

E. NABEDRYK & J. BRETON Intr. by P. MATHIS. Service Biophysique, CEN Saclay, 91191 Gif-Sur-Yvette cedex, France

The possibility that light-induced protein conformational changes accompany the formation of the M412 species of bacteriorhodopsin (BR) has been investigated by recording polarized Fourier transform infrared (FTIR) spectra of oriented films of BR in the dark and during illumination ($\lambda > 500$ nm). Comparison of light-induced FTIR difference absorption (ΔA) and linear dichroism (ΔLD) changes between M412 and BR indicates that several highly reproducible dichroism signals correspond to identified bands in the M412 ΔA spectrum. With our conventions, a ΔLD signal associated with a ΔA signal of the same sign reflects a change in a transition that is oriented at less than 55° from the normal to the membrane plane. It appears that the transition absorbing at 1762 cm^{-1} in M412 (which has been identified to C=O groups of protonated Asp) is oriented rather perpendicular to the membrane plane while the BR C=C retinal vibrations at 1527 cm^{-1} preferentially lie in the membrane plane (in agreement with previous LD studies on the BR chromophore). In the $1660\text{--}1695\text{ cm}^{-1}$ spectral region, several ΔLD signals could be due to peptide and/or isolated amino acid side chains carbonyl groups. Indeed their small magnitude excludes any significant protein conformational change during the M412 formation. This observation rules out a large tilting of the α -helices away from the membrane normal as recently proposed by Draheim and Cassim (*Biophys. J.* 1985, 47, 497-507).



W-Pos95 EVIDENCE FOR A 13,14-CIS CYCLE IN BACTERIORHODOPSIN Klaus Schulten and Paul Tavan, Dept. of Physics, Technical University of Munich, Fed. Rep. Germany

We provide evidence that the vibrational spectra of bacteriorhodopsin which have been observed by Mathies et. al. and Stockburger et. al. by means of Resonance Raman spectroscopy and by Gerwert and Siebert by means of infrared absorption are in agreement with a photocycle of bacteriorhodopsin which involves the sequence Br (all trans) \rightarrow K(13,14-cis) \rightarrow L(13,14-cis) \rightarrow M(13-cis) \rightarrow N(13-cis) \rightarrow O(all trans) \rightarrow B(all trans). Our conclusion is based on quantumchemical (MNDO) calculations of the vibrational spectra (MOPAC, QCPE 455) of the relevant isomers of the protonated and unprotonated Schiff base of retinal. In particular, we investigated the effects of different charge environments on these isomers. Evidence is also presented for a 13, 14-cis cycle in halorhodopsin (collaboration with Hegemann and Oesterhelt).

W-Pos96 ARE C₁₄-C₁₅ ISOMERIZATIONS OF THE RETINAL CHROMOPHORE INVOLVED IN THE PHOTOCYCLE OF BACTERIORHODOPSIN? S.O. Smith, I. Hornung, R. van den Steen, J.A. Pardoen, M.S. Braiman, J. Lugtenburg and R.A. Mathies. Dept. of Chemistry, Univ. of Calif., Berkeley, CA 94720 and Leiden University, 2300 RA Leiden, The Netherlands.

It has been proposed that bacteriorhodopsin's K and L intermediates contain 13-*cis*, 14-*s-cis* chromophore structures (Schulten & Tavan, Nature 272, 85 (1978)). This ideal is appealing since thermal 14-*s-cis* \rightarrow 14-*s-trans* isomerization could function as a "reprotonation switch" in the proton pump mechanism. To test this idea we have developed a method for establishing the *in-situ* structure of the retinal chromophore about C-C single bonds using resonance Raman vibrational spectroscopy. Normal mode calculations have shown that the vibration containing predominantly C₁₄-C₁₅ stretch character is ~ 70 cm⁻¹ lower in frequency in the 14-*s-cis* conformer than in the *s-trans* case. Isotopic substitutions of K₆₂₅ with ¹³C and ²H show that significant C₁₄-C₁₅ stretch character is observed in normal modes at ~ 1185 - 1195 cm⁻¹. The relatively high frequency of the C₁₄-C₁₅ stretch argues that K₆₂₅ contains a 13-*cis*, 14-*s-trans* chromophore. Similarly, isotopic derivative spectra indicate that L₅₅₀ has a 14-*s-trans* chromophore as well. These results argue that the primary step in bacteriorhodopsin is a C₁₃=C₁₄ *trans* \rightarrow *cis* photoisomerization that does not involve C₁₄-C₁₅ *s-cis* structures. Based on these results, we present two alternative models for the "reprotonation switch" in BR. First, inversion of the Schiff base nitrogen during the decay of the M₄₁₂ intermediate could produce a 13-*cis*, C=N *syn* structure similar to BR₅₄₈. A two-bond bicycle pedal isomerization, analogous to the BR₅₄₈ \rightarrow BR₅₆₈ interconversion would then complete the photocycle. The second possibility is that structural changes in the protein form the reprotonation switch.

W-Pos97 RECENT STUDIES OF BACTERIORHODOPSIN PHOTOCYCLE. Aihua Xie¹, John F. Nagle¹, and Richard H. Lozier². ¹Departments of Physics and Biological Sciences, Carnegie-Mellon University, Pittsburgh, PA 15213, and ²Department of Biophysics and Cardiovascular Research Institute, University of California, San Francisco, CA 94143.

The bacteriorhodopsin (bR) photocycle is probed using time resolved flash photolysis spectroscopy. Experiments were performed at 7 mM sodium chloride with a buffer consisting of 1 mM sodium acetate, 1 mM sodium hydrated phosphate and 1 mM boric acid, under several conditions: at seven temperatures, 5°C, 10°C, 15°C, 20°C, 25°C, 30°C and 35°C; at three pH's, pH 5, 7, and 9; in deuterated water, D₂O, buffered at pD 6.8; and at multiple wavelengths and wide time windows (from 1 μ s to 30 ms or 300 ms). In addition, data quality was improved by better temperature control and ensuring that the bacteriorhodopsin samples were light adapted at higher temperatures. Assuming simple exponential kinetics, the number of intermediates required is five or six, while a distributed kinetics analysis, assuming that the decay of L to M is distributed, requires four or five intermediates. A variety of kinetic models, which includes biphasic L model, biphasic M model, and a model with both O to M backreaction and M to bR branch, are analyzed using this data set. Each model is discussed in view of various physical criteria to determine whether it is acceptable.

W-Pos98 EFFECTS OF ARGININE MODIFICATION ON THE HALORHODOPSIN PHOTOCYCLE. Masahiro Ariki, Brigitte Shobert and Janos K. Lanyi Dept. of Physiology and Biophysics, University of California, Irvine, CA 92717

Exhaustive reaction with phenylglyoxal modified 9 of the 12 arginine residues in detergent-solubilized halorhodopsin (HR), without affecting the chromophore spectrum. The consequences of this modification on various Cl^- binding equilibria in HR were evaluated. No significant effects were seen on the affinity of binding Site I to Cl^- and on the increase in the pK_a of Schiff-base deprotonation, which is caused by the Cl^- binding at this site. The affinity of binding Site II to Cl^- was also not affected. However, kinetic modeling of the observed changes in photocycle kinetics suggests that the modification increases the affinity of the main photointermediate (HR_{520}) to Cl^- by about 4-fold while the velocity constant in the recovery step, HR_{640} to HR_{565} , is not influenced by the significant loss of positively charged groups. This inhibitory effect might be related to the early finding that phenylglyoxal treatment of HR vesicles inhibits light-induced Cl^- transport. Since HR contains only one free lysine, the results indicate that the observable Cl^- -dependent equilibria do not depend on a large number of positively charged residues in the protein. The present study suggests, contrary to previous assumptions, that Cl^- binds to the positively charged groups in domains buried in the protein.

W-Pos99 SOLID STATE ^{13}C - AND ^{15}N -NMR STUDIES OF RETINAL AND TYROSINE IN BACTERIORHODOPSIN G.S. Harbison^{1,2}, D.P. Raleigh^{2,3}, S.O. Smith², J.E. Roberts², J.A. Pardo⁴, J. Lugtenburg⁴, J. Herzfeld¹, R.A. Mathies⁵, and R.G. Griffin². ¹Harvard Medical School, ²Francis Bitter National Magnet Laboratory and ³Department of Chemistry, Massachusetts Institute of Technology. ⁴Leiden University, The Netherlands and ⁵Department of Chemistry, University of California, Berkeley.

Solid-state NMR techniques are used to probe the structure and protein environment of the retinal chromophore and the protonation state of tyrosine in bacteriorhodopsin (bR). Spectra were obtained of hydrated dark-adapted bR selectively labeled with ^{13}C at fourteen positions on the retinal prosthetic group, with ^{15}N at the retinal Schiff base nitrogen, and with ^{13}C at the 4'-position of tyrosine. In addition, selected spectra have been obtained of the light-adapted pigment. The ^{13}C -retinal spectra indicate that dark-adapted bR contains a mixture of all-*trans* and 13,15 *di-cis* protonated Schiff base chromophores. The C_6 - C_7 single bond is shown to be *trans* and there is evidence for a negative bacterio-opsin charge near C_5 and a positive charge near C_7 of the retinal. These spectra also indicate that the Schiff base is protonated and weakly hydrogen-bonded. Based on these results, we present a new model for the retinal binding site in bR which has important implications for the mechanism of the "opsin shift". Finally, we have obtained spectra of hydrated dark-adapted bR labeled with ^{13}C at the 4'-position of tyrosine and observe a strong line at 157 ppm. The isotropic chemical shift (157 ppm) and the asymmetry parameter (0.9 ± 0.1), calculated from the sideband intensities, are similar to those measured from protonated tyrosines in other peptides indicating that the observed tyrosines in dark-adapted bR are protonated.

W-Pos100 PHOTOACTIVE RETINAL PIGMENTS IN HALOALKALIPHILIC BACTERIA D.B. Bivin and W. Stoekenius, Cardiovascular Research Institute and Department of Biochemistry and Biophysics, University of California San Francisco, CA 94143

Light-induced fast transient absorbance changes are detected by time-resolved spectroscopy in 38 out of 51 haloalkaliphilic isolates from alkaline salt lakes in Kenya and the Wadi Natrun in Egypt. They indicate the presence of two retinal pigments, P_f and P_s , which undergo cyclic photoreactions with halftimes of 2ms and 500ms respectively. P_f absorbs maximally near 580nm and P_s near 500nm. The pigments differ in their sensitivity to hydroxylamine and detergent bleaching and the photoreactions of P_f are strongly dependent on chloride concentration. Of the 38 pigment-containing strains, 29 possess both P_f and P_s , 9 only P_s . Inhibition of retinal synthesis with nicotinic blocks pigment formation and addition of retinal restores it. Hydroxylamine-bleached pigments can be reconstituted with retinal or retinal analogues. Their similarity to the retinal pigments of *Halobacterium halobium* strongly suggest that they are also rhodopsin-like retinylidene proteins. P_f in all properties tested is almost identical to halorhodopsin, the light-driven chloride pump of *H. halobium*, and may serve the same function in the haloalkaliphiles. P_s has photocycle kinetics similar to sensory rhodopsin and a far blue-shifted long-lived photocycle intermediate but its ground state absorption maximum is near 500nm instead of 587nm. We have not found a bacteriorhodopsin-like pigment in the haloalkaliphiles.

W-Pos101 TRYPTOPHAN IMAGING OF BACTERIO-OPSIN RECONSTITUTED INTO LIPID VESICLES.
*A. M. Kleinfeld, J. D. LeGrange and †S. R. Caplan, *Harvard Medical School, Boston, MA 02115 and †Weizmann Institute of Science, Rehovot, Israel.

The spatial distribution of tryptophanyl residues of reconstituted bacterio-opsin (bo) was determined by resonance energy transfer (RET) from Trp to the n-(9-anthroyloxy) (AO) fatty acids ($2 \leq n \leq 16$). Purple membrane was bleached, retinal was extracted and the solubilized protein was reconstituted into liposomes of egg phosphatidylcholine by dialysis. Reaction of the reconstituted bo with n-bromosuccinimide (NBS) was used to assess the Trp quantum yield heterogeneity. The results indicate that 3 to 4 of the 8 Trp are only weakly fluorescent. Steady state anisotropy measurements were carried out on vesicles treated with amounts of NBS sufficient to quench 0, 25 and 75% of the Trp fluorescence and results from each sample are consistent with significant Trp mobility ($r(300 \text{ nm}) < 0.20$). Energy transfer was measured for each of eight different AO probes, added to the vesicles at fatty acid to lipid ratios between 0.5 and 5%. RET efficiencies (T) were determined from the quenching of Trp fluorescence intensity as well as the sensitized emission of the AO probes. T values were found to increase almost linearly with probe position and the increase with concentration was in excellent agreement with that expected for RET. In all cases the average T values obtained from Trp quenching were about twice those from sensitized emission, as expected from the observed Trp quantum yield heterogeneity. A Monte Carlo analysis of the T values (Kleinfeld, 1985, Biochemistry 24, 1874) indicates that the fluorescent Trp are distributed deep within the bilayer. This work was supported by NSF grant PCM-8302687 and was done during the tenure of an Established Investigatorship (AMK) of the American Heart Association.

W-Pos102 SPECTROSCOPIC STUDIES ON THE CONFORMATION OF BACTERIORHODOPSIN REGENERATED WITH α -RETINAL, Cynthia Y. Robinson, Wayne J. Brouillette, Donald D. Muccio, Department of Chemistry, University of Alabama at Birmingham, Birmingham, AL., 35294.

A bacteriorhodopsin analogue was prepared by regenerating bacterio-opsin with all-*trans* - α -retinal, a retinoid with an altered trimethylcyclohexene ring. A membrane preparation with a difference absorption maximum (regenerated minus bleached) at 475 nm was observed, which is significantly shifted to the blue from preparations regenerated with all-*trans* -retinal ($\lambda_{\text{max}} = 570 \text{ nm}$). Regeneration times under different conditions were, in general, slower for the α -retinoid than the β -retinoid. Near and far UV circular dichroic (CD) studies yielded nearly identical spectra for these two preparations. This indicates that the secondary and tertiary structure of the regenerated membranes are very similar. Visible CD spectra, on the other hand, have indicated that the exciton CD bands are eliminated, suggesting that the orientations of the α -retinyl chromophores have either changed to a more symmetric environment or have increased in mobility. A comparison of the structural stability of the α -retinoid analogue to that of the β -retinoid analogue is currently under investigation. These results will be discussed in terms of the conformation of the trimethylcyclohexene ring relative to the polyene chain in the α -retinoid preparation.

W-Pos103 SPECIFIC CHROMOPHORE-PROTEIN INTERACTIONS ARE REQUIRED FOR THE STRUCTURE AND THE COLOR OF BACTERIORHODOPSIN- A SOLVENT PERTURBATION STUDY. C. Pande, A. Pande* and R. Callender. Physics department, City College of New York, U.S.A.; † Universitatsspital Zurich, Switzerland.

In aqueous solutions containing 60% DMSO, the native dark-adapted bR₅₆₀ (Abs. Max. 560 nm) converts, reversibly and completely, to a new species, bR₄₆₀ (Abs. Max. 460 nm). The kinetics of this reaction show that the transformation from bR₅₆₀ to bR₄₆₀ takes place predominantly through the all-*trans* chromophoric pigment. Thus, the 13-*cis* pigment has to undergo a rate limiting thermal isomerization to the all-*trans* form, before conversion to bR₄₆₀. Resonance Raman spectroscopy shows that the chromophore is linked to the protein by a protonated Schiff base linkage in bR₄₆₀. The frequency of the Schiff base vibrational mode, as well as the magnitude of its shift upon deuteration, are quite different from those of the native bR₅₆₀, and are, in fact, similar to those observed for the protonated Schiff bases of the model chromophores, suggesting minimal protein-chromophore interaction near the Schiff base in bR₄₆₀. Furthermore, comparison of the I.R. spectra of bR₅₆₀ and bR₄₆₀ suggests that the formation of bR₄₆₀ is associated with protein structural changes.

We attribute these changes, associated with the solvent perturbation, to the structural alteration of the protein. The 13-*cis* chromophoric pigment appears to be resistant to this solvent induced protein structural change. Conversion of the dark-adapted bR₅₆₀ to bR₄₆₀, therefore, proceeds via the all-*trans* pigment form. The changes in protein structure presumably result in the opening up of the structure, causing displacement of the protein counterion(s) responsible for the opsin-shift observed in the native bR₅₆₀.

W-Pos104 SPECTROSCOPIC PROPERTIES OF BACTERIAL SENSORY RHODOPSIN (SR) AND BACTERIORHODOPSIN (BR) CONTAINING ACYCLIC AND RING DESMETHYL ANALOGUES OF ALL-TRANS RETINAL. D.A. McCain^{ab}, V.J. Rao^c, Masami Okabe^c, Koji Nakanishi^c, and John L. Spudich^{ab}, ^aDept. of Anatomy and Structural Biology, and ^bDept. of Physiology and Biophysics, Albert Einstein College of Medicine, Bronx, NY, 10461, ^cDept. of Chemistry, Columbia Univ., New York, NY, 10027.

Analogues of all-trans retinal were synthesized with the methyl group(s) removed from the C-1, C-5 and both C-1 and C-5 positions of the β -ionone ring, along with the acyclic analogues 3,7,11-trimethyl-2,4,6,8-dodecapentaenal and 3,7,11-trimethyl-8-isopropyl-2,4,6,8-dodecapentaenal. Each of the 5 analogues generates photochemically reactive pigments when added to BR or SR apoprotein with reconstitution times and yields similar to those of all-trans retinal at the same chromophore:apoprotein ratio. Measurement of the absorption spectra and opsin shifts indicate: (1) Of the 3 methyl groups, the C-5 methyl is both sufficient and necessary for a large SR opsin shift, but does not contribute substantially to the opsin shift of BR. (2) The SR analogue absorption maximum and opsin shift values differ from the corresponding BR analogue values only when the C-5 methyl group is present. (3) The C-1 and C-5 methyl groups, even when present on an incomplete ring, are sufficient to generate the native absorption and opsin shift values in both BR and SR. Flash photolysis of the SR analogue pigments indicates the formation of photo-intermediates similar to the S₃₇₃ intermediate in the native SR photochemical reaction cycle with the thermal decay of this intermediate being significantly slower in the analogue SR pigments. First order rate constants (23°) range from 0.93 sec⁻¹ for the native SR to 0.17 sec⁻¹ for the 3,7,11-trimethyl-2,4,6,8-dodecapentaenal pigment.

W-Pos105 LOCATION OF THE RETINAL IN BACTERIORHODOPSIN'S M INTERMEDIATES BY PHASE MODULATION OF ENERGY TRANSFER. C.A. Hasselbacher and T.G. Dewey, Department of Chemistry, University of Denver, Denver, Colorado 80208.

A novel application of modulation excitation spectroscopy has been used to measure the position of the retinal chromophore in the M intermediates of the bacteriorhodopsin (bR) photocycle. This technique uses phase modulation of fluorescence resonance energy transfer to determine the distance from a lipid fluorescent donor to a chromophore in a photocycle intermediate. BR was incorporated into asolectin vesicles labeled with a fluorescent lipid probe. Vesicles were characterized with respect to size and orientation of the protein. Energy transfer was measured from the fluorescent probes located either on the surface of the membrane or buried in the interior of the bilayer. This allowed the measurement of distances to the retinal in the M intermediate from a variety of locations. The concentration of M intermediates was varied by changing the frequency of modulation of the actinic light that drives the photocycle. Simultaneous measurements of the M absorbance and of the fluorescence quenching due to resonance energy transfer were made using phase-sensitive detection. In each case the signal amplitude decay was biphasic, indicating the presence of two M intermediates. Distances of closest approach of lipid to retinal were found for each intermediate. From this information the location of the retinal in each M intermediate could be determined. Our results show that the chromophore in the slow-decaying M intermediate is located farther from the membrane surface of the vesicle exterior than the chromophore in the fast-decaying M intermediate. These results indicate the dynamic, flexible nature of bR as it proceeds through its photocycle.

W-Pos106 EFFECT OF pH ON THE ABSORPTION AND PHOTOCHEMICAL REACTION CYCLE OF MEMBRANE-INSERTED AND DETERGENT-SOLUBILIZED SENSORY RHODOPSIN (SR) FROM HALOBACTERIUM HALOBIVM. Danny Manor^a and John L. Spudich^{a,b}, ^aDept. of Anatomy and Structural Biology and ^bDept. of Physiology and Biophysics, Albert Einstein Coll. of Med., Bronx, NY 10461.

The effect of pH on the spectral properties of SR was studied using both cell envelopes (sonicated vesicles) and detergent-solubilized vesicles (5mM CHAPS). At pH 7, both preparations show indistinguishable absorption spectra and flash-induced difference spectra, indicating conversion of the resting form SR₅₈₇ to the long lived photointermediate S₃₇₃. While SR₅₈₇ recovery from a flash is fitted well by a single first order rate constant ($k = 1.05 \text{ sec}^{-1}$, 26°) for the vesicle preparation, in the solubilized state SR shows biphasic recovery kinetics ($k_{\text{slow}} = 0.34 \text{ sec}^{-1}$, $k_{\text{fast}} = 1.10 \text{ sec}^{-1}$). Upon alkalization of vesicles, the absorption maximum of the pigment shifts from 587 nm to 550 nm, as observed previously (Spudich and Bogomolni, *Biophys J.* (1983), 43:243-246; Hazemoto et al. *Biophys. J.* (1983) 44:59-64). We observe this shift also in the solubilized preparation. The transformation is characterized by a defined titration curve with a $pK = 8.5$. Flash excitation of the alkaline species (SR^{alk}₅₅₀) generates a long lived photointermediate with maximal absorption near 370 nm, similar to that observed after photo-excitation of SR₅₈₇. The kinetics of recovery from a flash of SR₅₈₇ is independent of pH in the range of $8 > \text{pH} > 5$. However the thermal decay step S^{alk}₃₇₀ \rightarrow SR^{alk}₅₅₀ is markedly retarded by increasing pH. The effect of pH is most pronounced on k_{slow} which decreases from 0.34 sec⁻¹ to 0.017 sec⁻¹. In general the results indicate that, although kinetic details differ, similar photochemical processes occur in SR in its native membrane and in the CHAPS solubilized state.

W-Pos107 FLASH-INDUCED CONDUCTIVITY CHANGES IN SUSPENSIONS OF PHOSPHOLIPID VESICLES CONTAINING BACTERIORHODOPSIN. Tim Marinetti, The Rockefeller University, 1230 York Avenue, New York NY 10021

Light-induced conductivity changes were observed in suspensions of bacteriorhodopsin (bR) incorporated into phospholipid vesicles (approx. 1000 lipid/bR) at neutral pH and ionic strength under 100 mM. The vesicles were prepared by detergent dialysis using octyl glucoside, followed by brief sonication. In the light, they raise the pH of the external medium, indicating a net orientation of the bR opposite to that of whole cells. Net proton uptake is confirmed by the uncoupler-sensitive baseline shift in the conductivity long after the flash. The conductivity method detects changes in the external aqueous phase only. On the timescale corresponding to the proton uptake phase of the bR photocycle (10-50 ms), conductivity transients are seen which vary with the composition of the external buffer but not as expected if the signal is due solely to protons. These transients are present above and below the melting temperature of the lipid, suggesting that a small amount of ion release accompanies the proton uptake. The large non-proton ion movements seen in purple membranes¹ which are abolished by solubilization in Triton X-100 are not seen in these vesicles. This behavior is consistent with bR being present as monomers in the vesicles under these conditions².

¹ Marinetti and Mauzerall, *Biophys. J.* 47 96a (1985).

² Dencher and Heyn, *FEBS Lett.* 108 307 (1979).

This work was supported by NIH grant GM 32955-02

W-Pos108

Effects of $\Delta\psi$ and ΔpH on proton pumping efficiency of Bacteriorhodopsin reconstituted into large liposomes. M. SEIGNEURET and J.L. RIGAUD. Service de Biophysique, Departement de Biologie, CEN Saclay, 91191 Gif sur Yvette, Cedex, FRANCE.

Bacteriorhodopsin has been incorporated into large phospholipid vesicles by phase reversion. The kinetics of the light-induced proton uptake, the steady-state pH gradient and the subsequent release of H^+ in the dark have been analyzed for their quantitative dependence on system parameters: light-intensity, internal and external buffer capacity, internal and external pH, lipid to protein ratio, passive permeability (to H^+ and other ions) and nature of phospholipids.

Proton movements in the BR vesicles were assayed with pH meter, ¹⁴C-Methylamine distribution as well as with pyranine entrapped inside liposomes. Yield of M_{412} formation and its decay kinetics were detected by rapid absorption spectroscopy.

The results show clearly that the light-activated proton pumping is inhibited by the electrochemical potential generated through a back-pressure effect: Bacteriorhodopsin is inhibited either by the membrane potential (60mV) or by the pH gradient (up to 2 pH units) it develops across our reconstituted systems.

The relative influences of $\Delta\psi$ and ΔpH on the proton pumping efficiency will be discussed.

W-Pos109

PROTON MOVEMENT IN BACTERIORHODOPSIN DETECTED BY FTIR SPECTROSCOPY

P. Roepe, P. Ahl, P. Scherrer, J. Herzfeld, R. Bogolomoni and K.J. Rothschild

Depts. of Physics and Physiology, Boston University, Boston, Massachusetts 02215 (P.R., P.A. and K.J.R.),

Depts. of Biochemistry and Biophysics, University of California, San Francisco (P.S. and R.B.)

and The Biophysical Laboratory, Harvard Medical School, Boston. (J.H.)

Tyrosine contributions to the $\text{BR}_{548} \rightarrow \text{BR}_{570}$, $\text{BR}_{570} \rightarrow \text{K}_{630}$ and $\text{BR}_{570} \rightarrow \text{M}_{412}$ FTIR difference spectra have been identified by using isotope labelling of bacteriorhodopsin tyrosine residues. Measurements are made at several temperatures and pH. Analysis of deuterium/hydrogen exchange sensitivity of these peaks and of model compounds enables us to reach the following conclusions: i) A tyrosine group appears to deprotonate during the $\text{BR}_{548} \rightarrow \text{BR}_{570}$ transition. ii) A tyrosinate \rightarrow tyrosine conversion occurs during the $\text{BR}_{570} \rightarrow \text{K}_{630}$ transition at low temperature (Rothschild *et al.*, PNAS (1985), in the press). iii) The tyrosinate which becomes protonated at K remains protonated through the formation of M. iv) A second tyrosine group deprotonates between L550 and M. v) Concomitant with M formation several carboxyl groups are altered. In order to identify the position of these tyrosine groups in the primary sequence, bacteriorhodopsin selectively nitrated at tyrosines 26 and 64 (Scherrer and Stoerkenius, *Biochemistry* (1985) 23, 6195) has been studied. It is concluded that neither of these residues is directly involved in the $\text{BR}_{570} \rightarrow \text{K}$ transition. Furthermore, tyr-26 does not appear to undergo a change up to M_{412} . Nitration of tyrosine 64 drastically perturbs the electronic environment of the chromophore, and appears to induce changes in the behaviour of this group during the photocycle. (This research was sponsored by NSF grant DMB-8509857 to KJR.)

W-Pos110 PROTONATION STATES OF TYROSINE AND CARBOXYLIC ACIDS IN THE BACTERIORHODOPSIN PHOTOCYCLE.

Laura Eisenstein, Gavin Dollinger, Shuo-Liang Lin and Joseph Vittitow, Physics Dept., University of Illinois, 1110W. Green St., Urbana IL, and Koji Nakanishi*, John Termini and Kazunori Odashima, Dept. of Chemistry, Columbia University, New York, NY, 10027.

Earlier we reported some results on our FTIR work on bacteriorhodopsin (bR) from *Halobacteria halobium* grown on standard media and medium containing L- $\{\delta 1, \epsilon 3, \zeta 2, \xi 3, \eta, -2H5\}$ tryptophan or L- $\{\epsilon 1, \epsilon 2, 2H2\}$ tyrosine, which pointed to protonation/deprotonation changes of tyrosine during the photocycle. We could detect no such changes for isotopically labeled tryptophan. (*Biophys. J.*, 47 99a, (1985)) The completion of analogous experiments utilizing L- $\{\epsilon 1, \epsilon 2, \gamma 1, \gamma 2, -2H4\}$ tyrosine has allowed us to identify vibrations in the FTIR difference spectra of bR(LA)-K(620), M(412) and bR(DA) as tyrosine or tyrosinate. Assignments were based upon FTIR studies of these amino acids in H₂O and D₂O at high and low pH utilizing an attenuated total reflectance cell. Our results are consistent with the notion of a tyrosine protonation upon dark adaptation. We can definitely assign two and probably three protonated tyrosine lines in the bR(K) spectra on the basis of isotopically shifted tyrosine frequencies, one of which becomes deprotonated during the transition to M(412). We also report some results on FTIR studies for bR labeled with L- $\{4-13C\}$ and $\{2,3,3'-2H3\}$ aspartic acids and describe experiments in progress with L- $\{5-13C\}$ and $\{2,4,4'-2H3\}$ glutamic acids. The ¹³C labels have allowed us to unambiguously assign the CO₂H vibrations for aspartic acid in bR(LA) and bR(M). No protonated aspartic acids in K could be detected. The ²H₃ derivatives have enabled us to identify the CO₂- vibrations in the FTIR spectra of bR intermediates. This work was supported by HEW PHS GM 32455 (LE) and NSF CHE 84-12513 (KN).

W-Pos111 PROTON MOVEMENT IN BACTERIORHODOPSIN DETECTED BY UV SPECTROSCOPY

Patrick L. Ahl, Paul Roepe, and Kenneth J. Rothschild

Depts. of Physics and Physiology, Boston University, Boston Massachusetts 02215

The protonation state of at least one tyrosine, several carboxyl groups, and the Schiff base apparently change during the bacteriorhodopsin (bR) photocycle. It is thus possible that these groups are part of the proton pathway through bR. In order to further examine proton movement in bR, we studied the low temperature UV-visible difference spectrum from 210 to 700 nm of purple membrane films and suspensions. These data reveal tyrosine protonation changes and tryptophan H bonding changes during the formation of the K, L, and M intermediates, along with tyrosine protonation changes during light-dark adaptation. Titration studies with tyrosine model compounds showed the maximum absorbance increases are at 244 and 296 nm for deprotonation. In the bR → K difference spectra (T=80 K) a strong negative peak at 244 nm was observed indicating a tyrosine protonation during this step. This peak coexisted with two large positive peaks at 289 and 294 nm. Model compound studies with H bond acceptors interacting with 3-methylindole, 1-methylindole or p-cresol indicated that these two peaks result from increased H bonding at the indolyl NH of tryptophan, rather than H bonding at the OH group of tyrosine. In contrast, the bR → L difference spectra (T=170 K, pH 4.8) was distinctly different, showing a small positive peak at 240 nm, while the positive peaks at 289 and 294 nm were significantly decreased. These results indicate a tyrosine deprotonation and reduced tryptophan H bonding during the formation of L. In the bR → M difference spectrum (T=210 K, pH 6.4), strong positive peaks at 240 and 300 nm were observed clearly indicating a tyrosine deprotonation by the M intermediate. Light adaptation of humidified purple membrane films was accompanied by absorbance increases at both 243 and 308 nm consistent with a tyrosine deprotonation. Model compound difference spectra of various Schiff base retinal isomers indicated all of the observed bR absorbance changes were not due to UV retinal transitions. (Supported by NSF grant DMB-8509857 to KJR)

W-Pos112 PROTON-DEUTERON EXCHANGE OF THE SCHIFF BASE IN BACTERIORHODOPSIN. H. Deng, R. Callender and T. Ebrey. Department of Physics, City College of New York, N.Y. 10031 (H.D. and R.C.) and Department of Physiology and Biophysics, University of Illinois at Urbana-Champaign, Urbana, IL 61801 (T.E.).

We have remeasured the exchange kinetics of the bR Schiff base deuteron for a proton, using continuous-flow resonance Raman spectroscopy (Doukas et al., *Biophys. J.* 1980, 33, 275), with an improved mixing chamber, that allows us to kinetically resolve this process. Experiments were done both with the light- and the dark-adapted bR. To test for the effect of high salt concentration on the exchange kinetics, the bR sample in D₂O was rapidly mixed with water, with or without 4M NaCl. For studying the effect of pH, the bR sample in D₂O was mixed with water at the desired final pH, again with or without 4M NaCl.

The half-life of this reaction more than doubles (from 1.3 ms to 2.8 ms) on going from the light- to the dark-adapted bR. Furthermore, in contrast to the dark-adapted bR which is insensitive to the presence of NaCl, the half-life of the light-adapted sample increases to 2.7 ms in 4M NaCl. Interestingly, within the experimental resolution, these exchange rates are insensitive to the solution pH in the range from 2 to 12.

The data have been fitted to various kinetic models, and the plausible reaction schemes, that emerge from these analysis, will be discussed.

W-Pos113 PROTON PUMPING AND ABSORPTION KINETICS IN GLUTARALDEHYDE TREATED PURPLE MEMBRANE. Drake C. Mitchell and G. W. Rayfield, Department of Physics,

University of Oregon, Eugene, OR 97403. Our recent measurements (1) of charge motion within bacteriorhodopsin (bR) in highly viscous solutions suggested that conformational changes may be necessary for proton translocation. Recent work by Ahl and Cone (2) has shown that light-induced rotations of bR can be eliminated by cross linking with glutaraldehyde. To investigate the possible coupling between conformational changes and proton pumping we have treated purple membrane with glutaraldehyde following the protocol of Ahl and Cone. The absorption kinetics measured with a flash spectrophotometer are significantly slowed relative to untreated bR for all the wavelengths measured. When incorporated into egg PC vesicles, cross linked bR has about two thirds the proton pumping activity of normal bR when measured by a pH electrode. Proton uptake and release from cross linked purple membranes, followed with a pH sensitive dye, are also retarded. When normal purple membrane is suspended in a glycerol solution its absorption kinetics and proton translocation kinetics (1) are slowed. The same effect is observed when cross linked purple membrane is substituted for normal purple membrane, suggesting that these effects are additive. Parameters of proton uptake and release, absorption kinetics, and intra-protein charge motion will be presented.

1. Rayfield, G. W. 1985. Photochem.-Photobio. in press
2. Ahl, P. L. and R. A. Cone. 1984. Biophys. J. 45:1039-1049

W-Pos114 PARTICIPATION OF THE CARBOXYL GROUP IN PROTON TRANSFERS. Steve Scheiner, Department of Chemistry & Biochemistry, Southern Illinois University, Carbondale, IL 62901.

The carboxyl group appears to participate in a number of important proton transfer reactions involved in bioenergetic phenomena. For example, this group is probably the counterion and proton acceptor for the Schiff base cation in bacteriorhodopsin. Yet surprisingly little is known about the conditions under which such a proton transfer can take place. Ab initio calculations were therefore carried out to study the effects on the transfer process (1) of the geometrical relationship between a carboxyl and a proton donor group. Despite the intrinsic energetic preference of a proton for the carboxyl, a distance between the two groups of greater than about 2.9 Å leads to a high barrier to transfer and hence a small likelihood of proton shift toward the carboxyl. Angular reorientation can drastically alter the energetics of the process, e.g. the equilibrium position of the proton can be shifted from one group to the other (2). Motions of either group, caused by small protein conformational changes, can therefore be used as a mechanism to push a proton across the H-bond from the Schiff base to its counterion or vice versa. This process may be described as a coupling of conformational to "protonic" energy; the latter term refers to placement of a proton on a group of normally lower pK.

- (1) S. Scheiner, Acc. Chem. Res. 1985 18, 174
- (2) S. Scheiner & E. A. Hillenbrand, Proc. Nat. Acad. Sci., USA 1985 82, 2741

W-Pos115 ANTI-BACTERIORHODOPSIN POLYCLONAL ANTIBODIES INHIBIT THE PHOTOREACTIONS OF BACTERIORHODOPSIN AND LIGHT INDUCED PROTON UPTAKE. J. G. CHEN; R. GOVINDJEE; C.-H. CHANG AND T.G. EBREY. DEPARTMENT OF PHYSIOLOGY AND BIOPHYSICS, UNIVERSITY OF ILLINOIS, URBANA, ILLINOIS 61801.

Polyclonal antibodies against bacteriorhodopsin (bR) were obtained from an immunized rabbit and they were initially tested with Western blotting and dot assays. The antibodies were purified from rabbit serum by dextran sulfate and ammonium sulfate precipitation. Fab fragments of the antibodies were obtained by papain treatment; these were further purified on a bR-affinity column. Addition of the Fab fragment of anti-bR polyclonal antibodies to bR slows both the decay of the M photointermediate and the rate of light-induced proton uptake.

In order to determine the specific antigenic determinants at which the binding of an antibody perturbs the photochemistry and proton pumping, we have begun to use monoclonal antibodies. An anti-bR monoclonal antibody which binds to the C-terminal region of the bR polypeptide has been identified. A bR affinity column was used to purify and concentrate the monoclonal antibody. Addition of this antibody to a bR sample in an equimolar quantity however showed only a slight effect on the M decay and proton uptake.

W-Pos116 PHOTOTAXIS IN HALOBACTERIUM HALOBIUM. E. Wolff, R.A. Bogomolni, B. Hess, W. Stoeckenius; Max-Planck Institute, Dortmund, W. Germany and Dept. of Biochemistry and Biophysics, University of California, San Francisco, CA 94143.

H. halobium is attracted by long wavelength and repelled by short wavelength light. Sensory rhodopsin (sR) has been identified as receptor for both responses. Absorption of light in its 587nm absorption band generates the attractant response and also generates a photointermediate absorbing at 373nm (S₃₇₃). When this is photoconverted back to sR₅₈₇, a repellent response results. We have used a light microscope to record the responses. A suspension of cells is illuminated through a dark-field condenser with >750nm light, which is not perceived by the cells. Shorter wavelength background light can be added. Through the objective lens, a 150µm spot of light, which can be varied in wavelength and intensity, is projected into the center of the field and the >750nm light scattered from this spot is monitored by a photomultiplier (PM). The PM current is proportional to the number of cells in the spot and its initial rate of change when the light intensity and/or wavelength in the measuring spot are changed, measures the reactivity of the cells. The resulting action spectra show a broad peak between 560nm and 620nm with one or two subsidiary maxima for the attractant response and an even broader peak in the blue and near UV for the repellent response. The point of crossover from attractant to repellent response depends on wavelength and intensity of background light. Without it, crossover occurs between 460 and 480nm and for a mutant lacking the major carotenoids, at 535nm. This is incompatible with sR₅₈₇ and S₃₇₃ as the only photoreceptors and suggests a second repellent receptor absorbing near 500nm, which we have also detected spectroscopically.

W-Pos117 HIGH TIME-RESOLUTION MEASUREMENTS OF PHOTOTAXIS RESPONSE LATENCIES IN HALOBACTERIUM HALOBIUM. Steven A. Sundberg*, Maqsoodul Alam[†], Diana Cherbavaz*, and John L. Spudich*, Dept. of Anatomy and Structural Biology, and Dept. of Physiology and Biophysics, Albert Einstein College of Medicine, Bronx, New York, 10461, and [†]Biochemistry and Biophysics Program, Washington State University, Pullman, Washington, 99164.

Reversals of swimming direction can be induced in H. halobium both by sudden increases in "blue" light ($\lambda < 520\text{nm}$) or decreases in "red" light ($\lambda = 600 \pm 20\text{nm}$). We have measured the latency of the response following delivery of light stimuli using a computerized cell-tracking system (Motion Analysis Systems, Inc., Santa Rosa, CA) coupled to an electronic shutter. At present, we are able to detect reversals with approximately 67 msec resolution. Analysis of paths generated by digitizing video images of strain Flx15 (late log phase cells, 37 °C) indicates a clear difference in the distributions of response times for saturating red and blue stimuli. The minimum response latency following the blue-on stimulus was 310 ± 100 msec (mean \pm s.d. for 3 independent sets of data; 2000 paths total), with the maximum number of reversals occurring approximately 800 ± 140 msec after the onset of the stimulus. Responses to the red-off stimulus occurred at later times, with a minimum latency of 700 ± 140 msec (mean \pm s.d. for 2 independent sets of data; 1410 paths total) and a peak response at approximately 1340 ± 70 msec. The difference between red and blue response latencies is maintained at lower, non-saturating stimuli, for which the distributions are broadened and shifted toward later times. Experiments are presently being carried out to determine whether or not this difference can be accounted for in terms of the photocycle kinetics of sensory rhodopsin.

W-Pos118 Some Aspects of Electron Transfer Reaction Dynamics* -- Jose Nelson ONUCHIC, Caltech;
David N. BERATAN, Jet Propulsion Laboratory

Simple electron transfer without bond breakage or formation occurs in a broad range of biochemical reactions. These reactions are important in the primary photosynthetic events and in oxidative phosphorylation, for example. Standard non-adiabatic models of electron transfer reactions do not include a clear treatment of the dynamical aspects of the problem. We present a simple but complete quantum mechanical model for long distance transfer. It contains the elements necessary to calculate a rate: electron, reaction coordinate, and bath. The completeness of the model allows a full discussion of the dynamical aspects (validity of non-adiabatic, Born-Oppenheimer, and Condon approximations, for example) of the transfer problem. A discussion is given which tries to show when the standard non-adiabatic theory is expected to give qualitatively or quantitatively wrong answers for some experimental results, and whether biology will notice.

*Supported by the Brazilian agency CNPq, Universidade de Sao Paulo, and the NSF (#PCM-8406049); a NRC Resident Research Associateship at NASA/JPL, respectively.

W-Pos119 CHLORINATED CHLOROPHYLLS: COMPONENTS OF GREEN PLANT REACTION CENTERS? E. Fujita, J. Fajer, Brookhaven National Laboratory, Upton, NY 11973; B. Chadwick, H. Frank, Univ. of Connecticut, Storrs, CT 06268; D. Simpson, K.M. Smith, Univ. of California, Davis, CA 95616.

Chlorinated chlorophyll (Chl) derivatives, extracted from photosystem I preparations of spinach, cyanobacteria and green algae, have been proposed by Dornemann and Senger (1) to be integral parts of PS I reaction centers. δ -Chloro-Chl and 10-hydroxy, δ -chloro-Chl, possible candidates (2) for these chromophores, are readily synthesized by reaction of Chl a derivatives with mild oxidizing agents and chloride. The possibility that these compounds may function as either primary donors (P700) or acceptors (A_0 or A_1) is considered by comparing their properties with those of Chl a in vitro and of P700, P700⁺, A_0^- and A_1^- in vivo. The triplet zero field splittings and the redox, optical and ESR characteristics of the anions and cations of the chlorinated compounds do not differ widely from those of Chl a. These results do not offer, therefore, clear diagnostic signatures that would unambiguously identify the putative chlorinated species in vivo, nor do they provide obvious advantages (or disadvantages) for a biological role for chlorinated chromophores.

1. Dornemann, D. and Senger, H. FEBS Letters 126, 323 (1981). Photochem. Photobiol. 35, 821 (1982). Advances in Photosynthesis Research, Vol. II. Sybesma, C. (Ed.) 1984, pg. 77.
2. Scheer, H. et al. ibid. pg. 81.

(Work supported by the Div. of Chemical Sciences, U.S. Dept. of Energy and the National Science Foundation.)

W-Pos120 THE EFFECT OF ETHYLENEDIAMINE CHEMICAL MODIFICATION ON THE ELECTRON TRANSPORT PROPERTIES OF PLASTOCYANIN. G. Anderson, D. Sanderson, C.H. Lee, J. Draheim, and E. L. Cross, Dept. of Biochemistry, The Ohio State University, Columbus, Ohio 43210.

Plastocyanin (PC) acts as a mobile electron carrier in photosynthetic electron transport between cytochrome f and P700. PC was modified by ethylenediamine plus a water soluble carbodiimide which has the effect of changing a negative charge into a positive charge. The conditions were adjusted in order to produce a series of singly and doubly-modified forms. These forms were separable on the Pharmacia FPLC with a Mono Q column on the basis of their different dipole moments. These forms are being used to examine the importance of site charges versus net charge on PC and its interaction with its reaction partners cytochrome f and P700. Four singly-modified forms were obtained which showed differential inhibition of cytochrome f oxidation, (from 36 to 77%). This indicates that inhibition is dependent on location of the modification. The most inhibited forms were located on the 'East face' in the negative patches 42-45 and 59-61, whereas the form modified at 68, on the opposite side, showed the least inhibition. The doubly-modified forms are all highly inhibited regardless of location. It can be concluded that the 'East face' contains the binding site for cytochrome f. The effect of these modifications on oxidation-state dependent conformational changes is also being investigated.

W-Pos121 STEADY-STATE SPECTROELECTROCHEMISTRY: COOPERATIVITY BETWEEN SURFACE EXPOSED PROTONATION SITES AND THE COPPER CENTER IN SPINACH PLASTOCYANIN

D.G. Sanderson, L.B. Anderson, and E.L. Gross Departments of Chemistry and Biochemistry, Ohio State University, Columbus, Ohio 43210.

Thin-layer, steady-state spectroelectrochemistry employing twin-interdigitated filar electrodes (D.G. Sanderson & L.B. Anderson, *Anal. Chem.*, Nov. 1985) has been used in a structure-function investigation of the blue copper electron transport protein plastocyanin (PC). This steady-state voltammetric technique has enabled simultaneous determinations of the formal redox potential and diffusion coefficient ($D = 8.7 \times 10^{-7} \text{ cm}^2 \text{ s}^{-1}$) for spinach PC.

Native PC exhibits positive shifts in formal potential with decreasing pH. However, when the protonation sites 18 Å away from the copper center (acidic residues 42-45) are blocked by chemical modification with ethylene diamine in the presence of a water soluble carbodiimide, the formal potential of the modified PC exhibits no positive shift in potential with decreasing pH. This suggests a cooperative relationship between residues 42-45 and the copper center. Such a relationship may be important in the regulation of photosynthetic electron transport since PC is exposed to dramatic fluctuations in pH within the lumen of the chloroplast.

W-Pos122 PHOTOELECTRIC EFFECT IN BILAYER LIPID MEMBRANE CONTAINING METALLO-PORPHYRINS AND DYES. Jan Kutnik and H. Ti Tien, Department of Physiology, Michigan State University, East Lansing, MI 48824

Photoelectric effects in the bilayer lipid membrane (BLM) system have been extensively studied for the purpose of elucidating details of the mechanism of light-initiated redox reactions in photosynthesis and vision. Our present studies deal with the BLM system containing metallo-porphyrins (TPP) and dyes as sensitizers and electron mediators. BLMs were formed in the usual manner, to which various redox agents and modifiers were added. Charge separation and electron transfer across the membrane, induced by light, resulted in redox reactions. Two types of photoeffects were measured: photovoltage and photoconductivity. Cyclic voltammetry was used for determining electrokinetic parameters of photo reactions. The system containing Mg-TPP in the BLM phase, and MV^{2+} (methyl viologen) in the aqueous phase yielded large photoconductivity (an increase of around two orders of magnitude) under illumination which resulting in $1.7 \times 10^{-6} \text{ A/cm}^2$ photocurrent when 100 mV voltage was applied. Addition of iodine to the aqueous phase was used for lowering of the membrane resistance. Photovoltage vs. time plots showed the existence of two components; a fast one (less than 0.1 ms risetime) and a slow one (3 s risetime). A number of dyes have been tested and some of them proved to be photoactive, especially Malachite Green, Crystal Violet, Ethyl Violet, Methylene Blue and Brilliant Yellow. The results are explained in terms of redox reactions and electron transfer processes.

[Supported by ONR Grant N00014-85-K-0399]

W-Pos123 A SEMIQUINONE EPR SIGNAL ELICITED BY Q_2 ADDITION TO CYTOCHROME b_6f COMPLEX. J.W. McGill, Swatantar Kumar, J.C. Salerno, Biology Department, Rensselaer Polytechnic Institute, Troy, NY 12180

A relatively weak free radical signal was observed in cytochrome b_6f complex isolated by the method of Hurt and Hauska with the addition of a $CaPO_4$ column. Addition of oxidized Q_2 decreased the intensity of the signal; Q_2 partially reduced with borohydride increased the signal five fold without altering its characteristics. The linewidth of the signal was 8 gauss and the g value approximately 2.005. At 50K, it was slightly saturated 50 μW and had an apparent ' P_1 ' of around 250 μW . 'Quinone analogs' such as UHDBT and HHNQ greatly decreased the signal amplitude; the site specificity of the inhibitors may have been lowered by working at high concentrations. These observations strongly suggest that the $g=2.005$ signals correspond to bound semiquinone species analogous to those observed in other bc -type complexes.

Addition of NADPH to cytochrome b_6f complex in the presence of excess oxidized Q_2 elicited a large radical signal with characteristics similar to Q_2H_2 induced species (pp ~ 8 gauss, $g=2.005$, P_1 50K $\sim 250 \mu\text{W}$). The complex is NADPH reducible because of the associated NADPH-ferredoxin reductase flavoprotein, which remains associated with it during $CaPO_4$ column step, and has NADPH- Q_2 reductase activity. The characteristics of the radical suggest that it is also a semiquinone species generated during turnover rather than a flavosemiquinone.

W-Pos124 ENDOR CHARACTERIZATION OF THE SECONDARY DONOR IN PHOTOSYSTEM II, T.K. Chandrashekar, I.D. Rodriguez and G.T. Babcock, Dept. Chemistry, Michigan State Univ., E. Lansing, MI 48824

The molecular identity of Z^+ , the electron carrier which links the reaction center of PSII, P680, with the oxygen evolving complex (OEC), has been further investigated by ENDOR spectroscopy. Recent studies from this laboratory have established that ENDOR is well suited for studying the hydrogen bond interaction in randomly oriented, immobilized quinone radical samples.¹ The application of this technique to Z^+ reveals lines which most likely can be assigned to hydrogen bonded proton(s) and they show orientation selection. An in-plane orientation for the hydrogen bond is indicated. Attempts to replace the H-bonded proton(s) with deuterium by soaking samples in D₂O have not yet produced quantitative exchange despite fairly extreme conditions. However, the intensity of the resonances from the H-bonded proton(s) do decrease in these experiments and a pair of resonances in the matrix region disappear indicating that the site is insulated from the solvent to a large extent but that solvent accessibility can be induced. The methyl coupling attributed to the 2-CH₃ in PQH₂⁺ have also been observed. Overall, these data are consistent with the postulated PQH₂⁺ origin for the Z^+ EPR spectra² as they indicate hydrogen-bonding to the radical in a site which is in poor equilibrium with the aqueous phase.

This work was supported by the McKnight Foundation and USDA/SEA/CRGO).

References: 1) (a) O'Malley, P.J., Chandrashekar, T.K. and Babcock, G.T. (1985) in "Primary Processes in Photosynthetic Bacteria" (Michele-Beyerle, ed.) Springer-Verlag, Berlin, in press; (b) O'Malley, P.J. and Babcock, G.T. (1985) J. Am. Chem. Soc., submitted. 2) O'Malley, P.J. and Babcock, G.T. (1984) BBA 765, 370.

W-Pos125 EFFECTS OF AMINE BINDING ON THE MANGANESE SITE OF THE OXYGEN-EVOLVING COMPLEX OF PHOTOSYSTEM II. Warren F. Beck and Gary W. Brudvig, Department of Chemistry, Yale University, New Haven, CT 06511 (Intr. by P. B. Moore)

Amines inhibit photosynthetic O₂ evolution by binding to the O₂-evolving complex (OEC) of Photosystem II (PSII) in competition with chloride. Ammonia, however, competes additionally for another site independently of the concentration of chloride (Sandusky and Yocum (1984) BBA 766, 603-611). We have used low-temperature EPR spectroscopy to study the effects of amine binding on the Mn site of the OEC. Past studies indicate that ammonia binds to the S₂ and S₃ states of the OEC, but not to the S₁ state (Velthuys (1975) BBA 396, 392-401). The S₂ state normally exhibits a multiline EPR signal that can be produced by illumination at 210K, a temperature below which ligand substitution occurs, or at 0°C in the presence of DCMU. We find that adding up to 300 mM Tris, 2-amino-2-ethyl-1,3-propanediol, or methylamine to PSII membranes at pH 7.5 has no effect on the S₂ state multiline EPR signal produced either at 210 K or 0°C. In contrast, a new S₂ state multiline EPR signal is produced by 0°C illumination in the presence of 100 mM ammonium chloride. This new EPR signal exhibits an average spacing of the hyperfine lines of 67 G which is reduced from the average spacing of 87 G observed in the EPR signal from untreated samples. 210 K illumination fails to produce a new multiline EPR signal in ammonia-inhibited preparations. These results indicate that ammonia binds directly to the Mn site, producing the novel multiline EPR signal, only after a structural change occurs in the Mn site during the S₁ to S₂ transition. The results also suggest that the observable Mn site in the OEC is the ligand-binding site involved in photosynthetic water oxidation, and that the chloride-binding site, competed for by amines, is not on the Mn site.

W-Pos126 EFFECTS OF INHIBITING O₂-EVOLUTION (MILD HEAT OR TRIS TREATMENT) ON THE HILL ACTIVITY AND THE BINDING OF CHLORIDE IN SPINACH THYLAKOIDS. W. J. Coleman^a, Govindjee^{a,b}, and H. S. Gutowsky^c, Departments of ^aPlant Biology, ^bPhysiology and Biophysics, and ^cChemistry, University of Illinois, Urbana, IL 61801.

Binding of Cl⁻ to the oxygen-evolving complex (OEC) of Photosystem II is required for O₂-evolution, and can be studied by ³⁵Cl-NMR. Measurement of the excess ³⁵Cl-NMR linewidth as a function of [Cl⁻] for Cl⁻-depleted spinach thylakoids gives a descending hyperbola between 0.1 mM and 10 mM Cl⁻, indicating specific Cl⁻ binding. The curve also shows three maxima in linewidth at 0.3 mM, 0.75 mM, and 3.25 mM NaCl, suggesting that the addition of Cl⁻ exposes previously nonexchanging sites. These maxima correspond to inflection points observed in plots of the Hill activity as a function of [Cl⁻] at low light intensity. The stair-step dependence of the Hill activity vs. [Cl⁻] may indicate that the binding of Cl⁻ ions alters the affinity of the OEC for other Cl⁻ ions. Two inhibitory treatments were used to test the relationship between Cl⁻ binding and Hill activity: 1) Mild heat treatment (38°C for 3 min; 50-60% inhibition of the Hill activity) abolishes the linewidth maxima in the NMR binding curve, producing a simple hyperbola. This treatment also removes the inflections from the Hill activity curve. These effects of mild heating are consistent with the possibility that heating destroys the interactions between polypeptides of the OEC. 2) Tris treatment (0.8 M Tris-phosphate, pH 8.0) for 30 min., which is known to detach some of the extrinsic polypeptides from the OEC, destroys 90% of the Hill activity, and abolishes almost all of the specific Cl⁻ binding observed by NMR. These data suggest that cooperative binding of Cl⁻ to the polypeptides of the OEC may be responsible for activation and regulation of O₂ evolution.

W-Pos127 STRUCTURE-FUNCTION STUDIES IN REACTION CENTERS: CHARACTERIZATION OF AN HERBICIDE RESISTANCE MUTATION IN RHODOPSEUDOMONAS SPHAEROIDES. C. C. Schenck; Department of Biochemistry, Colorado State University; Fort Collins, CO 80523 and W. R. Sistrom and R. A. Capaldi; Institute of Molec. Biology; University of Oregon; Eugene, OR 97403. Intr. by M. M. Elkind.

Recent studies have shown that triazine herbicides and other inhibitors of electron transport exert their effect as competitive inhibitors of electron transfer to a special reaction center-bound ubiquinone, Q_B. Biophysical experiments demonstrate that a mutant strain of *R. sphaeroides* is resistant to terbutryn, a triazine herbicide. The mutation decreases the ability of herbicide to block electron transfer to Q_B in intact membranes. In purified reaction centers depleted of Q_B and terbutryn, soluble analogs of ubiquinone are decreased in their ability to accept electrons from the primary quinone, Q_A. Single turnover flash experiments show that the equilibrium $Q_A \rightleftharpoons Q_B$ is shifted to the right in the ter^R mutant.

A molecular genetic approach has been used to map the resistance mutation to a plasmid bearing a piece of *R. sphaeroides* DNA 4.8 kb in length. DNA sequence studies show that the ter locus encodes the reaction center L subunit gene. A single point mutation is observed in the N-terminus side of the fifth putative transmembrane helix. We propose that this mutation localizes the Q_B binding site on the protein.

W-Pos128 FLASH-INDUCED FLUORESCENCE MEASUREMENT OF PHOTOSYSTEM II FUNCTIONING OF WILD-TYPE AND HERBICIDE-RESISTANCE TRANSFORMED STRAINS OF ANACYSTIS NIDULANDS R2. H.H. Robinson, C-Y. Yun, Dept. of Physiology and Biophysics, University of Illinois, Urbana, Illinois and S.S. Golden, R. Haselkorn, Dept. of Molecular Genetics and Cell Biology, University of Chicago, Chicago, Illinois.

Wild-type and transformed strains of the cyanobacterium *Anacystis nidulands R2* were studied by a flash-induced fluorescence technique to examine the functioning of their photosystem II quinone acceptor complexes. The transformed strain (R2-Taql) has a mutated psbA gene with a single nucleotide substitution at the start of codon 264. The polypeptide from this gene has an alanine where there had been a serine in the primary sequence of the 32-kD herbicide-binding protein of the thylakoid membrane (S.S. Golden and R. Haselkorn, *Science*, 229, 1104, 1985). Flash-induced fluorescence studies on intact cells show that the quinone acceptor complex of photosystem II becomes blocked upon binding of the herbicide DCMU. In the wild-type strain, all the photosystem II centers become inactivated with a single association binding constant of about 25 nM. The photosystem II centers from the transformed strain R2-Taql, similarly become inactivated with a single association binding constant which is 100 times larger (2800 nM) than the wild-type strain R2. There are three separate psbA-type genes in *Anacystis* which encode highly homologous polypeptides (S.S. Golden, J. Brusslan and R. Haselkorn, unpublished). In the transformed strain R2-Taql only one of these genes is altered. Since this strain shows only a single inhibitory low affinity binding of DCMU, we suggest that proteins from the other two genes are not associated with functional photosystem II centers.

W-Pos129 CHEMICALLY-INDUCED DYNAMIC ELECTRON POLARIZATION IN PHOTOSYSTEM 2 REACTION CENTERS. Joseph T. Warden and Karoly Csatorday, Department of Chemistry, Rensselaer Polytechnic Institute, Troy, N.Y. 12180-3590.

Time-resolved electron spin resonance spectroscopy has been utilized to probe secondary electron transfer processes at cryogenic temperatures in photosystem 2 (PS 2) subchloroplast preparations isolated from spinach. Control samples, during photolysis with a 600 ns laser flash (665 nm), exhibit a transient resonance centered at $g=2.0025$ ($\Delta H_{pp}=0.82$ mT) with a lifetime of circa 4.5 ms. The control samples do not display the spin-polarized triplet resonances associated with ³P680.

Treatment of the PS 2 preparation with the fatty acid, linolenic acid (Golbeck and Warden, *Biochim. Biophys. Acta* (1984) 767, 263-271), eliminates the 4.5 ms kinetic electron spin resonance transient and abolishes optical absorption changes observed at room temperature arising from P680⁺ and Q_A⁻. Although the linolenic acid inhibited sample displays a high initial fluorescence yield, significant formation of the polarized P680 triplet is not observed.

Chemical redox poisoning ($E_h \approx -500$ mV) of the control PS 2 particles or the linolenic acid inhibited sample facilitates formation of the light-induced P680 triplet. Additionally, the fatty-acid treated samples exhibit a reversible, spin-polarized esr transient, centered near $g=2.003$, which is characterized by mixed absorption and emission components.

These observations combined with published peptide sequence data are interpreted within the framework of the current model for the acceptor locus of the PS 2 electron transport chain. This work was supported by the National Institutes of Health (2R01 GM26133-06).

W-Pos130 LIGHT-INDUCED FOURIER TRANSFORM INFRARED (FTIR) SPECTROSCOPIC INVESTIGATIONS OF THE INTERMEDIARY ELECTRON ACCEPTOR REDUCTION IN BACTERIAL PHOTOSYNTHESIS.

J. BRETON*, E. NABEDRYK, B.A. TAVITIAN* and W. MANTELE† (Intr. by P. RIPOCHE)

*Service de Biophysique, CEN Saclay, 91191 Gif-sur-Yvette cedex, France

†Institut für Biophysik und Strahlenbiologie, Albertstrasse 23, D-7800 Freiburg, FRG

Molecular changes associated with the light-induced reduction of the intermediary electron acceptor H (a bacteriopheophytin b molecule) in *Rhodospseudomonas viridis* were studied by means of Fourier transform infrared (FTIR) difference spectroscopy. Films of chromatophore membranes and reaction centers reconstituted in lipid vesicles were prereduced to trap photochemically the state H⁻. FTIR spectra of these samples were recorded before, during and after illumination (715 nm < λ < 1100 nm), with an accuracy better than 10⁻³ absorbance units (W. Mantele, E. Nabedryk, B. Tavitian and J. Breton, 1985, Proc. 1st European Conf. Spectroscopy Biological Molecules, Reims 370-372). Difference spectra of H⁻ in chromatophores and in reaction centers closely correspond to each other. In the carbonyl stretching frequency region between 1750 cm⁻¹ and 1640 cm⁻¹, bands are tentatively attributed to a decrease in absorbance strength of both ester C=O groups of the bacteriopheophytin, a shift in position of a keto C=O group and possibly a change of an acetyl C=O group after reduction of H. As already reported in the case of the photooxidation of the primary donor (W. Mantele, E. Nabedryk, B. Tavitian, W. Kreutz and J. Breton, 1985, FEBS Lett 187, 227-232), the absence of strong bands in the amide I and amide II regions excludes large protein conformational changes associated with these two primary reactions in bacterial photosynthesis.

W-Pos131 Antenna And Reaction Center Proteins in Monomolecular Layers

W. Heckl, M. Lösche and H. Möhwald, TU Munich, Physics-Dept. E22, D 8046 Garching

Lipid monolayers containing proteins are valuable tools with which to study protein/lipid interactions, because the lipid phase state can be easily controlled and because proteins are oriented in a membrane of macroscopic size. This model system in particular enables studies of interactions with the adjacent aqueous phase and also provides interesting routes in developing a biological sensor. On the other hand, reconstitution into monolayers is very critical and difficult to monitor due to the low molecular density at the air/water interface.

Using the technique of fluorescence microscopy and spectroscopy at this interface we studied reconstitution of antenna proteins (LHCP) of the bacterial photosynthetic apparatus into phospholipid monolayers. Monitoring the intrinsic protein fluorescence we elaborated conditions to maintain the protein functional and to achieve a homogeneous protein distribution. Maintaining coexistence between fluid and solid phases yields a regularly inhomogeneous protein distribution. This is ascribed to the higher protein solubility in the fluid compared to the gel phase. The fluorescence quantum yield drastically depends on surface pressure indicating pressure-induced protein conformational changes.

As detected from a reduction in pressure corresponding to the phase transition the protein tends to order acidic phospholipids. Additionally incorporating reaction centers (RC) into the monolayer reveals efficient energy transfer LHCP→RC indicating binding of the different proteins. Electron microscopic studies of monolayers transferred onto solid supports demonstrate a statistical distribution of monomeric RC but linear aggregates of LHCP.

W-Pos132 Interactions of Photosynthetic Reaction Centers and Antenna Proteins with Phospholipid Membranes

U. Riegler, J. Peschke and H. Möhwald, Physics Dept. E22, D 8046 Garching

The functioning of the photosynthetic unit depends to a large extent on the organization of interacting proteins within the membrane. Its understanding therefore necessitates studies of protein-protein- and protein-lipid-interactions. Performed with structurally and functionally well characterized proteins (from the photosynthetic apparatus) these studies may additionally display model character for many functional membranes.

We reconstituted reaction centers (RC) and the B800-850 (LHCP) antenna proteins of the photosynthetic bacterium *R. sphaeroides* into vesicles of saturated diacyl-phosphatidylcholines varying the chain length. Protein distribution is studied electron microscopically, protein function is assessed by fluorescence spectroscopy and by transient absorption measurements and lipid phase transitions are investigated by static light scattering.

RC reconstituted into vesicles cause a shift and a broadening of the gel/fluid phase transition. The sign of the shift depends on lipid chain length determining the hydrophobic thickness of the membrane. The results can be explained by an elastic (mattress) model assuming a thickness of 28 Å for the hydrophobic membrane spanning part of the RC. Elastic forces are also responsible for protein segregation within the membrane, being most pronounced for a large mismatch of protein and membrane thickness and for a gel phase lipid. Lipid solidification does not influence the back reaction after electron transfer within RC but does reduce the fluorescence quantum yield of LHCP. Yet this does not affect the efficient LHCP RC energy transfer.

W-Pos133 SUPRAMOLECULAR ORGANIZATION OF THE B800-850 AND B875 LIGHT-HARVESTING PIGMENT-PROTEIN COMPLEXES OF *RHODOPSEUDOMONAS SPHAEROIDES* STUDIED BY EXCITATION ENERGY TRANSFER AND

SINGLET-SINGLET ANNIHILATION IN PHOSPHOLIPID-ENRICHED MEMBRANES. W. H. J. Westerhuis^a, M. Vos^b, R. J. Van Dorssen^b, R. van Grondelle^c, J. Amesz^b and R. A. Niederman^a. ^aRutgers Univ., Piscataway, NJ, ^bState Univ., Leiden and ^cFree Univ., Amsterdam, The Netherlands.

Liposomes were fused to chromatophores of *R. sphaeroides* by a freeze-thaw method (Casadio, R. et al., *J. Biol. Chem.* 259:9149-9157, 1984) which limited loss of B800 in the peripheral B800-850 complex. Fluorescence excitation spectra at 4 K showed that ~5-fold phospholipid enrichment resulted in decreased energy transfer between B850 and the B875 core complex from near 100% to ~65%, while that from B800 to B850 was essentially unaffected. The temperature dependence of fluorescence emission indicated that energy distribution was no longer determined by a thermal equilibrium but instead, was shifted toward B850. These data suggested further that the antenna complexes are disconnected upon fusion. Singlet-singlet annihilation was used to measure domain size (N_D), i.e. the number of connected bacteriochlorophyll molecules. In unfused chromatophores, N_D values were >550 at ~300 and 65 at 4 K which can be explained by decreased connectivity of B875 units at low temperatures and lack of back transfer to B850 (Vos, M., van Grondelle, R., van der Kooij, F. W., van der Poll, D., Amesz, J. and Duysens, L. N. M., manuscript in preparation). In fused preparations, N_D of 75-90 were found at ~300 and 4 K, reflecting dissociation of B800-850 from B875 as well as decreased B875 connectivity. In unfused chromatophores from strain 2.4.1, the N_D for B850 at 4 K was ~30 (Vos et al.); after fusion, N_D were only 3-12, suggesting phospholipid-induced dissociation of B800-850 multimers into smaller units. (Supported by NSF grant PCM82-09761)

W-Pos134 TRIPLET-TRIPLET ENERGY TRANSFER IN LIGHT-HARVESTING COMPLEXES OF PHOTOSYNTHETIC BACTERIA AND SYNTHETIC CAROTENOPORPHYRIN MOLECULES.

Harry A. Frank, Barry W. Chadwick and Chaoying Zhang, Department of Chemistry, U-60, University of Connecticut, Storrs, CT 06268; Richard J. Cogdell, Department of Botany, University of Glasgow, Glasgow G12 8QQ, Scotland; and, Devens Gust, Paul A. Liddell and Thomas A. Moore, Department of Chemistry, Arizona State University, Tempe, AZ 85281.

Triplet-triplet energy transfer has been investigated using electron spin resonance techniques applied to B800-850 light-harvesting complexes isolated from several photosynthetic bacteria. The observed ESR spectra are attributable to carotenoid triplet states which are formed via triplet-triplet energy transfer from bacteriochlorophyll molecules. The zero-field splitting parameters and spin polarization patterns of the triplets were found to be very similar to those observed for several synthetic carotenoporphyrim molecules. The similarity in the spectra suggests a common mechanism for triplet-triplet energy transfer between porphyrins or bacteriochlorophylls and carotenoids in the two types of samples. Also, ESR spectra were taken from both free base and zinc-substituted carotenoporphyrim molecules. This substitutional change is known to affect the spin polarization which initially populates the porphyrim (energy donor). It was found that the spin polarization patterns of the carotenoid (energy acceptor) triplet state ESR spectra were insensitive to this change. This suggests that electron spin polarization is not conserved during the triplet-triplet energy transfer process. (Work supported by NSF grant PCM-8408201.)

W-Pos135 SPECTROSCOPIC AND VOLTAGE CLAMP MEASUREMENTS ON LANGMUIR-BLODGETT FILMS OF REACTION CENTERS FROM *RPS. VIRIDIS*. G. Alegria and P.L. Dutton. Department of Biochemistry and Biophysics, University of Pennsylvania. Philadelphia 19104, PA.

Langmuir-Blodgett (LB) films of reaction centers (RCs) from *Rps. Viridis*, have been prepared and transferred to fused quartz and glass slides for optical measurements. For electrical measurements capacitive cells were fabricated by coating Sn_2O_3 treated glass slides with variable numbers of arachidate layers on top of which the RC films were deposited. The glass/arachidate/RC array was dipped in a hexane solution of a polymer to protect the RCs. This cell permits signals to be measured on the same sample at different redox potentials. The blocking polymer can be washed off with hexane exposing the RCs. The film is then dipped in a medium with a given E_h and a new blocking polymer deposited. Observations include: a) Light induced absorbance changes in the α band of cytochromes c_{558} and c_{553} show that after the film making process all cytochromes are oxidized. Ascorbate and dithionite treatment respectively restores c_{558} and c_{553} photo oxidation. Spectra of flash induced c_{558} oxidation in LB films are identical to those seen in solution. b) Current clamp measurements of light induced voltages under steady state illumination and single flash excitation showed that films in which c_{558} is reduced generate voltages that decay with half times of ~1 sec. consistent with the decay of c_{558}^+ measured in solution. Films in which the cytochromes are fully oxidized show half times of ~30 ms. The present work shows for the first time the functionality and electrogenicity of the bound cytochrome c photo oxidation in a solid state environment and will allow us to study the effect of external electric fields on the electron transfer from cyt. c to the reaction center. Supported by DOE DE-AC02-80-ER 10590.

W-Pos136 STRUCTURE AND ASSEMBLY MECHANISM OF 29S PROTEIN, A MULTIMERIC COMPLEX WHICH BINDS THE LARGE SUBUNIT OF RuBisCO

Jane F. Koretz, Susan V. Cannon, Santa J. Tumminia, and Harry Roy, Dept. of Biology, Rensselaer Polytechnic Institute, Troy, NY 12180-3590 (Intr. by Robert H. Parsons)

29S protein complex is a multimeric aggregate of 12 identical subunits which weighs about 700,000 daltons in toto. Each of these complexes can bind a single large subunit of ribulose 1,5-bis phosphate carboxylase/oxygenase, which suggests a possible role in the control of RuBisCO assembly. The intact 29S complex consists of two hexameric rings stacked with a relative rotation of 30 degrees, and the central shaft is generally occupied by what is presumably a large subunit of RuBisCO. If the preparation is left at room temperature for about 60 minutes, a large proportion of these complexes exhibit a dark central shaft with negative staining, suggesting loss of the large subunit. The complex can be dissociated using increasing hydrostatic pressure; it first breaks down into single hexameric rings, which in turn dissociate at higher pressures into dimers. Dissociation studies using ATP are currently in progress as well, and preliminary results suggest that the double hexameric structure of the intact complex can "open" into a second form, also double hexameric, which has a larger central shaft. A shift between the open and closed forms may be the mechanism by which the large subunit is alternately bound or released.